NOVA SCHOOL OF SCIENCE & TECHNOLOGY

DEPARTMENT OF MECHANICAL AND INDUSTRIAL ENGINEERING

RICARDO ALBERTO HENRIQUES MANICA
BSc in Mechanical Engineering

Development of a modular extruder for the production of recycled and customizable polymers in filament form

Mechanical Engineering Integrated Master's Degree

NOVA University of Lisbon
September 2023

NOVA SCHOOL OF SCIENCE & TECHNOLOGY

DEPARTMENT OF MECHANICAL AND INDUSTRIAL ENGINEERING

Development of a modular extruder for the production of recycled and customizable polymers in filament form

RICARDO ALBERTO HENRIQUES MANICA

BSc in Mechanical Engineering

Adviser: Valdemar Duarte
Invited Assistant Professor, NOVA University Lisbon

Co-adviser: Bruno Soares
Assistant Professor, NOVA University Lisbon

Examination Committee:

Chair: Doctor Rui Fernando dos Santos Pereira Martins,
Associate Professor, Faculdade de Ciências e Tecnologia da Universidade NOVA de Lisboa

Members: Doctor António Gabriel Marques Duarte dos Santos,
Assistant Professor, Faculdade de Ciências e Tecnologia da Universidade NOVA de Lisboa

Doctor Valdemar Rebelo Duarte,
Invited Assistant Professor, Faculdade de Ciências e Tecnologia da Universidade NOVA de Lisboa.

Mechanical Engineering Integrated Master's Degree
NOVA University of Lisbon
September 2023

ACKNOWLEDGEMENTS

I would like to express my deepest gratitude to the individuals who have played significant roles in my academic journey and the completion of this master thesis.

Firstly, I extend my appreciation to Professor Valdemar Duarte, my thesis advisor. His guidance, expertise and support throughout this academic endeavour have been invaluable. His vast knowledge, feedback and encouragement have been greatly contributed to the success of this master thesis. I am equally thankful to Professor Bruno Soares, my co-advisor, for his valuable insights and contributions for this work.

To Rui Gonçalves, a dear friend, for his unwavering support and assistance throughout this thesis journey. His knowledge was indispensable, providing me with the necessary encouragement to persevere through challenging moments.

To my parents, Nereida and Alberto, and my grandparents, I am forever grateful for their endless love, support, and sacrifices that have paved the way for my academic and life achievements. Their believe in me has been a pillar of strength throughout my life.

To Leonor, my girlfriend, I owe a debt of gratitude for her support, understanding and encouragement during the challenging times of the past two years. Her presence and unwavering belief in my abilities have been a constant source of strength and motivation.

A special thanks to my cousins, Santiago and Adrian, for their support and presence during critical junctures for this journey. Your support has been a great source of comfort and motivation.

Lastly, I would like to express my heartfelt gratitude to my dear friend Diogo Oliveira for his friendship since the beginning of my academic journey. I wish him every possible success throughout his life because he really deserves it.

To all mentioned and those not, thank you for being part of this important phase of my life.

ABSTRACT

Up to the present day, extruders utilized in the polymer extrusion industry have been designed to guarantee the extrusion of a vast quantity of polymeric materials. However, when the need arises to extrude a different material not compatible with the existent equipment, a complete replacement of components becomes necessary, thereby aggravating project's overall costs. Hence, the development of a modular extruder for the production of recycled and customizable polymers in filament form is evident within the industry. Such modular approach would allow for equipment customization, lowering project costs and broadening the spectrum of materials previously deemed incompatible with current extrusion machinery. To achieve this, the extrusion barrel was divided into three different sections, being each correspondingly aligned with the extrusion stages in which they are situated. The results manifest a promising outlook, showcasing a substantial reduction in production costs when compared with the extruders implemented nowadays in the industry, along with the potential for lowering specific energy consumption levels associated with the extrusion process.

Keywords: Single screw extrusion; Modular extruder; Extrusion barrel; Extrusion of polymeric materials; Specific energy consumption

RESUMO

As extrusoras utilizadas na extrusão de polímeros, até aos dias de hoje, são construídas com base na garantia de extrusão de vários tipos de materiais poliméricos. Contudo, com o crescer da necessidade de extrudir materiais não compatíveis com estes equipamentos existentes, torna-se assim necessária a sua substituição, agravando assim os custos associados ao projeto. Sendo assim, o desenvolvimento de uma extrusora modular para a produção de polímeros reciclados e customizáveis é cada vez mais evidente na indústria. Este equipamento irá trazer redução de custos associados ao projeto, aumento ainda a quantidade de matérias capazes de serem extrudidos com este equipamento.

De modo a desenvolver este equipamento, o barril de extrusão foi dividido em três secções diferentes, tendo cada uma correspondência com a etapa de extrusão que estas albergam. Os resultados apresentados são bastante promissores uma vez que apresentam uma significativa redução de custos acompanhada ainda de uma potencial descida da energia específica de consumo associados ao processo de extrusão.

Palavras-chave: Extrusão de fuso único; Extrusora modular; Barril de extrusão; Extrusão de polímeros; Energia específica de consumo

CONTENTS

LIST OF FIGURES

LIST OF TABLES

ABBREVIATIONS

PLA	Polylactic acid
SSE	Single screw extruder
L/D	Length-to-diameter ratios
SEC	Specific energy of consumption
IR	Infrared

SYMBOLS

τ_a	Allowable shear stress	$\mathbf{I}$	Electrical current
$\dot{\gamma}_{w,a}$	Apparent shear rate	$\mathbf{U}$	Electrical potential
$\dot{\tau}_{w,a}$	Apparent shear stress	$\mathbf{P_e}$	Electrical power
$\mathbf{A}$	Area	$\mathbf{R_i}$	Electrical resistance
$\mathbf{D_b}$	Barrel diameter	$\mathbf{Q_e}$	Energy
$\mathbf{t_b}$	Barrel thickness	$\mathbf{d_e}$	Extrudate diameter
$\mathbf{V_b}$	Barrel velocity	$\mathbf{Q}$	Extruder throughput
$\mathbf{w}$	Channel width	$\mathbf{t_1, t_2}$	Geometrical tolerances
$\mathbf{V_{bx}}$	Cross channel velocity	$\mathbf{c_p}$	Heat capacity coefficient
Δ	Deviation	$\mathbf{K}$	Heat conductivity
$\mathbf{D}$	Diameter	φ	Helix angle
$\mathbf{L_e}$	Die exiting length	σ_o	Hoop stress
$\mathbf{R_e}$	Die exiting radius	$\mathbf{L}$	Length
$\mathbf{S}$	Die swell ratio	α	Linear expansion coefficient
$\mathbf{V_{b,z}}$	Down channel velocity	$\mathbf{m}$	Mass

$\mathbf{D_m}$	Mean diameter	$\boldsymbol{\tau}$	Shear stress
$\boldsymbol{\delta}$	Melt film thickness	**h/w**	Slenderness ratio
$\boldsymbol{\omega_m}$	Melting rate per unit length	$\mathbf{V_{sy}}$	Solid bed velocity
J	Moment of inertia	**X**	Solid bed width
P	Pressure	$\boldsymbol{\sigma}$	Stefan Boltzmann constant
ΔP	Pressure differential	**F**	Tangential force
$\mathbf{T_k}$	Rated coupling torque	**T**	Temperature
n	Safety coefficient	**ΔT**	Temperature differential
h	Screw channel depth	**t**	Time
R	Screw outer radius	$\mathbf{T_r}$	Torque
r	Screw radial position	**V**	Velocity
N	Screw rotational speed	**η**	Viscosity
γ	Shear rate		

1

INTRODUCTION

Plastics have become one of the most crucial materials in the 21st century owing not only to their cost-effectiveness, lightness and durability but also for its importance in advancing sustainable development. Over the past 50 years, the production of plastics has experienced tremendous growth, with Europe alone accounting for more than 55 tons of the global plastic production, representing nearly a quarter of all the plastic production in the world [1].

The packaging market stands as the larger consumer of these materials, representing nearly 40% of the market share. Additionally, the building and construction sectors also present a significant role with nearly 20% of market share [1].

Today, the increasing accessibility of additive manufacturing equipment, such as 3D printers, has the potential to revolutionize the market. These machines are affordable and relatively user-friendly, promoting for its in-house use. Additive manufacturing, like 3D printers, rely on the use of filaments to feed the machine. These filaments are made from polymer and polymer composites due to their lightweight, durability, corrosion and chemical resistance as well as its low-cost-manufacturing.

Extrusion is one of the primary techniques employed in the production of these materials. It is estimated that roughly 50% of polymeric material produced employs this technique in their manufacturing process. Although the extrusion process involves high energy levels, this parameter is overlooked in favor of optimizing the final product quality [2].

The objective of this project is to obtain a comprehensive understanding of process variables during the extrusion process. This knowledge aims to meet manufacturing demands and validate information presented in the vast bibliography on the subject. Additionally, this project searches to create a single screw extruder reducing, as much as possible, the costs associated with the project, while serving as an enabler for future projects and research in the fields of plastic extrusion and additive manufacturing, including 3D printing.

1.1 Motivation

Addictive manufacturing, the foundation of 3D printers, is a powerful technique that has a lot of potential to change the way that we see prototypes and small product quantities in the manufacturing industry. In order to implement this technique on 3D printers, it is necessary to feed the equipment with a polymer-based filament that is usually produced through extrusion.

The functionality of a polymer extruder is notably contingent upon the specific material intended for extrusion, a topic to be expounded upon in forthcoming chapters. Typically, this equipment is implemented in places where only similar density types of polymer are to be extruded. However, the necessity to modify or upgrade the extrusion process equipment can pose cost challenges due to the need for compatibility with the distinct polymer properties, thereby potentially increasing project expenses.

Therefore, the creation of a customizable extruder depending on the polymer requirements for the extrusion process, is a huge advantage for industrial settings as well as for academic research where costs are more limited. Also, by building this equipment it is possible to study and optimize the extrusion process in future works, more specifically on how the material behaves inside the equipment when changing the extrusion parameters due to its rheological properties.

Finally, the conception of such equipment would bring an enormous advantage when referring to acquisition costs of filament, since it is estimated by implementing this equipment that a 50% cost reduction when acquiring filament for 3D printers would take place.

1.2 Objectives

The objective of this dissertation is to develop and produce a modular extruder of filaments with 1,75 mm in diameter. In the first approach, to validate the developed equipment, these filaments will be obtained through extrusion of virgin polylactic acid (PLA) due to its low cost as well as it does not require any expensive equipment for its extrusion. Despite the vast existence of this equipment within the market, the in-house development of this equipment presents many advantages like:

- **Reduction of cost**
- **Flexibility and customization** – The equipment will be developed considering a possible adaptation for the production of other polymeric materials or even the implementation of non-polymeric materials like ceramic or metallic particles, glass or carbon fibers.
- **Inclusion of instrumentation** – This will allow the development of research in the area of moulding injection, particularly into the energetic efficiency and sustainability of the extrusion process.

To these advantages, it can be added the contribution that this equipment will have on the mechanical and industrial engineering of 3D printers, enabling the expansion of this area of research, having access to another step of the cycle of products produced by Fused Filament Fabrication (FFF).

2

EXTRUSION FUNDAMENTALS AND STATE OF ART

The extrusion process can be defined by the feeding of raw plastic material in the shape of grains (pellets) into a heated barrel that melts the polymer until it reaches the adequate point of viscosity (around 250° C for PLA), and by a compressive effort, this melted material is pushed to an orifice (nozzle) whose shape defines the cross-section of the extrudate. This procedure is highly dependable upon frictional, thermal and rheologic properties of the material [4–6].

The equipment employed in this procedure is the extruder, which can be delineated by its operational mode, categorized as either continuous or discontinuous. Continuous extruders primarily feature the utilization of a rotating element, typically a conveying screw or a rotating disc. In contrast, discontinuous processes, as implied by the nomenclature, entail intermittent operations applied by a plunger that exerts pressure on the material, forcing it to flow through the nozzle.

This chapter is dedicated to elucidating the phases of the extrusion process, along with its inherent characteristics, drawing upon investigations conducted by various researchers who have devoted their efforts to the comprehensive examination and optimization of this subject.

2.1 Equipment

The extrusion of plastic filament typically requires the production of substantial lengths of filament with a continuous feed of raw material into the equipment. Consequently, discontinuous extruders are unsuitable for such purposes, making continuous extruders the most apt and practical solution.

There are two types of continuous extruders: disk or drum extruders and screw extruders (single or multiple). Disk or drum extruders, often referred as screwless extruders, employ a disk or drum mechanism for the extrusion of materials, therefore, being categorized according to their conveying mechanism (viscous drag transportation or elasticity of polymer melt) which develops the necessary die-head pressure for the extrusion to occur [7].

The viscous drag conveying mechanism can be visualized in Figure 2.1.a, where it is also possible to see a schematic of a stepped disk. The main feature of this type of machine is the stepped disk positioned at a small distance from a flat disk. When the polymer starts its melting in the axial gap, a pressure build-up will occur at the transition of one gap size to another smaller gap size and, if an exit channel is incorporated into the equipment, the polymer can be continuously extruded [7]. A practical disadvantage of this type of extruders is its difficult to clean due to its intricate design of the flow channels in the stepped disk. The elasticity of the polymer melt conveying mechanism makes use of the polymer melt viscoelastic properties. When a viscoelastic fluid is exposed to a shearing deformation, unevenly normal stresses will be developed in the fluid, as opposed to a purely viscous fluid. The shearing occurs between two plates, one stationary and one rotating, Figure 2.1.b. However, despite its ingenuity, this type of extruders has not been able to acquire a position of importance in the extrusion industry [7].

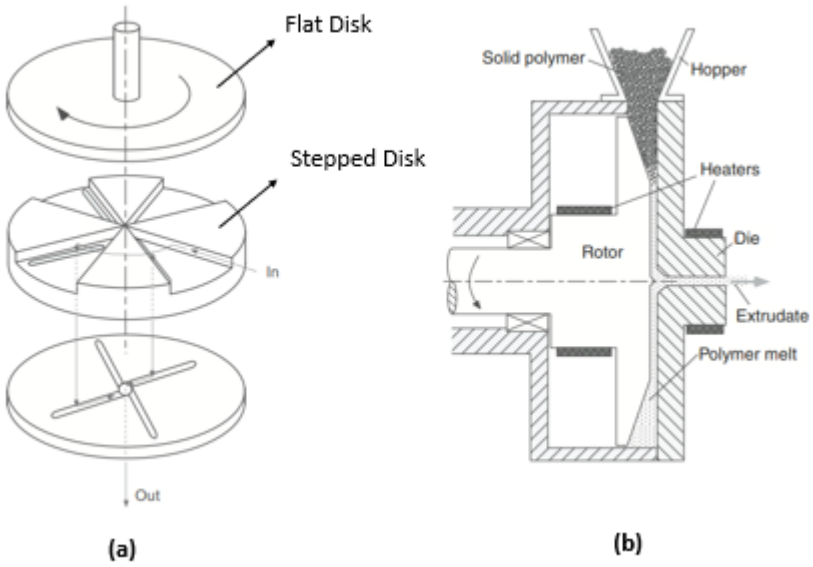

Figure 2.1 Disk/Drum extruders according to its conveying mechanism **(a)** viscous drag transportation **(b)** elasticity of polymer melt [7]

Currently, the most common extruder applied in the industry for the continuous extrusion of polymeric materials is the single screw extruder (SSE), belonging to the screw extruders classification mentioned above. The low cost, uncomplicated design and favourable performance-to-cost ratio established this equipment as the main choice for these applications, supplanting the utilization of disc/drum extruders. In this type of extruders, the main operating conditions are determined by the material properties and by the geometry of its components. The SSE is composed of some components like the: feed hopper, conveying screw, extrusion barrel, extrusion die, adaptor, breaker plate, cooling system, band heaters and the motor. However, the main component in this system is the conveying screw, due to its importance in promoting the material's movement, compression and plasticisation along the extruder's length during the process. The conveying screw can be divided into three different geometric sections

(feeding, transition/compression and metering) each of them important for the fundamental plasticizing stages of the extrudate material.

Conventional SSE features different rotation speeds for the conveying screw; however, these speeds are not higher than 150 RPM. As a result of this, the energy levels generated due to friction caused by the material when in contact with the screw and the barrel will be lower when compared to twin screw extruders. Consequently, this type of extruders tends to have higher screw lengths and low rotational speeds, which will cause higher residence times within the extruder. In terms of dispersion (the ability of the extruder to uniformly shred and mix the material throughout the plasticizing process), the single screw extruder isn't capable of presenting high levels of mixing, unlike the twin screw extruders.

Also, this extruder cannot extract volatile substances inside the mixture. Normally the presence of these substances occurs in high length-to-diameter ratios (L/D), so the extraction can occur in ventilation areas that consist of smaller holes in the barrel, commonly encountered in vented extruders. Furthermore, owing to these regions, it is possible to add more material or additives, at any juncture of the process, rendering the extruder adaptable to the desired product specifications. Despite the enhanced adaptability of the process with the implementation of these regions, this type of extruders tend to be more expensive and poses more manufacturing challenges primarily due to their intricate geometric and production complexity.

2.2 Extrusion process

The extrusion process in single screw extruders has several sequential steps, that demand careful attention from the operator, as an inadequate manipulation of any of these steps, can compromise the quality of the end product. Within the scope of this research project, some of these steps will be addressed in consideration of product limitations and the focused content of this study, namely the drying, extrusion, filament formation and cooling,

2.2.1 Drying

As previously mentioned, the extrusion process has numerous interrelated stages. Therefore, it's imperative to ensure the quality of all factors influencing the process, beginning with the material admission and extending to its ultimate formation.

There is no external factor as critical to a plastic before processing as moisture. The pellets admitted into the extruder must present low moisture levels so as not to affect the remaining stages of the process [8]. If the moisture levels are higher than what its supported by the extruder, it is possible to verify the formation of air bubbles at the end of the process [9].

The results of high moisture levels in the admission phase were studied by Sousa et al. [8]. His study suggests a relation between the end quality of PLA and the moisture levels presented in the admission phase when in the form of granulate. It was observed that the porosity of the pellets increased as the proportion of water insoluble material in the formulation increased. Also, it was observed that the mechanical properties of the pellets were related to the feeding material porosity. Pellets with low porosity were stronger than those with a high porosity being opposite also observed in this study. These high moisture levels in the granulated feed into the extruder can cause substantial drops in the thermal coefficient, modulus transition and the elasticity of the material [10]. Therefore, justifying the effects presented above.

To grant acceptable levels of moisture on the granulate before being admitted into the extruder, the material has to pass through a drying stage. The dehumidifier will be responsible for this stage. This equipment can be equipped in-line with the extruder by applying a heat closed loop, or as a separated machine which is usually more implemented.

To obviate the need to incorporate this parameter into the process, dehumidifiers are placed upstream of the extruder's administration zone. Within this equipment, hot dry air circulates through the lower portions of the container and, by diffusion, eases the expelling of residual water from the pellets. Although this equipment can function as a dehumidifier, they are also capable of functioning as material pre-heaters, the amount of energy required to heat the pellets being proportional to the total mass of this product and its initial temperature.

Due to cost implications associated with this machinery, the decision was made to abstain from its integration into this project. Instead, the pellets are submitted to a prior drying/dehumidifying process in a separate machine.

2.2.2 Extrusion

Once the moisture levels in the granulate reach an acceptable value, it becomes necessary to introduce the polymeric material into the extruder via the administration zone. Once the material is inside the preheated extruder, the extrusion phase commences.

The extruder is without a doubt the most important equipment in the polymer processing machine [7,11]. The majority of polymer process components involve extrusion, representing around 50% of the total process energy. According to the research conducted by Kent et al. [12], when applying no-cost or low-cost practices it is possible to reduce up to 20% of the energy consumed by the process. Also, Drury et al. [13] claims that nearly 40% of the energy given to the process is lost without being transmitted, nor used, in the procedure and that there exists very low potential for its recovery. Hence, meticulous practices, including a good comprehension of process variables and familiarity with extruder components, are imperative for the operator.

As stated before, this step is the most crucial in the whole process as this is where the material will move from its solid state to a molten state, where it can then be shaped in the following step. If this step is not performed well, it might lead to imperfections in the final product that can only be seen once the material leaves the equipment. For this reason, the extrusion components (barrel, screw and heaters), Figure 2.2, must be well designed.

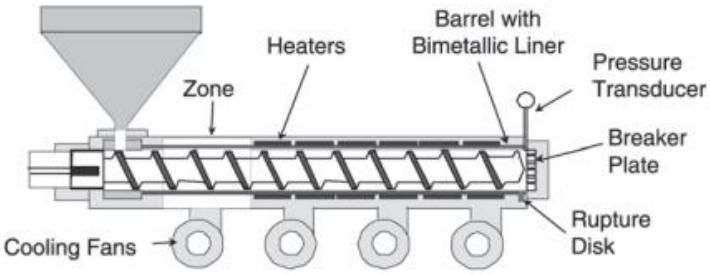

Figure 2.2 Components which form the extrusion process and formation of the filament [42]

The process of plasticizing polymeric materials is inherently time-extensive. Agassant et al. [14] explained that most of polymeric materials require some time to reach the same temperature on the surface due to their low thermal conductivity. So, to optimize the process, the material must also be heated by the friction caused through the conveying screw's rotation. The amount of energy transmitted to the material is directly proportional to the conveying screw's rotational speed. This is also corroborated by the study made by Cantor [15]. Cantor asserts that increasing the rotational speed of the conveying screw results in reduced energy consumption by the band heaters. This is due to the greater heat generation resulting from friction between the material and the screw as well as between the barrel and the material, at higher speeds.

For this reason, the efficiency of this process tends to be relatively low. In their article, Chung et al. [16] offer insight into the efficiency of some single screw extruders. He notices that the efficiency of single screw extruders started to decrease once the geometric conditions reach a specific value. For a 63.5 mm diameters this equipment presented 62% of efficiency and for extruders with higher diameters, its efficiency began to decrease even more. Strauch et al. [17] also presented some information on the efficiency of this equipment for a single screw extruder with 63.5 mm screw diameter. He observed that most of the thermal energy given to the system came from the mechanical components, with the remaining energy coming from the heaters applied along the barrel, Figure 2.3.

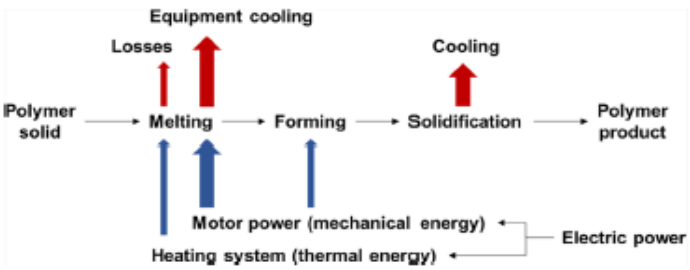

Figure 2.3 Energy consumption and loss in each step of the extrusion process [2]

Anderson et al. [18] stated in their paper that the majority of polymeric material required specific energies in the motor, between 0.0822 and 0.1644 kW h/kg, in the administration zone of the extruder, when at room temperatures. He also said that when the specific energy of consumption (SEC) was above 0.3288 kW h/kg, this was a parameter that indicated the excessive consumption of the extruder, which is also related to the rheological properties of the material. Javier et al. [6] point out that the higher the viscosity of the extruded material, the higher the SEC values and lower end material's homogeneity.

Nowadays there are lot of information to reduce SEC levels, providing better efficiency to the equipment by ensuring that the temperature being supplied to the process is distributed evenly throughout the barrel. Deng et al. [19] explored the energy consumption in the motor zone and the heaters along the system. His work concluded that lower energy SEC levels were obtained from the combination of lower temperatures in the heating system with higher rotations from the conveying screw. The number of band heaters used along the barrel was also one of the subjects studied by Rasid and Wood [20] as well as their influence on the material's melt temperature. They observed that the only section of the barrel which had an impact on the melt temperature was the metering section, implying that this is the only zone which requires a heater to optimize the process. When applying a heater to the feeding section, the melt temperature had a neglectable variation. However, the power consumption was noticed to have lowered when the temperature of this section was increased, Table 2.1. These observations go in full agreement with the observations made by Deng [19] in his work.

Table 2.1 Power consumption according to temperature values [20]

Barrel Temperatures (°C)	**Power Consumption (kW)**			
	Feeding Zone	Compression Zone	Metering Zone	Die Zone
140	1.78	1.66	1.63	1.63
180	1.53	1.53	1.53	1.53
Percentage change (%)	11	4	2.5	2.5

The barrel temperature mentioned earlier is evenly distributed for the entire barrel's length, and the power consumption represents the amount of energy consumed by the extruder.

Kelly et al. [21] conducted a study to investigate the influence of molten material flow on energy consumption. By implementing some sensors to measure the melt temperature, pressure and energy consumption in different zones of the extruders, she concluded that the screw's geometry had a high relation with the conveying stability of the process, during the molten material phase.

2.2.2.1 Plasticising process

The plasticising process of polymeric materials occurs in the transition/compression section of the extruder. To better understand it, Tadmor [22] used a simplified model in which the channel is unwound from the screw and located along a rectangular coordinate system, being the Z-axis in the

down channel direction, Y-axis channel depth direction and X-axis in the cross channel direction, Figure 2.4.a. The barrel surface is at the top moving at a constant velocity, V_b, with velocity components $V_{b,x}$ and $V_{b,z}$ in the cross channel and down channel directions, respectively, depending on the helix angle (φ), Figure 2.4.b. The screw surface is at the bottom being the screw flights represented at the sides of the model.

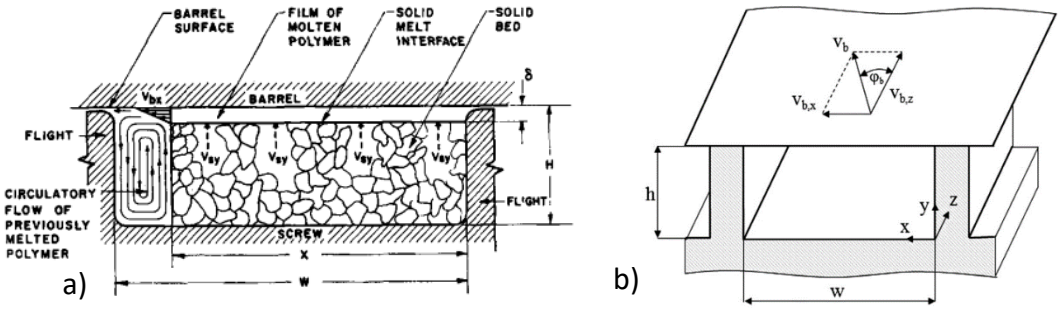

Figure 2.4 (a) Channel cross section [22] **(b)** Barrel velocities decomposition [27]

In this model, heat is not only conducted from the barrel surface heaters through the moving film to the solid-melt interface but is also generated through viscous dissipation within the film. Note that the actual melting of the solid particles takes place exclusively at the solid-melt interface. The steady state is maintained as the molten material is carried along by the barrel surface toward the rear of the channel, while the solid bed maintains a constant velocity as it approaches the interface [8,22,23].

This model incorporates several simplifications. Firstly, it assumes that the film thickness is extremely small, on the order of 0.2 mm, while the barrel presents high velocities, typically around 20 cm/sec. This justifies the presumption that within the molten film, there is a pure drag flow, which occurs between two infinitely long parallel plates. Additionally, it is assumed that the barrel maintains a constant velocity, denoted as V_b, and both lower and upper plates have a constant temperature, T. The plastic's melting point is assumed to have a constant down channel velocity $V_{b,z}$. Consequently, the fluid is approximated to display Newtonian characteristics as a consequence of the high shear rates within the film, which results in significant heat generation [22].

As the melt is considered as a Newtonian fluid, it becomes possible to calculate the material's melting rate by evaluating the thickness of the melt film. The temperature distribution within a Newtonian fluid confined between two parallel plates, each at a different velocity and temperature, while taking into consideration the heat generated due to viscous dissipation, has been previously derived by Bird et al. [24].

Due to the constant upward velocity in the solid bed, a time independent temperature profile will be developed, which decreases exponentially from the interface melting temperature to the solid bed's initial temperature. The rate of this decrease is associated, not only with the physical properties of the plastic, but also with the unknown solid bed velocity, V_{sy} [22]. The material's temperature distribution inside the extruder is presented in Figure 2.5.

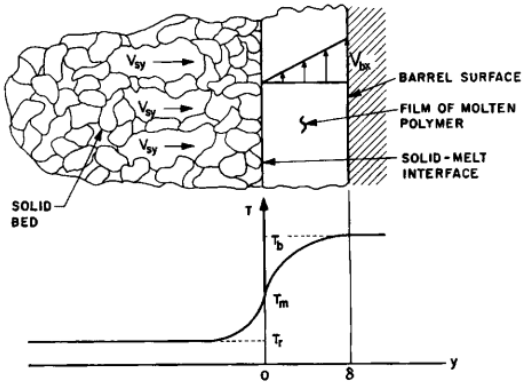

Figure 2.5 Temperature profile in the molten film and the solid bed [22]

The solid bed's melting rate will therefore be dependent on this unknown velocity V_{sy}. However, due to the similarity present between the solid bed's mass flow rate within the interface, per unit length, and the melt's flow rate value in the rear channel, per unit length, it is possible to say that the melting rate per unit length will be unattached to the value of the unknown velocity of the solid bed, as it is possible to see in Eq.1. Where (ω) is the melting rate per unit length, (V_{sy}) is the solid bed's velocity, (X) is the solid bed's width, (ρ_s) is the solid bed's density, (V_{bx}) is the barrel's constant velocity cross channel, (δ) is the film thickness and (ρ_m) is the melt film's density.

$$\omega \cong V_{sy} X \rho_s = \frac{V_{bx}}{2} \delta \rho_m \qquad (1)$$

It is worth emphasizing that the efficiency of the plasticising process will depend on the rate at which the material is melted. This can only be achieved when a uniform and consistent heat source is provided into the process.

Pioneer studies like these, based on the assumption of Newtonian fluids, provided analytical solutions in function of independent terms like drag flow and pressure flow. To refine this analysis, Griffith [25] , Zamodits and Pearson [26] and Karwe and Jaluria [27] suggested some numerical solutions for a two-dimensional non-Newtonian flow in an infinitely wide screw channel.

Numerical techniques, despite their high relevance, have limited usefulness in practice, since they require professional expertise to achieve stable solutions and tend to be time-consuming as well as cost-expensive [28].

2.2.3 Filament formation

Filament formation takes place once the plasticising process has been completed. At this stage, all solid material has transitioned into its molten state, and as a result, it proceeds to a pressure zone adjacent to the die. Therefore, the material must exhibit good mixing and maintain a homogeneous temperature for this step to be successful.

In order to provide the desired shape, several dies can be applied onto the extruder. Depending on the desired product, it is possible to have: 1) sheet dies; 2) flat-film and blown-film dies; 3) pipe and tubing dies; 4) profile extrusion dies and 5) co-extrusion dies. However, due to the uncertain nature of the profile when extruded, detailed knowledge of material characteristics, flow, heat transfer phenomena and extensive experience with extrusion processing is required when implementing any of these types presented above.

The traditional extrusion procedure was studied by Tadmor and Gogos [29], which observed that the production of components with regular geometry such as film, slits, conduits and rods are easily formed. However, the production of irregular shape profiles with polymeric materials is very difficult to obtain. This tends to happen due to the die swell.

Die swell, often referred to as the Barus effect or extrudate swell, is a phenomenon that occurs when a viscoelastic fluid flows out of a die as it undergoes compression through the die. Consequently, the diameter of the extruded is usually larger than the dimensions of the die orifice, as presented in the works made by Malkin et al. [30] and Nishimura et al. [31].

In order to avoid this effect when extruding irregular shape profiles with polymeric materials, computer simulations are applied, enabling a quicker way to solve many sophisticated problems involving different physical models and conditions. A cohesive understanding of the computational implementations made throughout the years when extruding polymeric materials, is illustrated by Wilczynski et al. [32] in his work.

Although the material homogenisation can be achieved by incorporating multiple filters or screens before the die, it remains necessary to optimize process parameters for a better control over the process, as discussed by Abeykoon et al.[33,34], Kelly et al. [35] and Rasid & Wood [20]. They believed that thermal homogeneity within the process will be mostly affected by process variables like melt temperature, pressure, screw speed and polymer type. This also refers to a molten material's temperature variation along its radial position inside the barrel. Unfortunately, as Rasid & Wood [20] found, it is quite difficult to monitor the melt temperature profile within a production environment since most extruders are only instrumented with wall mounted thermocouples which do not capture melt temperature variations across the melt flow, or detect rapid melt temperature variations.

As previously noted, in numerous extruders, wall-mounted thermocouples are placed in different barrel sections, sometimes only in a few of them, with a common practice being the implementation of a thermocouple at the die. Despite the high usage of wall-mounted thermocouples, their implementation

on the barrel's outer surface does not grant the true molten material temperature, being then necessary to immerse these thermocouples into the molten material. However, these are intrusive methods, which may disturb the melt flow steadiness as well as the temperature reading, which is affected by shear heating effects as stated by Kim et al. [36] in his work.

Additionally, certain industrial extruders use alternative techniques such as infrared (IR) temperature sensors and resistance temperature detectors. Kelly et al. [37] conducted a study using a thermocouple mesh developed by Brown et al. [38], to capture radial profile temperatures along the die's flow. By capturing different temperature values, it was possible to notice the result's radial symmetry according to the thermocouple mesh centreline, when averaged over significantly long periods of time. The maximum temperature, observed at the centreline of the thermocouple mesh, was dependable upon pressor values within the extruder. These pressure values were directly affected by the screw's rotational speed, generating more heat as a consequence of increased shear forces, as depicted in Figure 2.6.a.

Later, Abeykoon et al. [39], optimized this equipment generating a model capable of predicting the die melt temperature profile with reductions of up to 60% on melt temperature variations. At Figure 2.6.b, it is possible to compare the measures captured by the equipment (red), the results obtained by the model developed by Abeykoon (black) and finally the experimental average measured temperature traces at the 8th minute (blue).

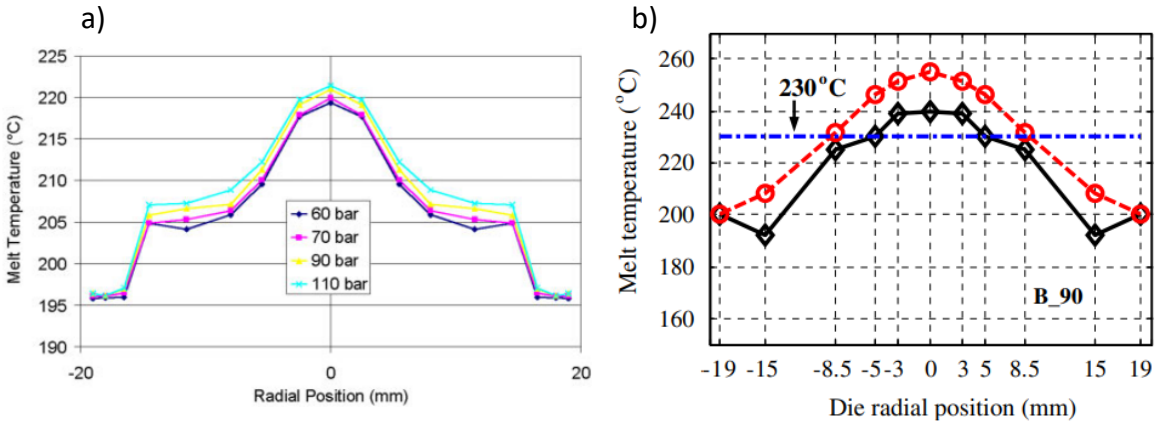

Figure 2.6 (a) Melt temperature profiles measured at a range of die head pressures at a set temperature of 200°C on a single screw extrudir with a 50 rev min^{-1} **(b)** Measured and optimized melt temperature profile [38]

2.2.4 Cooling

As previously mentioned, the main working element of a single-screw extruder is the conveying screw. Considering the nature of the extrusion process, both the solids conveying and melting sections must function at sufficiently high rates to ensure complete material melting and pressurization into the metering section. If solid conveying rates are less than optimal, then the downstream sections of the extruder screw can be partially filled, leading to solid degradation and reduced transportation rates [40,41]. Furthermore, flow surging can occur, creating challenges in maintaining product stability. The solid conveying optimal values occur when forwarding forces on the compacted solid bed are

maximized accompanied by the minimized retarding forces [40]. These forces are dependable on various factors, including the coefficient of dynamic friction specific to the resin, the temperature of the metal surface, pressure and the geometrical configurations of the screw [42]. Nonetheless, as until this day, these forces remain inadequately understood. While numerous solid conveying models exist, none of them can fully describe the performance of solid conveying with precision [40].

Since one of the factors that affects solid conveying inside of the extruder is the coefficient of dynamic friction, the temperature of the metal surface is one of the most important factors to control in the extruder, because of its direct relation with this variable. An optimized process maximizes the forces and coefficient of friction at the barrel wall while simultaneously minimizing them at the screw surface. Implying that the screw surface should be maintained at a lower temperature compared to the rest of the equipment, requiring cooling mechanisms.

The rate of cooling applied in these materials affects their crystalline structure. Faster cooling rates tend to result in more grain boundaries and, consequently a better crystallization. Likewise, filaments with larger cross-sectional areas tend to exhibit a better crystallisation when rapidly cooled, due to the relations between these properties [43].

Womer [42] suggests in his work, the advantages of screw cooling when the feedstock being processed has a high percentage of regrind and the material has poor feeding characteristics. If the regrind has several small particles, which melt prematurely as compared to the larger regrind particle sizes, the small particles will melt and stick to the screw and inhibit the solids conveying of the feedstock. Screw cooling mitigates this effect.

Mikulionok and Radchenko [44] explain in their work that, in the feeding zone, a more severe screw cooling is required to prevent premature polymer melt and ensure reliable initial polymer granules transportation along the extruder. Therefore, single screw extruder's cooling devices have been developed throughout the years, Figure 2.7.

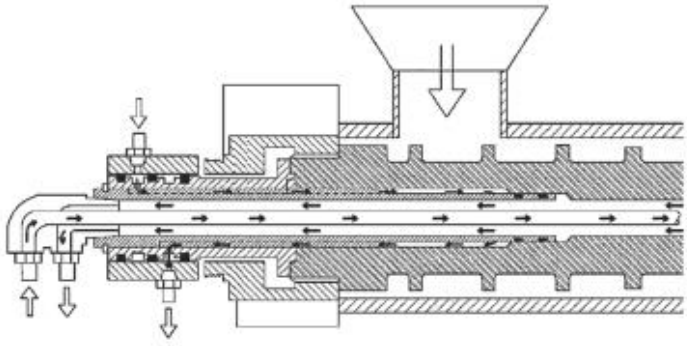

Figure 2.7 Schematic of the device with two-zone thermal stabilization of the screw (Patent No. KR20160141947A)

These devices, in the words of Mikulionok [45], can be classified according to the:

- **Refrigerant type**: devices with liquid refrigerant, gaseous refrigerant and combined.
- **Number of cooling zones**: devices with one, two (or more) cooling zones.
- **Cooling intensity along the screw**: devices with variable and constant cooling intensity.

- **Possibility of adjusting the cooling zone length**: devices with non-adjustable length and adjustable length of the cooling zone or its separate sections.
- **Material of the main structural elements**: devices made of metals and alloys, as well as polymer and composite materials. The elements of most cooling devices are made of metals and alloys. Also, the use of various polymers and composites that provide high strength, rigidity, chemical resistance, as well as low thermal conductivity have been applied to some device parts

As previously explained, heat within the extruder barrels can be added or removed through air or water cooling methods [46]. Air cooling stands out for its less expensive hardware, ease of maintenance, lower operational costs, and reduced space requirements when compared to fluid cooling. However, it possesses a lower heat removal capacity compared to water cooling.

Moreover, water cooling is best suited for processes that require high energy removal. Compared to air cooling, the equipment is more expensive, requires higher maintenance to prevent fouling and requires more space as well as a water circulation and cooling system. Large thermal gradients produced by water cooling can also contribute to excessive thermal strain and stress in the extruder, promoting lower equipment life.

In order to implement the most suitable cooling device for a specific equipment, it is crucial to understand how the material is conveyed along the process. As previously mentioned, being the feeding zone the most problematic when it comes to cooling, the understanding of the solid material movements in this section, takes greater importance than the viscous-elastic material flow properties present in the transition/metering section.

2.3 Process control

The extrusion process involves diverse variables that affect the quality of the final product. These variables can be categorized into four different major groups: material properties, process conditions, die design and equipment design. Material properties relate to factors such as viscosity, melt temperature and material elasticity. Process conditions consider factors such as screw rotational speed, the temperature profile of the extruded material, internal equipment pressure and cooling. Notably, die and equipment design are often overlooked in the early stages of the project, but can exert a greater impact on the overall extrusion process.

Among the variables involved in the extrusion of polymeric materials, the screw geometry emerges as the most important one. This is due to its direct influence on several aspects like: extruder throughput, the melting rate, mixing effectiveness, homogeneity of melt temperature and overall process efficiency. These variables are all dependent on polymer melt residence time, a variable that has a direct proportionality with the screw length and inverse proportionality with its rotational speed [11].

For obvious reasons, the polymeric melt residence time can’t be null at any cost, as the main function of the extruder is to deliver a homogeneous, well-mixed polymer melt to the die at a specified

uniform temperature and pressure. Consequently, a constant monitorization of the process variables, in particular melt temperature, is required during the process, as is the easiest one to measure and cares great value in the final product quality.

In the initial stages of the extrusion process, experiments, such as those conducted by Maddock et al. [47] and Street [48], employed a method named the "screw pulling out technique". In this approach, the extruder was stopped at steady state conditions, rapidly cooled, and then the screw was removed. By doing this, a first polymer melt analysis was removed from the screw cross-sectional area, enabling the evolution of the melting mechanism (contiguous solid melting). After, this analysis, in Figure 2.8, process variables were amended. The utilization of this method was initially motivated by simple estimating the effective temperature of the polymer within the extruder. This difficulty was obtained by the high number of variables affecting the process, as underscored by Frankland et al. [49].2021

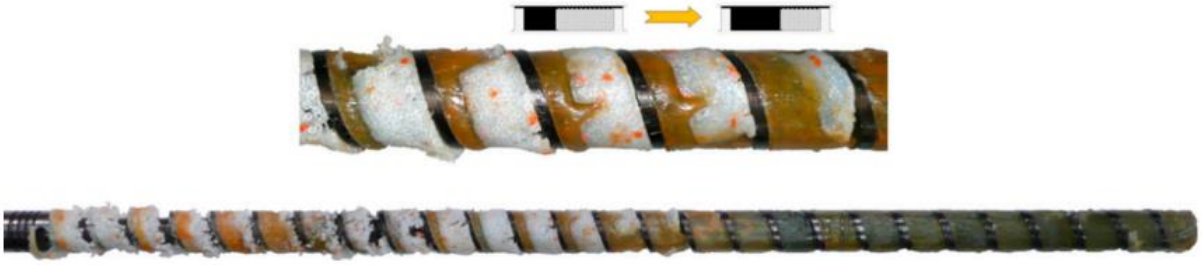

Figure 2.8 Contiguous solid melting mechanism observed for flood feed extruders [31]

Later, thanks to this technique, the first single screw extrusion melting model was developed by Tadmor et al. [22] and Marshall et al. [50], being a crucial contribution to the theory of extrusion and allowed the formulation of the first computer extruder model, "EXTRUD" [51]. Through the application of this model, it is possible to predict the velocity and temperature profiles within the melt film, as well as the temperature profile within the solid bed that would occur throughout the process. By applying an energy balance at the interface between the melt and solid and incorporating mass balance within the melt film and solid, it is possible to calculate the melting rate.

Throughout the years, many researchers have been validating the "screw pulling out technique" as well as the model developed by Tadmor. However, this technique is relatively time-consuming and costly when applied to studying melting within extruders. As a result, other approaches have been explored to directly observe the melting behaviour during the process.

In further experiments, Maddock et al. [52] employed wall-mounted thermocouples to monitor the extrusion melt temperature under different process conditions. Product quality was defined by uniformity of melt temperature and pressure. These components are still in use today due to their simplicity and ease of integration into extruder systems.

Many wall-mounted thermocouples with different probe design arrangements are commercially available. Depending on their arrangement, they can be classified as invasive, as they submerge into the melt. However, as invasive thermocouples disturb melt flow steadiness, they may also be influenced by

shear heating effects, as noted by Kim and Collins [36]. Despite their vast implementation, Schoppner et al. [53] observed that these components are not capable of capturing melt temperature rapid variations due to their relatively slow response time, which then leads to the implementation of different components.

Another method to measure the melt temperature within the extruder is the Infra-red (IR) polymer bolt sensors, also called wall-mounted probes, which can offer non-intrusive measurements. This method was initially studied by Obendrauf et al. [54]; Maier [55] and Bendana and Lamontagne [56] who mainly used sensors flush mounted radially on the extruder die. With their implementation, IR radiation emitted by the molten material was captured using a sapphire window connected with fiber optic cables, being later converted by the detector into an electrical signal. This signal could then be correlated with the actual temperature of the heat source. However, an emissivity adjustment should be taken into consideration in order to adjust to the emitting characteristics of the polymer melt, Eq.2.

$$\text{Temperature} = \left(\frac{\text{Thermal radiation}}{\text{Emissivity} \times \sigma}\right)^{\frac{1}{4}} \quad (2)$$

This constant of proportionality (σ) is also known as the Stefan-Boltzmann constant. Despite, the high dependence on polymer melts emissivity due to technique penetration issues (1-5 mm), a study made by Vera et al. [57], corroborated the implementation of these components into the extruder barrel of production applications, since they could be readily employed to monitor the thermal dynamics of the extrusion process as complementary techniques that could detect sensitive fluctuations caused by melting instabilities. However, this technique is used for temperature measurements of the final product such as the surface temperature of extruded tubes, sheets, films, rods, etc. [34].

Ultrasonic sensors were examined for the measurement of polymer melt temperature in the early 1970s. However, as observed by Rauwendall et al. [58] and Hauptmann et al. [59], this technique is more complicated than conventional thermocouples and IR techniques. This complexity may have contributed to the limited adoption of this technique in production applications. This technique is established on the velocity of ultrasound waves (above 18000 kHz) passing through the molten polymer which depends on the pressure as well as the melt's temperature, providing measurements with $\pm$ 0.1 °C accuracy. It is also capable of working up to a maximum temperature of 1000 °C [60]. Generally, ultrasonic temperature sensors comprise two piezoelectrics, one working as a pulsar and the other as a receiver, respectively [61]. The temperature on this technique is determined based on delays between the ultrasonic echoes since the travel speed of the wave on the material varies with its temperature [34].

Other techniques, in addition to the non-intrusive ones discussed earlier, are presented in Table 2.2. This table offers insights into the type of measurement conducted by the technique, as well as its accuracy and response time. The accuracy ratings are presented into three levels: low, medium and high.

As shown in the previous table, some of these techniques are not yet developed enough to be implemented in industrial environments, such as the case of the fluorescent technique and the thermocouple mesh.

Table 2.2 Process control techniques in single screw extrusion of polymeric materials

No.	Technique	Operating Principle	Measurment Type	Invasive	Sensor acurracy	Response Time	Accuracy	Industrial
1	Wall-mounted Thermocouple	Thermoelectric effect (emf at thermocouple junction)	Point	Yes/No	± 0.5 °C	1 s	Low	Yes
2	IR probe (polymer bolt)	Detects emmited IR energy and converts into a current signal which is relative to the temperature	Point	No	± 0.5 °C	10 ms	Medium	Yes
3	Ultrasonic Technique	Wave velocity through the transmiting media is a function of the temperature	Point	No	± 0.1 °C	1 ms	Medium	Yes
4	Fluorescence Technique	Temperature sensitive fluorescent dye (changes in the fluorescence spectrum is a function of the temperature)	Point/Profile	No	-	-	Medium	Maybe
5	Thermocouple mesh	Thermoelectric effect (emf at thermocouple junction)	Point/Profile	Yes	± 0.1 °C	0.1 s	High	Maybe

The fluorescent technique was first studied by Bur et al. [62] and it consists of doping temperature-sensitive fluorescent dye into polymeric materials, which responds to temperature fluctuations by altering their spectral characteristics. Through this technique, it is possible to measure a temperature profile within a polymer melt flow or the overall bulk temperature.

Usually, the melt temperature can be determined based on employing statistical methods that establish relationships between wavelength into the changes perceived in the fluorescence spectra within a wide range of typical processing temperatures [62–65]. Overall, this technique seems rather complex and in need of doping the polymer with dyes may not be practical with some industrial processes.

The thermocouple mesh is a grid of thin thermocouple wires, designed to monitor melt temperatures at different radial positions within the die, developed by Brown et al [38]. This method represents an invasive approach to measure melt temperature in which wires of very small diameter, usually with a diameter of 0.5 mm, are used to minimize any disturbances in the flow mitigating shear heating effects on temperature readings, as illustrated in Figure 2.9. As thermocouple junctions are exposed to the target temperature source, this electromotive force can then be correlated to the temperature of the source. The number of mesh junctions required can be decided according to specific requirements, such as the desired level of accuracy and the size of the device into which is integrated [34].

This equipment has been widely used by Kelly et al. [35,37,66,67], Abeykoon et al. [68] and Vera et al. [57] to study the polymer melt temperature across the die over different process conditions in polymer extrusion. These studies demonstrated that the thermocouple mesh offers an accuracy of $\pm$ 0.1 °C and shows a faster response when capturing melt temperatures. It has been observed that the measured melt temperature profile is symmetrical across the centreline of the melt flow. Therefore, asymmetric placement of mesh wires/junctions can provide the opportunity to obtain a greater number of effective temperature readings radially across the die melt flow. Currently, this technique is only used

in research applications and holds potential for its application in industrial settings where is suitable and beneficial [34].

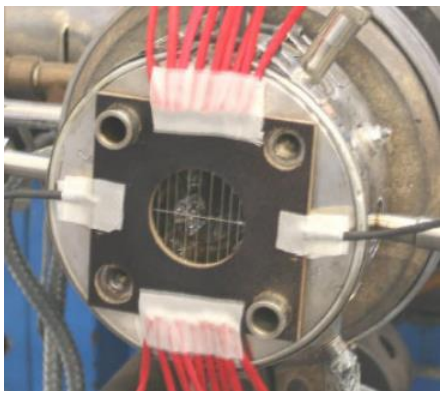

Figure 2.9 Thermocouple mesh [36]

3

COMPONENT THEORY

As observed in the previous section, the extrusion process depends on four main groups that can influence its end product quality: material properties, process conditions, die design and equipment configuration.

Material properties and process conditions are highly dependent on each other, with the flexibility to be adjusted according to the equipment being used, often without incurring in more costs to the extrusion process. In contrast, die design and equipment configuration have a direct impact on the final product quality, needing meticulous consideration as well as implementation before initiating the extrusion process.

Therefore, components such as the barrel, compression screw and extrusion die assume pivot roles to the well-functioning of the extrusion process. Consequently, this chapter is dedicated to explaining the component's design as well as their importance in the extrusion process.

3.1 Conveying screw

Designing a conveying screw for an extruder can be rather complex if considering all of the limitations that may affect the process. These limitations can promote melt material temperature fluctuations as well as promote some disparities in energy consumption levels within the equipment. To promote the absence of these issues, it is necessary to match the conveying screw design according to the polymeric material being extruded. Consequently, it will also be required to optimize the pumping consistency into the die [58,69,70].

The conveying screw will be responsible for the transportation and plastification process throughout the extrusion. This component can be categorized as being a barrier screw or a mixing screw.

An example of a commonly conveying screw present nowadays in extrusion processes is the barrier screw. The barrier screw is characterized by a single flighted design which promotes an effective material conveying within the feeding section. It also provides a good mixture as well as a uniform melt

throughout its length. Although its low capability to provide high mixture levels, compared to the mixing screw, its application doesn't affect the overall extrusion process neither its performance.

The barrier screw may encounter challenges when dealing with certain polymers, particularly those who production rate is governed by the screw. In such cases, this type of conveying screw cannot obtain higher rates due to its inability to melt all the material, requiring a better mixing for material homogenization[32,71]. Typically, these types of materials, such as PVC, PET, PP, PS, and others, present high melting points making them more complicated to extrude on a single screw extruder.

Several factors, including the extruder screw geometry, screw rotation speed and set temperature of the extruder, have been appointed in various studies as the responsible for both thermal homogeneity in the melt and overall process energy consumption [2,5].

When the production rate velocities present higher values, the polymeric material melt residence time is decreased, leading to a lower heat application from the band heaters to the polymeric material and consequently a lower mixture within the extruder. To obtain better mixture levels during the process, supplementary mixture screw sections, presented in Figure 3.1.a and Figure 3.1.b, are implemented in conjunction with the standard barrier screw [7,9,72].

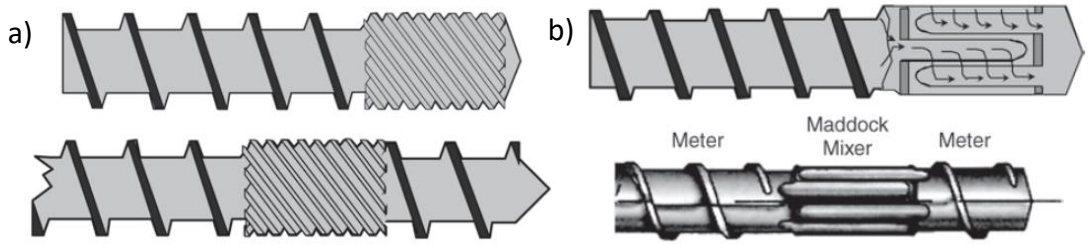

Figure 3.1 (a) Dulmage mixing section **(b)** Maddock mixer section [42]

The single flighted screw can be divided into three distinct stages, each playing an important role in the extrudate plastification process, namely the feeding, transition/compression and metering sections, Figure 3.2. The feeding stage is the responsible for conveying the granulated feed into the extruder to the transition area where the plastification process will initiate. The plastification process consists of the material compression against the heated barrel's inner walls, which with the conveying screw help will lower the energy required to fuse the material. Following the completion of the compression stage, the material progresses to the metering stage. Here it undergoes further blending, and, aided by the pressure generated from the other stages, the material flows into the die, where it takes the desired shape.

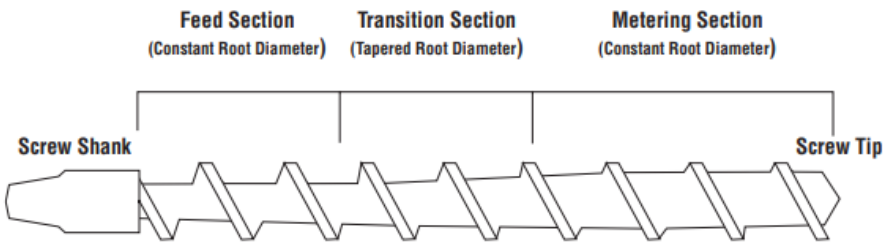

Figure 3.2 Single flighted screw with its three sections: feed, transition and metering [42]

The melting efficiency of the conveying screw can be improved by using multiple flights with an increased clearance in the transition area in order to break the solid bed formed within this phase. Despite this solution, mixing screws are normally implemented instead due to their lack of complexity when compared to these components. In contrast to barrier screws, where the flight performs the mixing and the extrudate conveying throughout the process, mixing screws lets the material be mixed in a specific zone where a supplementary mixing section is implemented within the conveying screw.

The primary objective of any mixing screw is to reduce non-uniformity composition. While mixing polymers, the highly viscous nature of the components to be mixed precludes the existence of turbulent eddy diffusion. However, due to the slow rate of polymeric diffusion, this effect can be neglected therefore becoming the bulk diffusion or convective mixing is the dominant distributive mixing mechanism in these processes [72]. Distributive mixing involves a material reconfiguration through the imposition of a deformation history involving shear, elongation and squeezing flows. The extent of mixing is therefore dependent on the total strain distribution and the ability of the mixer to reorient interfaces [29,73,74].

Revisiting the conveying screw, its capacity to uniformly melt the material, thereby achieving the desired properties as well as a stable output, is directly related to the conveying screw's dimensions in particular to its length to diameter ratio, also called L/D ratio [9], Figure 3.3.

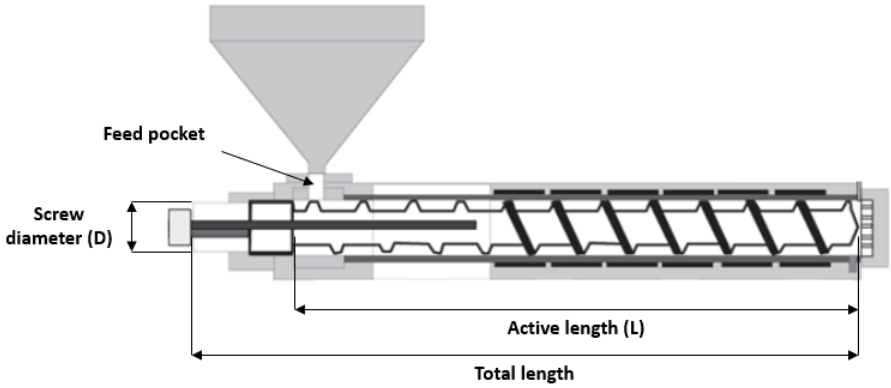

Figure 3.3 Extruder dimensions [42]

The L/D ratio can have different values, with each value offering distinct advantages according to its application. Higher L/D ratios result in greater melting and mixing capabilities, allowing the extruder to run at higher production rates. Conversely, shorter extruders require less physical space, lower initial implementation costs, reduced torque and consequently motors with less horsepower and size [43]. In order to choose its value, it is necessary to know: the type of material being extruded, as it directly affects the amount of energy required to melt it; the space where the equipment will be installed, and the throughput desired for the extrusion process. Some typical L/D ratios for extruders are: 18:1, 20:1, 24:1, 30:1, 36:1, and 40:1 [43]. However different ratios are possible to manufacture if scaling dimensions are respected.

The conveying screw's diameter can be directly related to the extruder throughput, as can be seen in Figure 3.4, where higher screw diameters correspond to higher throughput of the equipment.

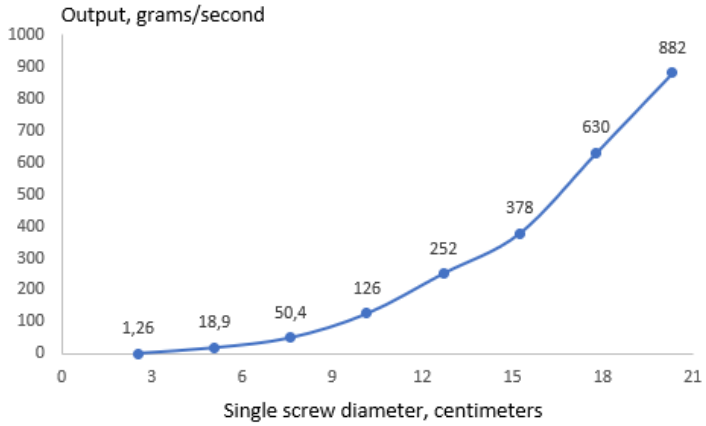

Figure 3.4 Typical Extruder output according to screw conveying diameter (D) Adapted from [42]

After knowing the L/D ratio as well as the conveying screw's diameter, it is possible to calculate the screw active length dimension by applying Eq.3. Where (L) is the conveying screw's active length and (D) is the conveying screw's diameter.

$$L = \frac{L}{D} \times D \ \ [mm] \qquad (3)$$

By knowing the active length of the component, it is necessary to define the length of each stage where multiple transformation stages will occur. Depending on its design purpose, each conveying screws can present different section lengths. Usually, the feeding section tends to be the smallest stage of the process, as it intends to convey the material to the transition stage where the plastification process will start. Depending on the manufacturer, this stage can or cannot include the feed pocket as it doesn't provide any work into the extruder procedure.

The transition stage, also referred as compression stage, represents the crucial stage of the extrusion process since it is where all the solid material will be transformed into its molten state. The length of this stage can vary depending on the chosen L/D ratio and the specific material being extruded.

When applying a conveying screw in injection molding, a so-called zero-meter screw is applied. This screw consists in the transition stage prolongation into the metering stage reducing the temperature build-up on the material. This type of screw is used to reduce the viscous heat generation in the melt conveying zone of the extruder. Despite its ingenuity, the obvious drawback in its application is the adverse pressure generation capability by the screw. Also, an extension of the zero-meter screw is the zero-feed zero-meter screw which consists of a conveying screw with only a compression stage. This allows a gradual material compression, and it has been applied in diverse scenarios and shown to be successful in many materials, more specifically nylon [7].

The compression of the channel depth tends to widen the solid bed. However, material melting tends to reduce the width of this solid bed [7,9,43]. As a result, the compression stage shouldn't be conducted too rapidly as the melting can be insufficient and the solid can grow in width causing channel

plugging. This plugging not only results in output fluctuations but can also lead to wear and damage to the conveying screw.

To avoid plugging, the compression stage's minimum allowable length must be respected. If the compression ratio is known, it becomes possible to determine this length by following the graphic shown in Figure 3.5, where a relation between these two variables is demonstrated.

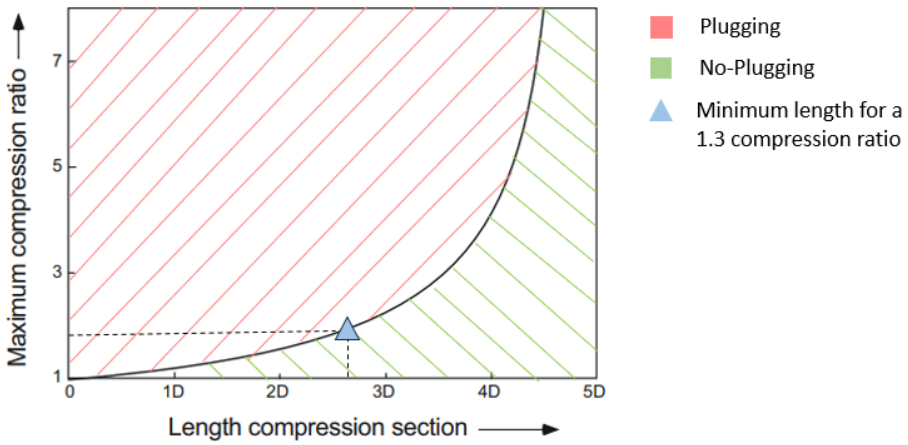

Figure 3.5 Minimum length of compression section versus compression ratio [7]

Also, it is possible to observe the compression stage's minimum allowable length according to a 1.3 compression ratio, which is about 2.5 diameters. Both of these values are set to be implemented in this project and will be looked at in better detail in future chapters.

The equipment's compression ratio can simply be calculated by performing the ratio between the depths of the feeding and metering channel, Eq.4. The channel depth is determined as the difference between the top of the screw flight and the screw root diameter. In the conveying screw, where a transition stage is used, this value will decrease along the screw's length.

$$\text{Compression ratio} = \frac{\text{Feeding channel depth}}{\text{Metering channel depth}} \quad (4)$$

The metering stage must also present a significant length since it's where the molten material's thermal homogeneity and mixing will occur. Additionally, this stage plays a crucial role in pumping the material into the die, thereby ensuring a consistent extrusion rate.

To force the material into the die in the metering stage, it is crucial to understand the plastic material's rheological properties. By examining the viscosity of materials, it is possible to establish a relationship between the imposed shear stress and the resulting shear rate, which allows for the determination of the material's resistance to flow, as described in Eq.5.

$$\eta = \frac{\text{Shear stress}}{\text{Shear rate}} = \frac{F/A}{V/h} = \frac{\tau}{\gamma} \quad [\text{N s/m}^2] \quad (5)$$

Where the shear stress (τ) is equal to the tangential force (F) divided by the surface's area (A) and the shear rate (γ) is equal to the velocity of the material (V) divided by the screw channel depth (h).

Within tubes or between two flat plates, the viscosity varies linearly from zero at its center axis to its maximum value at the wall.

On account of the non-Newtonian behaviour of the material (where viscosity is non constant), viscosity tends to decrease as the extrusion process progresses because the shear rate, which is referred to the rate at which a shearing deformation is applied to the material, increases. This phenomenon is characteristic of polymeric liquids and its often referred to as pseudo-plastic behaviour, as illustrated in Figure 3.6.

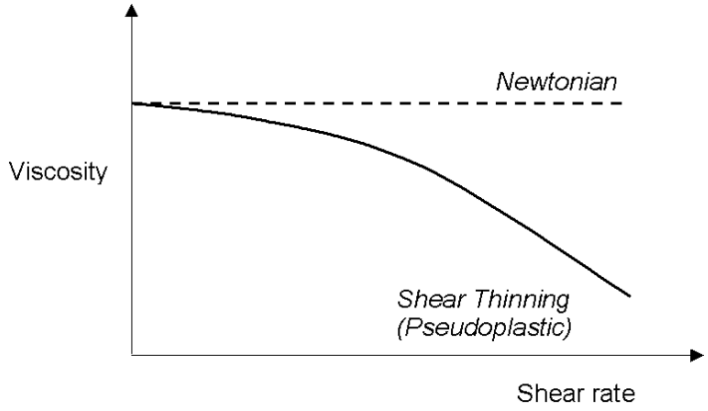

Figure 3.6 Newtonian and non-Newtonian material viscosity behaviour [7]

The extruder channel's shear rate can be calculated by applying Eq.6, where the screw channel depth (h), the conveying screw rotational speed (N) and the conveying screw's diameter (D) affect the shear rate value. This equation does not consider the clearance between the screw flight and the barrel as it is assumed that the material won't flow through there.

$$\gamma = \frac{\pi \times D \times N}{h} \quad [s^{-1}] \qquad (6)$$

The extruder throughput is determined by calculating the difference between the drag flow within the channel and the pressure flow generated by the friction between the material and the inner surface of the barrel and the screw root, Figure 3.7. In order to calculate the volumetric flow rate in the process, the simplified flow theory applied by Marschik [28] was considered, Figure 3.8. This theory applies the flat plates assumption, considering a rectangular screw channel of constant cross-section and infinite length. Also, by applying this theory it is possible to neglect the screw channel curvature and also consider the leakage between the top of the screw flight and the barrel to be inexistent. Another assumption made by this method is that the screw remains stationary while the barrel rotates around its axis at a velocity of $v_b = D_b \, \pi \, N$, as it eases the calculations needed for implementing this method [75]. This method allows for the theoretical calculation of the volumetric flow rate during the extrusion. The rate can be calculated using Eq.7, within the down-channel velocity ($v_{b,z}$) determined by Eq.8.

$$Q = v_{b,z} \times W \times h \quad [mm^3/s] \qquad (7)$$

$$v_{b,z} = \pi \times D \times N \times \cos\varphi \ \ [\text{mm/s}] \quad (8)$$

Where (Q) is the extruder throughput, (w) is the channel width, (h) is the channel depth, (D) is the screw diameter, (N) is the screw rotational speed and (φ) is the helix angle.

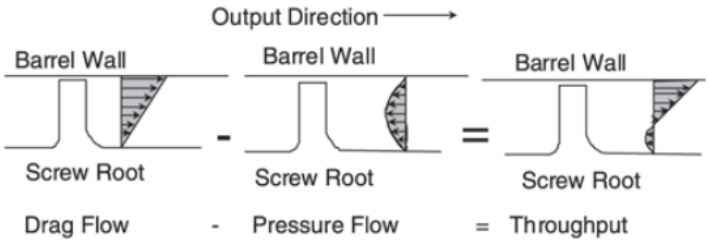

Figure 3.7 Extruder throughput calculation and representation [42]

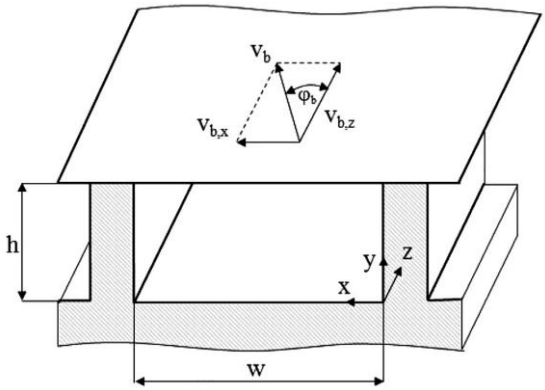

Figure 3.8 Simplified flow theory [27]

Despite the abundance of information available in the market regarding the screw channel dimensions, many operators who implement these components may not be informed of the latest studies on the subject. As a result, some active extruders do not operate at their full efficiency when compared with the situation where geometric conditions are considered.

The helix angle (φ) can be identified as the main responsible for the equipment's volumetric efficiency and it represents the angle formed between the screw flights and their transverse plane. Comparing to a combustion engine, where the volumetric efficiency represents the compressor efficiency when compressing gas, in the extrusion process this volumetric efficiency is referred to as the efficiency promoted by the conveying screw when compressing material in its molten state at a specific rate, being calculated by Eq.9 [7].

$$\frac{Q_{máx}}{Q_{ideal}} = 0.5\ (\cos\varphi)^2 \quad (9)$$

Unlike other efficiency variables, the volumetric efficiency has a maximum limit of 50%. Note that the maximum value does not represent the optimum condition. In fact, a 0° helix angle is not ideal

as it doesn't facilitate the proper conveying of material melt along the extruder's length and encourages the material's rotational movement within the barrel.

To calculate screw flight dimensions, it is necessary to analyse the stresses that occur during the extrusion process. The larger the screw flight, the greater the differential pressure submitted during the extruding process. Also, due to within the extruder, the screw flight's thickness will be dependable on the extrusion's shear forces, as is shown in Figure 3.9.

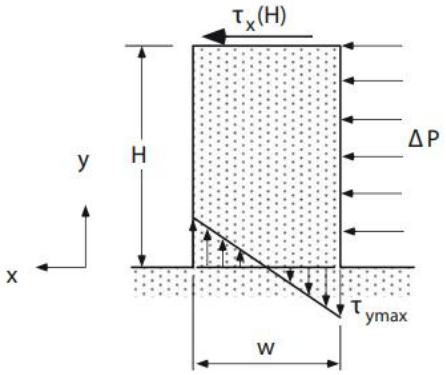

Figure 3.9 Stresses and their relationship with flight dimensions [7]

The feeding section is considered to be a critical area in which the combined forces present in the extrusion process are at their highest. According to the mechanical properties of a cylinder, the shear stress (τ) present in the outer surface can be calculated through Eq.10. This equation states that as the radius increases, the shear stress also increases.

$$\tau = \frac{Tr}{J} = \frac{2Tr}{\pi R^4} \quad [MPa] \qquad (10)$$

Where the shear stress (τ) depends on the product between the torque (T) and screw radial position (r) and its ratio with the screw's moment of inertia (J) which is dependable of the screw's outer radius (R).

To avoid compression screw failure due to torsional forces, a safety coefficient is applied, being then the allowable stress ($\tau_{allowable}$), the maximum value applied to this component. According to the allowable stress, it is possible to calculate, using Eq.11 [7], the maximum channel depth ($h_{máx}$) present in the screw's feeding section.

$$h_{máx} = \frac{1}{2}D - \left(\frac{2T}{\pi\tau_a}\right)^{\frac{1}{3}} \quad [mm] \qquad (11)$$

The channel width will have a significant role in determining the average melt film thickness during plasticization. A thinner melt film will improve heat conduction within the film, leading to increased viscous heat generation and improved melting performance [7]. To achieve this, multiple flights are usually incorporated into the conveying screw's design.

The correlations described above allow the examination of the following graphic presented in Figure 3.10, which illustrates the relation between the forces applied on the screw flights and the conveying screw's dimensions. The maximum height-to-flight width ratio can be considered as a slenderness ratio, indicating that values must be below the line in order to prevent the screw flight's failure. Consequently, it's then possible to conclude that the value obtained for the channel width of the extruder represents a minimum value that must be respected in order to the well-functioning of the equipment.

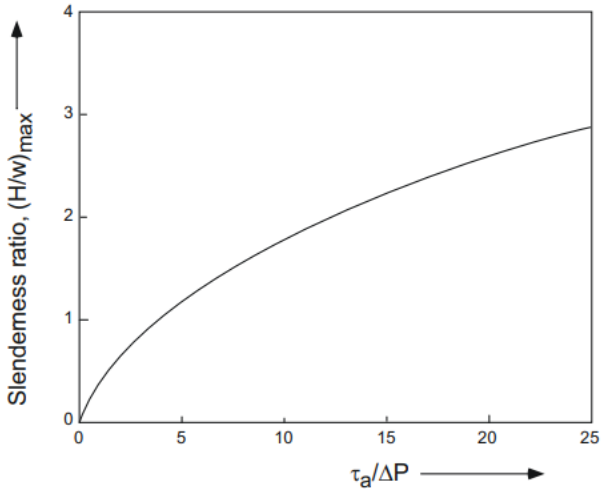

Figure 3.10 Relation between pressure and slenderness ratio [7]

Normally, the pressure generated in the flight clearance can be neglected since it does not reach significant pressure levels that could damage the component. The only situations in which these variables need to be considered are when there exists a metal-to-metal contact within the system. Consequently, it is normally recommended to avoid such scenarios when designing and implementing this type of equipment.

In addition to the geometric conditions, the screw's mechanical properties must ensure its proper functioning during the extrusion process. Therefore, the components must have good resistance to torsion and bending forces, and the channel flight must possess sufficient mechanical strength to withstand the pressure differential encountered along the extrusion process.

3.2 Extrusion barrel

Another crucial component for this project is the extruder barrel, which will host the compression screw in each section of the extrusion process. The barrel plays a multifaceted role, including containing and guiding the material along its transformation during the process. It is also responsible for the transmission of heat generated by the band heaters to the material. This is essential as the heat generated from the friction between the material and the barrel, as well as the material and the screw, may not be sufficient for the plastication process.

Due to its importance, this component must be manufactured with great precision, being its total out-of-alignment error, after proper matching, less than one half of the screw/barrel clearance to ensure optimal performance [9].

The barrel must be capable of handling the pressure generated at the beginning of the plastification process, which in industrial environments according to the literature, can reach up to values of 70 MPa [9]. The hoop stress in the extruder barrel can be calculated based on the values of pressure present during the extrusion process. To determine if the material chosen can withstand these pressure levels, the thin-walled assumption to a pressure vessel is applied, considering the wall thickness is no more than one-tenth of its radius. The equation for hoop stress (σ_θ), Eq.12, is given by an internal pressure (P) within a thin wall (t) in a cylindrical pressure vessel with a certain mean diameter ($D_m = \text{Outside diameter} - t$) is:

$$\sigma_\theta = \frac{P \cdot D_m}{2 \cdot t} \quad [\text{MPa}] \tag{12}$$

The allowable hoop stress is obtained by dividing the result obtained when applying Eq.12 by a safety coefficient factor of 2. Therefore, the material selected for manufacturing the extruder barrel must be capable to withstanding the allowable hoop stress to ensure its implementation into the equipment.

As nowadays, the majority of polymeric materials contain abrasive components meaning that the barrel must also be resistant to wear. When the wear factor is not considered the clearance between the screw flight and the inner barrel increases making it possible for the material to escape, consequently generating more back pressure and damaging the screw flight.

To prevent wear and promoting durability, barrels are usually fabricated from solid carbon steel or alternative materials such as stainless steel. Additionally, nitriding about 0.3 mm deep in the inner surface of the extruder barrel, hardens the surface improving wear resistance. However, nitriding is not particularly effective when abrasive materials are being extruded. For this reason, stainless steel barrels are implemented in smaller extruders, even though they may not provide as efficient heat transfer as solid carbon steel. Note that hardening stainless steel lessens the corrosive resistance of the material, so this should be taken into account [71].

As the pressure generated along the equipment will gradually increase due to the screw compression, it is possible to assume that the maximum pressure value will be reached immediately after the barrel and before the die zone. Consequently, a rupture disk is usually implemented for safety reasons as it functions as a safety valve that gets triggered when predetermined pressure levels are surpassed.

In order to admit the material to enter the equipment, a feed pocket is manufactured on the beginnings of the extruder barrel, Figure 3.11. The feed pocket, depending on the extruder, can have different configurations to allow the material to flow freely into the extruder with minimum restriction .

Figure 3.11 Feed pocket configurations [42]

Configuration A is the standard feed pocket design for pellets and powders. Configurations B and C are more commonly used in melt-fed extruders as the pellets applied in configuration C can wedge between the barrel and screw, causing the screw to deflect. The most common dimension value for the feed pocket's width is the value of the extruder diameter.

The barrels are equipped with band heaters along their length. These heaters will be responsible for generating the energy required for the plastification of the material during the extrusion process. However, since this energy is generated in the exterior zone of the extruder, it is essential to analyse how this energy will be transferred to the inside of the barrel through conduction. In other words, the heat flow within the process needs to be studied and understood.

The heat flow is defined as the movement of heat (energy) between two surfaces. In this case, the heat flow will be present between the barrel's outer surface and the inner surface of the band heaters both initially at room temperature, 25℃. To study this effect, it is also necessary to consider the material's heat conductivity (k) as it will affect the calculations and can also lead to an excessive production of energy, meaning more cost for the project. To calculate the heat conductivity of a 316 AISI Stainless Steel, with a metastable austenitic structure, it is necessary to apply Eq.13 [76].

$$\mathrm{k} = 9{,}2 + 0{,}0175\mathrm{T} + 2\mathrm{x}10^{-6}\mathrm{T}^2 \ [\ \mathrm{Wm^{-1}k^{-1}}\ ] \qquad (13)$$

This formula provides an accurate estimation of the thermal conductivity of a series 3 stainless steel for temperatures that do not exceed 1000 K [76]. Additionally, in order to calculate the amount of energy (Q_e) necessary to set the barrel with a specific mass (m) and a heat capacity coefficient (c_p) to a temperature (T), Eq.14 is utilized.

$$Q_e = \mathrm{m} \cdot \mathrm{c_p} \cdot \Delta\mathrm{T} \quad [\ \mathrm{J}\ ] \qquad (14)$$

The barrel of a single screw extruder is usually designed to accommodate a variety of materials without the need for its replacement. However, one of the main limitations of a single screw extruder is their low devolatilization capability compared to twin extruders. To solve this, some single screw extruders may incorporate vented zones. These vented zones consist of openings in the barrel which volatile materials can escape to the atmosphere not interfering in the final product quality.

While vented zones in single screw extruders offer advantages, they also come with a drawback, which is the need for an extended compression screw to accommodate the process requirements. These extended compression screws can reach lengths of 40 to 50 diameters, making them relatively long

components in the extrusion system. This happens because, in vented zones the material must present low pressure to prevent it from escaping through the ventilated openings. Consequently, in these zones, the compression screw presents a higher channel depth when compared with the previous section.

Following the decompression phase, the material must be recompressed to ensure uniform temperature and mixing. An example of a single vented extruder may be seen in Figure 3.12.

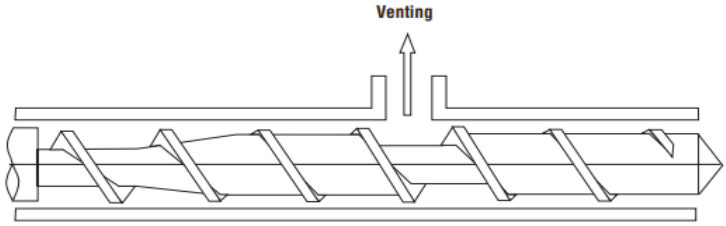

Figure 3.12 Single vented extruder [9]

According to the factors presented above, this type of extrusion barrel goes against the compression screw visualized in the previous chapter, as it involves a more complex manufacturing to its conception. The required length needed from the compression screw would also be problematic as it was more suitable to produce deflection and buckling issues when functioning. Also due to the space that it requires, its conception is not feasible and for this reason, despite its implications on the final product quality, this type of barrel will not be followed in this project.

Another type of barrels used in single screw extruders is the grooved barrel. These barrels feature a grooved section in the feeding stage to improve the feeding characteristics of the system. The grooved section usually has 3 to 4 screw diameters in length and tapers as it progresses through the barrel's feed stage, Figure 3.13.

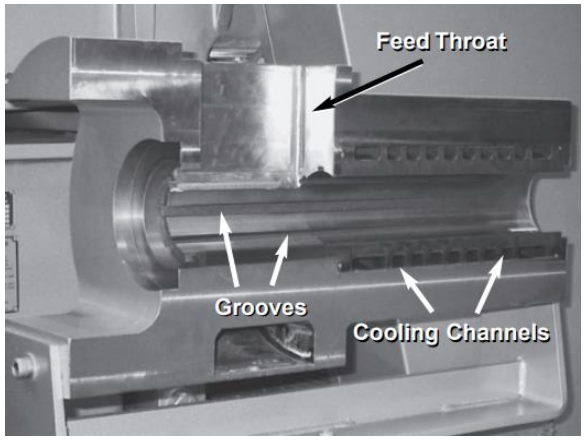

Figure 3.13 Grooved barrel in the feeding section [42]

As shown in Figure 3.13 above , these grooved zones are accompanied by cooling channels. Introducing grooved zones increases the friction between the pellets and the barrel's inner surface, leading to the temperature in the feeding section to increase drastically. Consequently, the implementation of water cooling system is necessary. The grooves shown above are orientated axially, but can also be helical, spiraling around the feed section.

Upon the introduction of these grooved barrels, the increased friction between the pellets and the barrel, leads to an increase in throughput. This is due to the fact that the material needs less residence time to melt and to be uniformly mixed. Despite its benefits, when implementing these components, it becomes necessary to produce three changes in the project [71]:

- Implementing an excellent feed throat cooling to dissipate the frictional heat generated and the capability of handling high pressures in the grooved zone
- Granting a good insulative barrier between the barrel and the feed section
- Designing a screw with a lower compression ratio to handle the increased throughput rate

The utilization of these barrels leads to an increased power consumption, approximately 10% [9]. Nevertheless, the output of the extruders that contain this component becomes less dependent on the back pressure generated by the breaker plate as the peak pressure is now generated at the end zone of the grooved section.

Despite its benefits, the implementation of this type of component would require more cost as more complex machinery within the project, not to mention the need to implement a water cooling system. For these reasons, the grooved barrels will not be incorporated into this project.

3.3 Extrusion die

The primary function of the die is to shape the molten plastic material as it exits the extruder into a desired cross-sectional shape. Predicting the required die profile to achieve the desired product dimensions is a highly intricate task which requires detailed knowledge of material characteristics, flow and heat transfer phenomena, as well as it requires extensive experience with extrusion processing. Given its complexity, the design and optimization of dies involves powerful computation techniques and modeling of complex flow and heat transfer processes, before, within, and after the die [77].

An ideal extrusion die would feature a passageway that provides [78,79]:

- Melt flow balance by providing a more uniform exit velocity across the entire die exit.
- Minimal pressure drop when achieving this flow balance.
- Streamline the flow to avoid abrupt changes in the flow passage that may cause stagnation areas. Stagnated flow may lead to thermal degradation of the plastic melt as the melt is exposed to high heats for long periods.

Despite the efforts to design an extrusion die, two material properties of molten plastics have a great impact on the extrusion process [58]: shear thinning and viscoelastic behaviour. Shear thinning behaviour refers to the capability of the molten material to become less viscous as they are sheared. This property causes the volumetric flow to be highly sensitive to the extrusion die design. While viscoelastic behaviour will be responsible for causing the “die swell” effect when exiting the extrusion die.

The "die swell" effect, also referred as the Barus effect, occurs when the viscoelastic fluids, such as polymer melts, are extruded with a larger diameter than the extruder exiting diameter [31]. This effect depends upon fundamental properties of the polymer such as the molecular weight and its distribution as well as on the flow conditions such as the shear rate, shear stress, L/D ratio of the die and melt temperature [31]. Its ratio (S) can be measured by applying Eq.15 in order to change the process variables to better approximate the extrudate diameter (d_e) to the extruder exiting diameter (D_e).

The ideal value for this ratio is one, indicating that both diameters coincide and die swell does not occur. However, as this value increases compared to its ideal, die swell becomes more significant in the process, requiring adjustments on the process variables.

$$S = \frac{d_e}{D_e} \quad (15)$$

To calculate the shear rate and the shear stress of an extrusion die, simplified approximations were employed. Therefore, the apparent shear rate ($\dot{\gamma}_{w,a}$) and apparent shear stress ($\dot{\tau}_{w,a}$) can be calculated using Eq.16 and Eq.17, respectively.

$$\dot{\gamma}_{w,a} = \frac{4Q}{\pi {R_e}^3} \quad [s^{-1}] \quad (16)$$

$$\dot{\tau}_{w,a} = \frac{PR_e}{2L_e} \quad [MPa] \quad (17)$$

Where (Q) represents the flow rate, (R_e) represents the die's exiting radius, (P) is the load in which the extrusion die is submitted to and (L_e) is the die's length.

Because of the non-Newtonian characteristics of polymeric materials when in their molten state (where they behave as pseudoplastic fluids as previously discussed), there isn't a direct relationship between pressure and flow that can be described by a single number. Consequently, a wide flow of testing conditions is required, as illustrated in Figure 3.14.

Using this type of plots allows the determination of the viscosity of the molten polymeric material when passing the extrusion die by calculating the slope of the flow curve. Flow curves are employed because the equations used to describe the flow behaviour of pseudoplastic fluids can be imprecise. Log-log plots are generally used to easily read the curves over several ranges of shear rate [9].

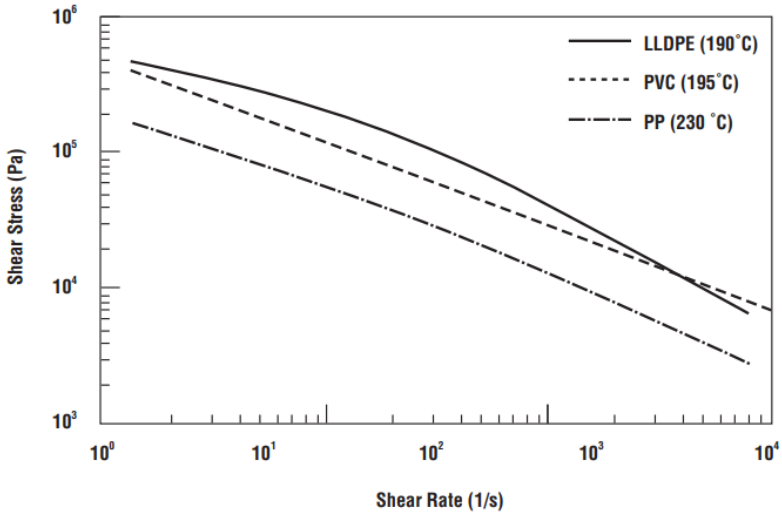

Figure 3.15 Viscosity curves for some polymeric materials [9]

As mentioned before, the extrusion process filament is shaped when the molten material converges with the cast material in the end zone of the extruder. Normally, the extrusion die is followed by a breaker plate, Figure 3.15.a and Figure 3.15.b. This component provides a better thermal homogeneity in the polymer melt and counteracts the rotary motion acquired by the material in the previous stage due to the screw's rotation, forcing it to flow in a direction perpendicular to its cross section.

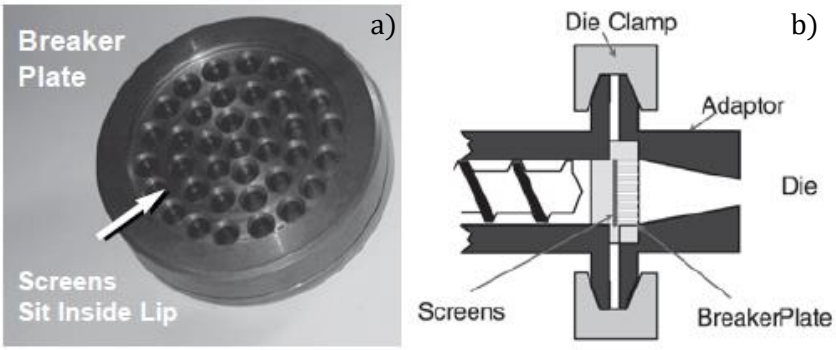

Figure 3.14 Breaker plate (a) and its implementation (b) [42]

As it is possible to see in the figure above, screens are also implemented before the breaker plate, serving as filters in the process. They contribute to a higher thermal homogeneity compared to using the breaker plate alone. However, the adding of these components into the extruder, leads to high levels of pressure at the extruder head causing a reduction in extrusion throughput.

In conclusion, a poorly designed die can lead to increased pressure at the metering section, promoting extruder stalling, as the required energy for its operation might not be obtained from the components installed in the equipment. Such a design can also cause screw wear and excessive heat buildup in the end zone of the extruder [9].

4

COMPONENT DESIGN AND MANUFACTURING

Based on the information presented in previous chapters, it can be deduced that the heat necessary to plasticize the material, is obtained from two sources: firstly, through the heat generated by the heat banders, and secondly, through the heat generated by the friction resulting from the rotation of the conveying screw. To obtain high extrusion rates (suitable for industry) most of the heat is generated by friction as heat transfer through the resistances is quite inefficient and time-consuming. It is for this reason that spindles typically have a large L/D ratio, which allows, on the one hand, a longer residence time for the material and greater heat generated by friction since the same material has to travel a longer length. As the conveying screw presents much importance in the extrusion process, its design is a critical part of performance of the remaining components during the process. The implementation of dimensional and geometrical tolerances are highly requested in big chain production sectors, as even slight modifications to their values may significantly affect project costs as well as the viability of the component when being used. These tolerances are highly dependable upon the machinery being used for component's manufacturing. Therefore, an effective design should be compatible with the existing machinery, minimizing project costs while meeting the requirement component specifications.

Therefore, this chapter cares to explain these component's design with the support of SolidWorks 3D modeling, also providing a comprehensive overview for the decisions taken along this stage as well as offering a brief description of the manufacturing process conducted. Additionally, the dimensional and geometrical tolerances implemented in this project are presented and explained throughout this chapter.

4.1 Conveying screw design

Extruders are typically sold according to screw or barrel dimensions [43]. Figure 3.4 provides guidance for choosing the extruder screw's diameter considering the desired extruder throughput. The extruder throughput wanted for this project, is significantly lower compared to those presented in

industrial environments. Consequently, the decision was made to opt for the lowest extruder throughput possible which equates to a conveying screw with 25 mm of diameter in this case.

The active length of the conveying screw is directly related with the extruder diameter and the length-to-diameter ratio (L/D). This ratio has an important role in determining the residence time of the material within the extruder, which is essential to its melting and thermal homogenisation.

To obtain the high levels of extruder throughput presented in industrial environments, the majority of heat must be generated by friction, as the heat energy supplied by the band heaters is inefficient and time-consuming. Therefore, the conveying screws typically present high levels of L/D ratios which allows for a higher material residence time as well as a higher heat generated from friction to be absorbed as the material travels a greater length. However, the extruder throughput desired for this equipment lower L/D ratios will be applied. Meaning, therefore, that the main heat source in the extruder system will be the heat banders.

Therefore, the extruder has 25 mm of diameter with a corresponding L/D ratio of 14:1. Resulting in an active length equal to 350 mm, having a total length of 420 mm, Figure 4.1.

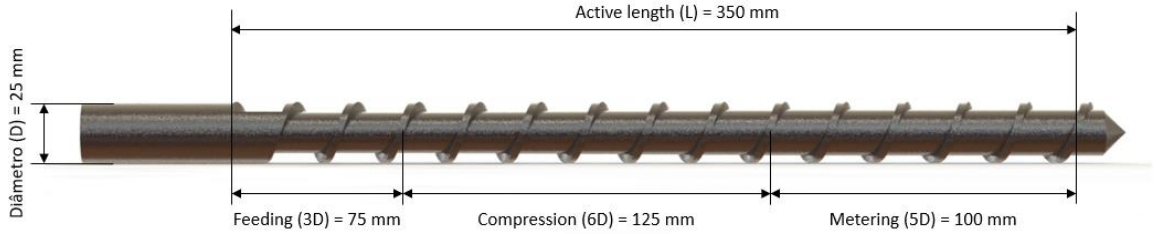

Figure 4.1 Conveying screw (L/D=14:1) and its dimensions

Based on Eq.10, the highest shear stress occurs at the top of the screw flight (r of 12.5 mm). Utilizing a stepper motor capable of applying a momentum, T of $100\ \mathrm{N \cdot m}$, and considering a safety coefficient of n=2, the material and the screw flight must withstand shear stress values, τ_a of 16.3 MPa.

With a differential pressure ΔP of 70 MPa inside of the extruder during the extrusion process, it is important to note that this assumption is made considering that the designed extruder will support lower pressures, ensuring safety. Using the allowable stress value and differential pressure ratio, for a $\tau_a/\Delta P$ of 0.23, the maximum slenderness ratio based on Figure 3.10 is $(h/w)_{máx}$ of approximately 0.23. According to the values presented above, the channel depth and channel width will be assumed to be 4 mm and 22 mm, respectively.

The conveying screw is divided into three stages, each responsible for fulfilling a specific part of the extrusion process. Therefore, each one of these stages has its specific length based on the time the material needs to spend in it. The feeding zone, as sole purpose is to convey the material to the transition zone in order to start the plastication process, does not require high lengths compared to the transition or metering zone. In this project, the feeding zone has a designated length of 75 mm (3D).

The compression ratio is required when choosing the compression stage length. As this compression ratio is chosen according to the dimensions of the extruder, bigger extruders present bigger compressing ratios [9,72]. Consequently, the compression ratio will have to go according to the L/D ratio. Industrial conveying screws, with higher diameters, are usually between 20D and 30D long with a feed channel depth normally up to 0.10D–0.30D, with a corresponding compression ratio comprehend between 2:1 and 4:1 [43]. For smaller extruders, these values can be scaled down accordingly and, in some cases, the extrusion can be performed even without compression ratio, as long as the final conditions of the process, including extruder throughput and final product quality, are not affected.

By applying a 1.3:1 compression ratio a more simplified design is followed as, by applying Eq.4, it is possible to know that the channel depth at the metering section is set to be $h = 3$ mm.

According to Figure 3.5, a 1.3:1 compression ratio requires a minimum compression stage length between 50-75 mm (2D-3D), as to ensure that all the solid polymeric material was melted before entering in the metering stage. However, implementing a longer compression stage can provide both safety and versatility for extruding different materials. Therefore, in this project, the compression stage is set to have 150 mm (6D) acting as a project safety measure. Additionally, having more screw flights can enhance the mixing and heating capabilities [7,43], eliminating the need for mixing zones and making the single barrier conveying screw the most suitable type of screw for this project.

The remaining conveying screw's length, 125 mm (5D), will be designated to the metering section. This design enables adaptability without significant design changes, allowing for flexibility in future projects to adjust the lengths of these sections as needed to optimize the process.

The shear rate caused by the conveying screw's rotation, $N = 5$ rpm, during the extrusion process, according to Eq.6, is set as $\gamma = 98.25\ s^{-1}$.

The conveying screw volumetric flow capability is calculated according to Eq.7 and Eq.8 which is highly dependable on the helix angle. The helix angle is set in this project, as recommended in the literature for a pitch value similar to the screw diameter (25 mm), as φ=17.66° providing a standard volumetric efficiency of 45.4%, according to Eq.9. Therefore, the down channel velocity for a conveying

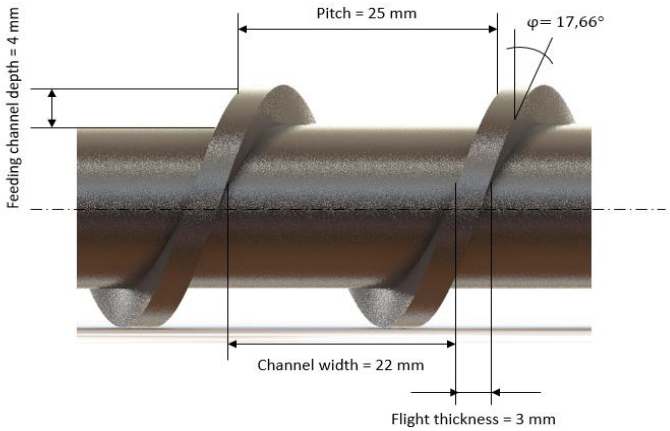

Figure 4.2 Feeding section channel dimensions

screw with a rotational speed of $N = 5$ rpm is $v_{b,z} = 6{,}2$ mm/s, meaning an extruder throughput of $Q = 411\ mm^3/s$. A representation of the feeding section channel can be seen in Figure 4.2.

A summary of all of the information given above is presented in Table 4.1.

Choosing the right material for the conveying screw is vital to ensure its durability and performance, especially considering the adhesive wear caused by metal-to-metal contact. Using the AISI 316 stainless steel bar for both the screw (25 mm) and the barrel (50 mm) is a prudent choice to minimize wear and maintain the equipment's integrity. The material properties according to its datasheet can be seen in

Table **4.2**.

Table 4.1 Variables of the conveying screw

Variables	**Value**
L/D ratio	14:1
Compression ratio	1.3:1
Diameter	25 mm
Active Length	350 mm
Pitch	25 mm
Feeding channel depth	4 mm
Metering channel depth	3 mm
Feeding zone length	3 D
Transition zone length	6 D
Metering zone length	5 D

Table 4.2 Datasheet AISI 316 [81]

Characteristic	**Value**
Designation (ISO)	4401-316-00-l X5CrNiMo17-12-2
Yield Stress (MPa)	> 220
Tensile Strength (MPa)	500-600
Density (kg/dm^3)	7.9
Elastic Modulus (GPa)	196
Thermal conductivity (W/m. K)	15
Expansion coefficient (K^{-1})	16.5 x 10^{-6} (at 200°C)
Specific heat (J/kg. K)	500

4.1.1 Conveying screw tolerances

The assembly of the conveying screw with the elastic coupler must provide a sufficiently rigid fixation while allowing for disassembly (slightly just adjustment), following the H7/j6 dimensional tolerance reference.

The elastic coupler, used for connecting the reduction gearbox to the conveying screw, bought at Juncor Lda. granting 25 mm of nominal diameter and a respective H7 dimensional tolerance, while the conveying screw has a 25 mm nominal diameter with a h9 dimensional tolerance. Both dimensions and their respective adjustment can be seen in Figure 4.3. Although this adjustment has higher clearance values compared to H7/j6 adjustment, the elastic coupler features a tightening system that helps to mitigate the extra clearance presented by this adjustment, enabling its application and significantly lowering project costs.

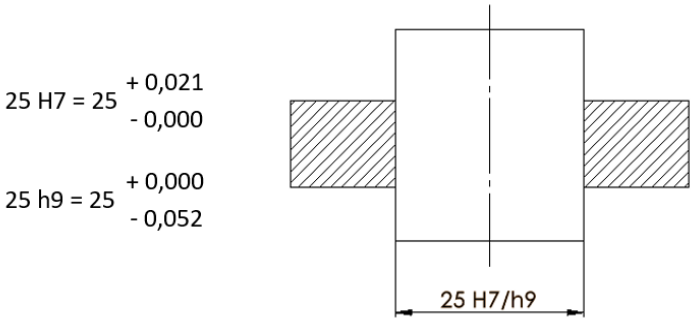

Figure 4.3 Dimensional adjustment between the elastic coupler and the conveying screw

Contrary to this adjustment, which only refers to dimensional tolerances, the assembly between the conveying screw and the multiple staged extrusion barrels involves both dimensional and geometrical tolerances. Additionally, the connections between the multiple staged extrusion and themselves are subjected to these tolerances, making it necessary its rigorous analyses in the subsection 4.2.2.

Focusing on the conveying screw mechanical drawing, the nominal dimensions and the respective functional dimensions for assembly with other components are specified, including the diameter (25 h9). In order to grant this dimensional tolerance throughout the conveying screw's length, it is, therefore, necessary to implement a cylindrical shape geometrical tolerance when manufacturing the components according to their revolution axis. This geometrical tolerance value will go according to the conveying screw's original length (2 m) and the manufacturing process used to produce the conveying screw, with the manufacturer being only responsible for specifying this tolerance in its mechanical drawing.

The conveying screw's keyseat is essential for facilitating the transmission of mechanical energy from the reduction gearbox to the component. According to technical drawing standards [80], this keyseat with a width of $w = 8$ mm, has a maximum deviation of 36 μm and the distance between the lower part of the keyseat and the end directly opposite is 20.9 mm, Figure 4.4.

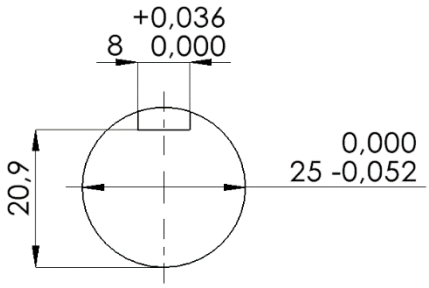

Figure 4.4 Conveying screw side view with the corresponding scatel

4.1.2 Conveying screw manufacturing

Due to the manufacturing complexity of the chosen conveying screw, a computer numerical control machine (CNC) was used, namely the HAAS Super Mini Mill 2, Figure 4.5 (a).

The G-code used in this machine was generated by a graphical computer aided design program (CAD), more precisely SolidCam. SolidCam is an extended version of the SolidWorks Cam extension, which is able to provide better tools to produce more complex designs as the conveying screw, due to its variable channel depth.

The HAAS Super Mini Mill 2 is a vertical milling type CNC capable of moving the spindle (or workpiece) for various locations which can go from 3 up to 6 axes. However, the HAAS Super Mini Mill 2 is only capable of moving its spindle in 3 axes. Therefore, a 4th axis was mounted into the equipment, Figure 4.5 (b), enables the rotational movement from the material along its revolution axis, thus allowing the milling to be carried out in this component. Consequently, to promote a better equipment support during the material revolution a counterpoint was implemented and fixed inside the CNC machine, Figure 4.5 (c).

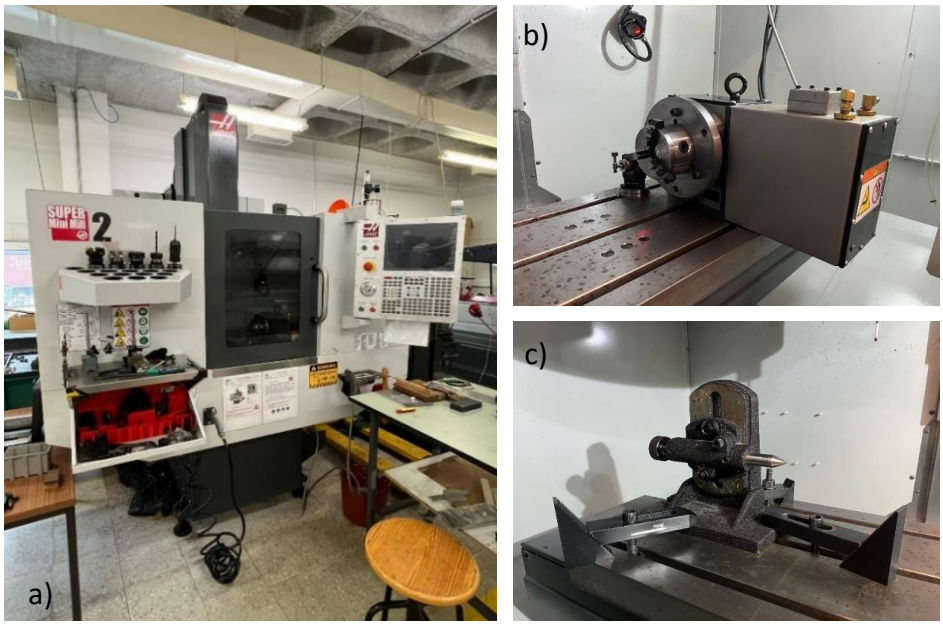

Figure 4.5 Equipment used to manufacture the conveying screw **(a)** Haas Super Mini Mill 2 **(b)** 4th axis device **(c)** Counterpoint

For the milling procedure to start, the raw material implemented at the CNC machine, needed to have add an extra amount of material (50 mm) which was later cut when the milling stage was concluded. Its purpose is to grant the fixation of the raw material onto the 4th axis device and also the counterpoint without having to affect the end product desired.

To ensure the alignment on the X-axis when setting up the equipment, a dial gauge with an associated deviation of $\Delta = 0.005$ mm was used during assembly, Figure 4.6, Dial gauges are used for checking flatness of surfaces, the parallelism of bars and rods and detecting small differences, if any, in linear measurement of identical objects. This equipment can also be used for measuring the concentricity of round objects.

Figure 4.6 Dial gauge with an associated deviation of $\Delta = 0.005\ mm$

The milling multi-axis feature of SolidCam was used to generate the G-code responsible for removing the unnecessary material from the 25 mm rolled bar with a 6 mm diameter flat end mill. Initially, the spindle enters the material as the 4 axes is activated when reaching the center plane, thus enabling material removal along the length of the conveying screw. After reaching the end of this process, the spindle was removed vertically leaving a smooth finish on the product. This process was repeated four times having each layer a 1 mm thickness.

Following the completion of the previous step, it was necessary to remove the excess material added to the front of the component to provide stability during the milling process in the CNC machine. During this material removal on the turning machine, a slight shortening of the transversal section was also performed, resulting in a cone with a 30° angle at the end of the conveying screw. This cone marks the end of the metering section and serves to prevent an abrupt pressure drop in that zone, facilitating the material flow through the die.

The final product can be seen in Figure 4.7, followed by a smooth imperfection originated during the manufacturing procedure.

Figure 4.7 Conveying Screw and flaw occurred during the manufacturing process

The imperfection observed represents a portion of the material that wasn't cut by the spindle during the manufacturing process, resulting in small zones where the material could potentially get trapped when in its viscoplastic form. To address this issue, the imperfection was resolved by using two files, one to remove the imperfection left during the component manufacturing and the other to smooth the material giving it a finish with reduced roughness.

The origin of this imperfection was concluded to be a bad pitch value implementation on the CNC machine code. The milling cutter has the ability to cut diverse types of materials by its high revolution. However, they are incapable of cutting through their own axis of revolution, resulting in a little distance between two consecutive phases where the milling cutter passes. To prevent this, it is not possible to implement its radius on its pitch value, Figure 4.8. When applying any value besides the cutter radius, the center zone where the tool did not cut will be targeted by the cutter teethes, leaving a smooth surface without any imperfections. In order to avoid this type of issues it is then necessary to implement a milling pitch between $]0;\ \text{Tool Diameter}\ [\ /\{\text{Tool Radius}\}$.

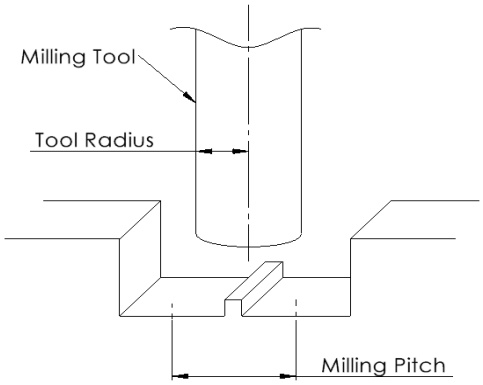

Figure 4.8 Milling cutter and milling pitch acceptable values

To complete the manufacturing stage of the conveying screw, a final milling stage was carried out on the side which was supported by the 4th axis to produce the keyseat.

4.2 Staged extrusion barrel

The barrel is another crucial part in the extrusion process because it confines the material against the conveying screw, enabling it to be melted and mixed during the extrusion process. This component must cover the active length of the conveying screw, in a way such as the material within the barrel won't flow in the opposite direction (leak), which could disrupt the extrusion process and damage the equipment. To achieve this, the barrel must follow a tight clearance between the top of the screw flight and the inner diameter of the barrel, typically around 0.01 times the screw diameter (0.25 mm). The manufacturing of this component must be carried out with the necessary precision to ensure it does not affect the extrusion process.

As previously mentioned, by implementing the same base material as the conveying screw for the extrusion barrel, it is possible to reduce adhesive wear, meaning that the extrusion barrel will be made from an AISI 316 stainless steel. According to Eq.12 the staged barrel's thickness considering an internal pressure ΔP of 70 MPa and a yield stress σ_{yield} of 220 MPa will need to be at least 0.25 mm however, for safety and production reasons the set thickness for these components will be of 2.5 mm.

Most barrels nowadays are manufactured using tubular extrusion, allowing the coverage of all process stages (feeding, transition and metering). In a first design analysis, the existing machinery was considered, being later observed that most of the machinery present wouldn't manufacture the barrel lengths necessary for this project (around 400 mm). However, this went according to one of the main objectives stated at the start of the project as it promoted the conception of a device able to be flexible and customized.

In spite of this circumstance, the decision was made to divide this component into three distinct sections, each aligning with a unique extrusion stage, Figure 4.9. Furthermore, provision was made for the possibility to change each one of these sections should a different procedure be implemented, all without having to change the overall of the entire equipment. This approach, however, leads to a reduction in the overall project cost.

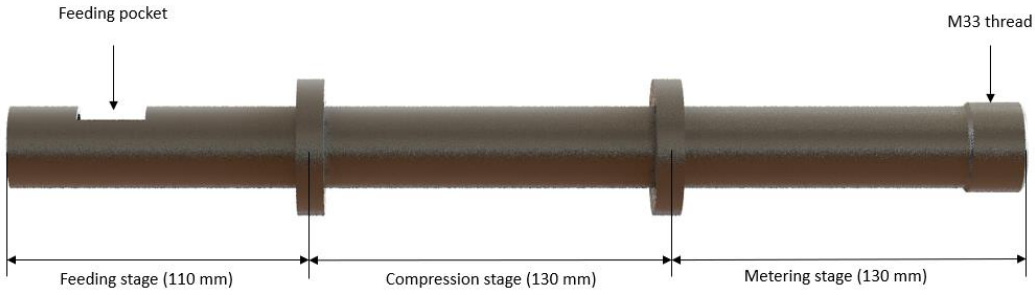

Figure 4.9 A three sectioned barrel according to the extrusion stage

Each of these sections, despite corresponding to a distinct conveying screw stage, exhibits unequal lengths. This discrepancy happens due to manufacturing limitations since the equipment does not

have the capability to manufacture components with such high lengths without having to compromise the tolerances associated with the manufacturing process. Consequently, a decision was made to maintain identical lengths for the compression and metering sections (130 mm) while assigning the remaining length to the feeding section (110 mm).

The implementation of various sections on the extrusion barrel, Figure 4.10, is anticipated to result in a more discrete temperature control for each of these sections. This is achieved by means of flanged coupling as the junctions are designed to function also as heat breakers. The objective of this feature is to ensure the coupling while enabling the desired temperature settings for each component of the equipment to be reached earlier than expected.

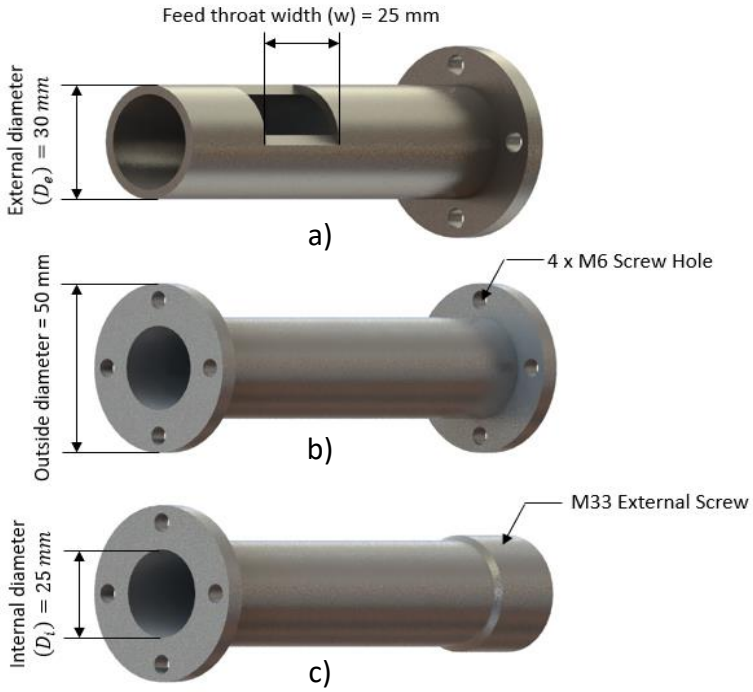

Figure 4.10 Sectioned barrel dimensions **(a)** Feeding **(b)** Compression **(c)** Metering

Normally, when heating an extrusion barrel, a uniform temperature is applied to all barrel stages. For instance, considering a temperature increase (ΔT) of $200℃$ for an extrusion barrel with a mass m of 0.64 kg and a specific heat c_p of $500\ J \cdot kg \cdot K^{-1}$, applying Eq.14 it is possible to see that approximately the required energy (Q_e) is around 64 kJ. When implementing a heat bander with 250 W of power to the system, the amount of time necessary to raise the temperature of the extrusion barrel by $200℃$ is around 4 min 16 s.

By dividing these sections is therefore possible to have more control over the temperature at which each section operates during the process. In this project, due to economic reasons and the absence of equipment optimization as a design variable, the compression stage ($\Delta T = 200℃$) and the metering stage ($\Delta T = 220℃$) will be subjected to temperature rising. On the other hand, the feeding stage will remain unheated throughout the process.

Applying the same procedure as presented above for the traditional extrusion barrel, it becomes evident that for a mass m of 0.318 kg and 0.295 kg, for the compression and the metering stages respectively, the energy required for achieving the determined temperature increases are 31.8 kJ and 32.45 kJ, respectively. By adding both of these amounts of energy, it is possible to visualize a total amount of energy of 64.25 kJ which is the same amount of energy required for the heating of a traditional extrusion barrel.

The time required to fulfill such requirement for the compression stage, equipped with two heat bands with 150 W each, thus totaling 300 W, is around 1 min 46 s. For the metering stage, equipped with a heat band of 250 W and another with 150 W, having therefore a total power supply of 400 W, the time needed is around 1 min 21 s. Consequently, the total time required for raising the temperature of the staged barrels is 1 min 46 s, given that both heating stages happen simultaneously. Additionally, a longer preheating time is recommended to ensure homogenization of the temperature at each stage.

Despite the benefits given by the flanged coupling, it was noticed that it could lead to an uneven expansion when providing heat to the material with the heat banders. This issue was then studied to ensure that no more problems were being added to the component manufacturing. It was concluded that no significant changes were observed by its implementation. The heat expansion of a ring was examined in order to study the variation of the staged barrel's diameter, Eq.18. This equation takes from the beginning that the component has a neglectable thickness (ring) providing a straightforward initial analysis of the process.

$$R_{final} = R_{initial} \cdot [1 + (\Delta T \cdot \alpha_l)] \quad [mm] \tag{18}$$

For instance, consider the metering stage, where the temperature is higher (ΔT) and takes greater values. The final inner radius (R_{final}) will depend on its initial inner radius ($R_{initial}$) as well as on the material linear expansion coefficient (α_l). Therefore, for an initial inner radius of 25 mm and a linear expansion coefficient of $16 \cdot 10^{-6}\ ℃^{-1}$, the final inner radius will be 25.088 mm. Therefore, it is important to choose the same material for both the screw and the barrel ensuring that the thermal expansion is similar in both components, maintaining the gap constant.

In the feeding stage barrel, a feed throat is implemented in order to feed the pellets into the equipment with minimum restrictions. This feed throat has a standard configuration, and its length is equal to the extruder's diameter (25 mm). This feature is placed at the 2nd diameter (50 mm) of the conveying screw for security reasons, allowing for material recovery in the event of any material leaks to the rear side of the conveying screw.

Lastly, an area threaded in the metering stage is observed. This section features a M33 thread with a 2 mm pitch in order to couple an adaptor device, facilitating the couple attachment of the die into the process, enabling the formation of the filament at the final extrusion stage.

4.2.1 Staged extrusion barrel tolerances

To ensure the assembly process for all staged barrels, it is essential to incorporate dimensional and geometrical tolerances. Geometrical tolerances serve to precisely define the form, orientation and position of elements and parts within a component. Furthermore, these tolerances can provide accuracy to the drawing, facilitate its interpretation and promote interchangeability with other components when followed by dimensional tolerances.

The most critical scenario during the assembly of these staged barrels is a result of their alignment along the axis, which could prevent the rotation of the conveying screw within the equipment. This misalignment can accumulate with the addition of each stage barrel. However, this issue can be mitigated by implementing a perpendicular geometrical tolerance for the contact surface between the transition and metering staged barrels. Additionally, a larger dimensional clearance in the feeding section can be implemented since it doesn't need tight tolerances like the remaining components, as its only purpose is the conveying of the material for the transition stage where the material will initiate its plastification process.

For the assembly between the conveying screw and the staged extrusion barrels, a rotational adjustment has been provided to facilitate faster movements, accommodate high temperature variations and enable the use of high viscosity lubricants. This adjustment utilizes a D9-h9 fit. In this configuration, the conveying screw has a h9 tolerance with a minimum deviation of -52 μm and a maximum deviation of 0 μm, while the inner hole of the staged barrel follows a standard dimensional tolerance with a minimum deviation of $+65$ μm and a maximum deviation of $+117$ μm.

Considering only dimensional tolerances there are two undesired scenarios to avoid. In one scenario the conveying screw may become unable to rotate, while in the other scenario, it rotates with excessive clearance causing material leakage. With this adjustment, the tolerance offers a clearance of $+65$ μm and $+169$ μm for these respective configurations.

To achieve a functional and well design staged extrusion barrel, these must be considered. Therefore, the feeding staged barrel will be designed with larger dimensional tolerances, as its only purpose is the conveying of solid material to the transition stage barrel. As a result, the 25 mm inner hole's dimensional tolerance will follow a C11 fit, considering the manufacturing process is turning. This fit will therefore allow a maximum deviation of $+240$ μm and a minimum deviation of $+110$ μm.

The transition staged barrel will play a crucial role in aligning both ends of the extrusion barrels, as a good assembly of these components with this barrel will ensure the proper functioning of the equipment. For this to happen, the barrel follows the D9/h9 adjustment as well as a perpendicular geometrical tolerance, as shown in Figure 4.11.

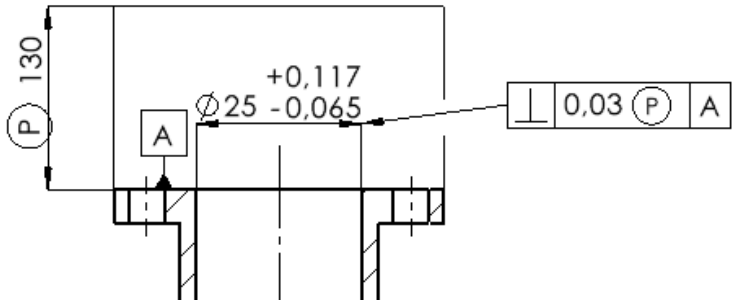

Figure 4.11 Tolerances representation in the transition staged barrel

To calculate the value for the perpendicular geometrical tolerance presented above, it is necessary to consider both components (transition and metering staged barrel) and consider their manufacturing process. Since their manufacturing process is the same, it can be assumed that both present the same difficulty in obtain both values of tolerance. According to Eq.19, their geometrical tolerance will be the ratio of the clearance minimum value divided by 2, therefore resulting in the 0.03 µm presented.

$$t_1 + t_2 = F_{mín} \quad [mm] \tag{19}$$

Where t_1 and t_2 denote the geometrical tolerances values employed in the assembly of the transition staged barrel and the conveying screw, respectively. $F_{mín}$ represents the minimum clearance value which is calculated by the maximum deviation of the conveying screw minus the minimum deviation of the transitions staged barrel when these components are assembled together. The same was applied to the metering stage barrel.

4.2.2 Extrusion staged barrel manufacturing

All these components, due to their rotational symmetry, were all manufactured on a lathe machine, namely the Optimum Mechanical Lathe D460 x 1500, Figure 4.12. As previously mentioned, this equipment was the responsible for the dimensioning of the extrusion staged barrel.

Figure 4.12 Optimum Mechanical Lathe D460 x 1500

All the extrusion staged barrels were manufactured from the same AISI 316 stainless steel rolled bar, which had a uniform length (L) of 500 mm. The order for manufacturing these components was chosen according to their complexity for manufacturing.

The initial component to be manufactured was the transition staged barrel. This component presents two flanged faces that cannot be realized in the same setup, being the change of the right cutting tool to a left cutting tool needed. Additionally, the length of 130 mm had an impact when opening the blind hole machining due to the increased vibrations.

Subsequently, the metering staged barrel was manufactured, following the same criteria of length (130 mm) and involving the threaded area, which requires a special cutting tool and a skilled operator to execute it precisely.

Finally, the feeding staged barrel was manufactured as it presented the shortest length of the three staged barrels (110 mm) and its manufacturing only required one setup.

The manufacturing process for all these components followed a consistent procedure. It commences with a facing stage to ensure a planar surface for connecting with other components and as a reference plane during the assembly process. Next, a turning stage was performed to reduce the initial external diameter to 30 mm, creating a 5 mm thicker flange coupling. Multiple stages of drilling were then held to create the 25 mm inner diameter. Afterward, a 24 mm drill was applied for the final diameter cutting.

Despite the similarities in the manufacturing procedure of these components, the metering staged barrel required the creation of its threaded area during its initial setup, to ensure a consistent setup and to avoid unwanted misalignment. This area was manufactured with an external thread tool. To produce

the M33 thread with a 2 mm pitch and a length of 25 mm, a 2 mm diameter reduction from the initial 33 mm of diameter was necessary.

Once all of the extrusion staged barrels had been concluded on the lathe machine, the milling machine was employed to open the feed throat of the feeding staged barrel. Finally, a drilling machine was utilized to create four M6 blind holes in each flanged coupling section.

4.3 Extrusion die

Following the manufacturing of the extrusion staged barrels, the focus shifts towards the production of the extrusion die and the corresponding adaptor, which are responsible for filament formation and coupling between the metering stage barrel and the die, respectively.

To guarantee a final temperature boost during the extrusion process, the material chosen for the adaptor and the die must withstand high temperatures before melting and respond rapidly to temperature changes. In particular, these materials should present a lower specific heat capacity and a higher thermal conductivity compared to the AISI 316 stainless steel rolled bar used in other components.

Brass is a suitable material choice, being an alloy of copper and zinc, typically with larger copper proportions, that can achieve multiple mechanical, chemical and electrical properties. Brass is known for its corrosion resistance and low friction properties. According to MatWeb, brass has the properties listed in Table 4.3.

Table 4.3 Properties of brass

Properties	**Value**
Yield Stress [MPa]	253
Ultimate Strength [MPa]	411
Density [kg/dm^3]	8.89
Elastic Modulus [GPa]	105
Thermal conductivity [W/m. K]	85.1
Specific heat [J/kg. K]	379

On account of the high thermal conductivity levels, which are visible in Table 4.3, it is possible to conclude that high quantities of energy (up to 85.1 W) will be transmitted through the material without having to be retained in it. This is an advantage since, as referred before, it leads to thermic modifications that may be necessary during the process, at the extrusion die, may occur at low operation times and without the unnecessary loss of material.

The specific heat capacity will also be a factor that has to be considered, as referred to before, since it will affect the time necessary to heat the material up to the desired temperature, which in this case will be around 240 ℃.

According to the values presented in previous chapters, the highest pressure levels will occur in the die zone, and it can reach values of around 70 MPa, when in industrial extruders. So, to design the component being inside the safety zone, this value of pressure was considered which leads us to admit the brass material as being sufficiently strong to withstand the pressure present during the process and therefore being an adequate material choice for this component.

As one of the objectives of this work is to make a customized extruder machine, it was decided to manufacture the die, Figure 4.13, as one separate component, making it possible to be changed according to the filament dimension needed.

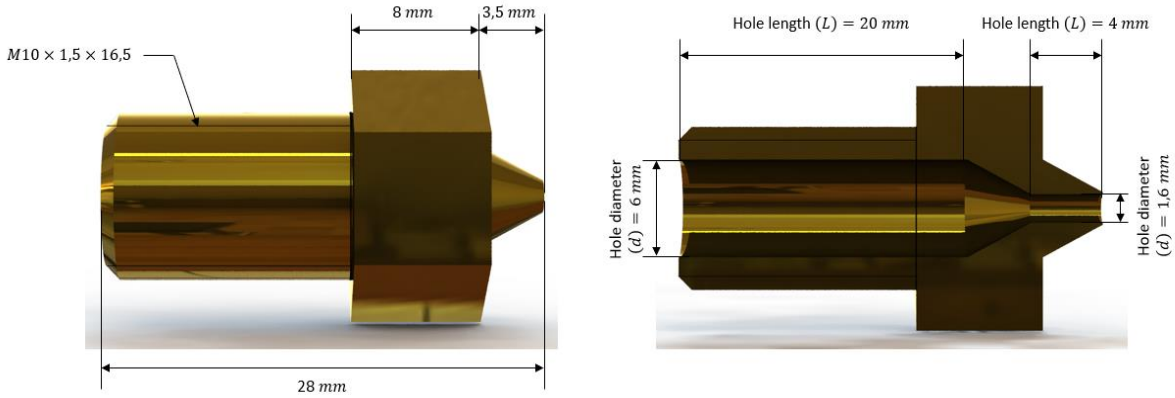

Figure 4.13 Die design

Considering this customization factor from the die, it was necessary to design it in a way that its implementation and removal were eased, not risking fracturing the component. To make it possible a 24 mm (between two parallel planar surfaces) hexagonal brass bar was used.

The die's total length, as seen above, is 28 mm. Of these, around 16.5 mm will be designated for a M10 external screw with a pitch value of 1.5 mm, in order to promote the connection between the adaptor and the die. The remaining length will be divided into a hexagonal section (8 mm), which eases the implementation of the component and by a conical section (3.5 mm) not affecting the material when leaving the extrusion process.

As the main function of the die is to distribute the melt uniformly through its cylindrical opening, depending on this orifice the filament may present several dimensions since this is not the only parameter that will be responsible for this formation process, since according to the extrusion velocity and also on the traction force applied by the puller (when implemented), this filament may have a greater dimension when comparing to the die hole.

In order to ease the die design process, the barus effect (die swell) was not considered in this stage. However, due to its relevance in the process and since it is an objective factor that indicates the quality of the final product, a final filament manual measurement is taken is carried out being applied the relation presented in Eq.15. By doing this a clear indication on how the variables that affect the extrusion process (temperature and screw rotational speed) is given and is, therefore, possible to obtain a better quality on the final product when leaving the equipment.

The die will be composed internally of a hole with a variable inner diameter. This hole starts having 6 mm of diameter (L = 20 mm) which will later be reduced to 1.6 mm (L = 4 mm), a bit lower to the expected value of the filament when leaving the extruder. This reduction in diameter will occur by a conical surface which presents the same inclination as the drill used to open the 6 mm hole in the die.

Having designed the extrusion die, it becomes therefore necessary to design the adaptor, since the implementation of the extrusion die in the equipment is highly dependable on this component. For this reason, the adaptor had to present on its surface the same characteristics presented by the die in order to guarantee their junction, and not to let the extrudate escape between the clearance left by a bad coupling of both components, Figure 4.14.

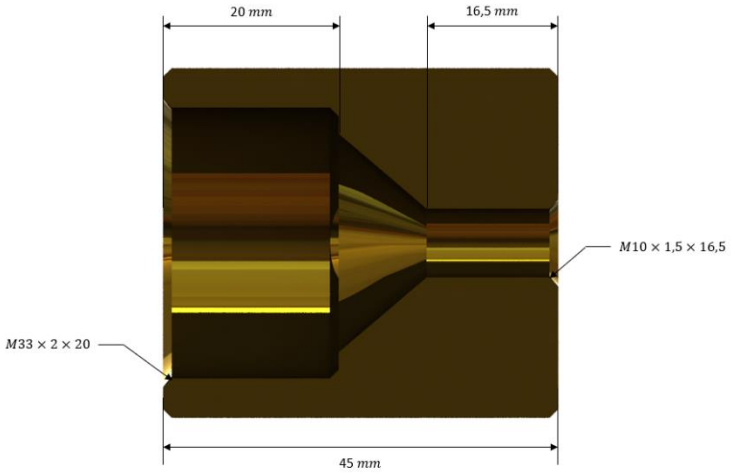

Figure 4.14 Adaptor and die

The adaptor has a total length of 45 mm and it is made from a round brass bar with 40 mm of diameter. Its design is very similar to the one presented at the extrusion die, where internally has a variable diameter hole. Although, despite its similarities, this component has two threaded areas in each of these sections in order to couple the designated components to it.

As it is possible to visualize in the Figure 4.14, this component starts by having a M33 internal screw area (L = 20 mm) with a pitch value of 2 mm in order to connect with the metering staged barrel with the corresponding external screw. Also, it has a M10 internal screw area (L = 16.5 mm) with a pitch value of 1.5 to connect with the extrusion die designed before.

The conical section visualized at this component will have the same inclination as the 25 mm drill used to open the first holes necessary to create the M33 threaded area.

Both of these components were manufactured at the mechanical lathe machine following the same procedures as the barrels. Firstly, a faced stage was done, and then a multiple staged drilling occurred with drills that presented different dimensions, as explained in the procedure made for the manufacturing of the staged barrels. A boring tool was then applied to remove the excess material remaining in the inner diameter of the adaptor, and finally, the threaded area was done with the help of an internal thread tool. The internal M10 thread area was done with a thread chaser.

For the die, the internal thread area was substituted by an external thread area. Also, as the conveying screw, a shortening of the transversal section was done in order to manufacture a cone with 30°. Both of the finished components can be seen in Figure 4.15.

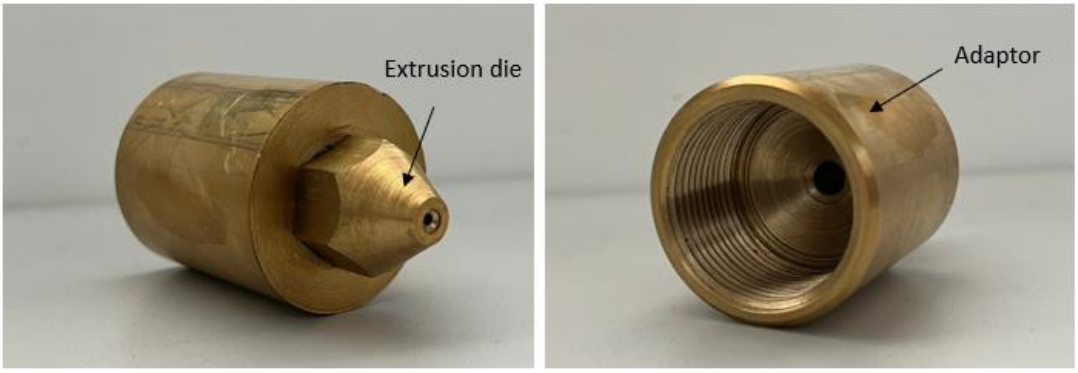

Figure 4.15 Extrusion die and adaptor

5

PROCESS CONTROL

As previously mentioned, the extrusion process is ruled by numerous interconnected variables. Some of the process variables that can be controlled during extrusion include screw speed and equipment temperatures, whereas die head pressure is primally dependent on factors like die geometry, melt viscosity and output rates, limiting the extent of control. However, by controlling equipment temperature and screw speed, it's possible to directly influence melt temperature, offering extreme advantages when optimizing process energy consumption and temperature homogenization of the viscous-elastic material being extruded [20].

Furthermore, the geometric properties of the extruder will also have an impact on these variables, such as die head pressure and melt temperatures. Nevertheless, once the extrusion process commences, these properties cannot be modified. Hence, the importance of early project planning, where this properties are studied and later engineered.

As to this, this project will primarily focus on two key variables: melt temperature and screw rotational speed. These variables are chosen due to their impact on other variables and for their ease of measurement and control.

5.1 Melt temperature control

To measure the melt temperature accurately, the implementation of a temperature control system is necessary. This system can take the form of either a feedback system (closed-loop system) or a non-feedback system (open-loop system). Normally, due to the nature of these systems, the system which provides feedback is usually implemented. In this setup, the information of the variable being measured, such as melt temperature, is transmitted to a control unit. This unit will then send a signal to the actuator that adjusts the control variable to stay as close as the desired value (setpoint) [58]. This closed loop feedback mechanism ensures control and regulation making it preferred for optimizing product quality.

There are two ways to limit variable readings within a certain level, the on-off method depicted in Figure 5.1, typically applied on automatic control systems, and the modular or continuous adjustment method.

The on-off method is highly dependable on setpoint values desired for the process. When temperature readings are below the setpoint value imposed, the power transmitted to the extruder is turned on at full capacity. Conversely, when readings are above the setpoint values imposed the power is completely shut off.

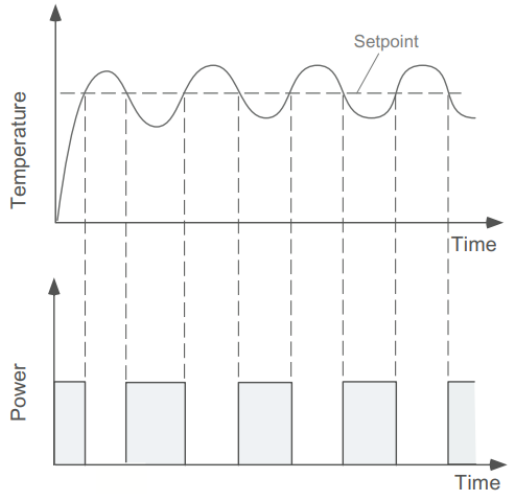

Figure 5.1 On-Off Temperature Control [9]

One of the problems when dealing with the extruder's heating and cooling, while applying the on-off method, is the significant thermal lag in these machines (delay between the time the controller asks for heat and when it actually receives it). This thermal lag can be quite significant, extending for several minutes long (e.g., 5 minutes for a 90 mm extruder), and tends to increase as the extruder's dimensions grow larger. One approach to avoid this lag is to position the sensor as close to the heater as possible. However, in polymer extrusion, the sensed temperature will be less representative as it primarily measures the heater's temperature rather than that of the polymer within the equipment [58].

When positioning the sensor as close to the heater as possible, the resulting temperature will be fluctuating around the setpoint, as its frequency is determined by the thermal lag of the machine. To solve this issue, an on-off differential is added to the controller function. This means that the temperature needs to exceed the setpoint by a certain amount (typically half the differential) before the output will be activated once again [58]. One type of controller that employs this approach is the Proportional-Integral-Derivative (PID).

A PID controller is an instrument used in industrial control applications. This controller uses a control loop feedback mechanism to regulate process variables such as temperature, flow, pressure, among others. These type of controllers are considered as being the most accurate and stable controllers on the market. Their main components can be grouped according to the following loop operations [81], as seen in Figure 5.2:

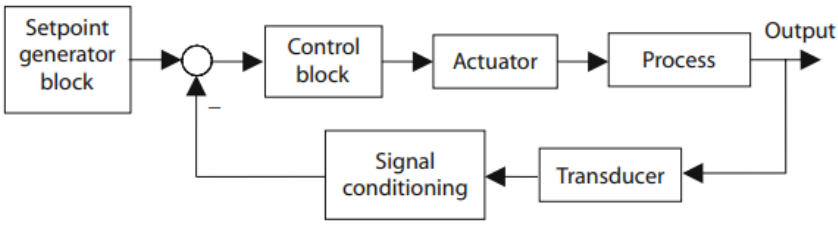

Figure 5.2 Components in a typical industrial control loop [79]

- **Process**: is the actual system where the variables are set to be controlled or regulated
- **Actuator**: is a processing unit where the material or power input is supplied to the process
- **Transducer and Signal conditioning**: this is where the measurement will occur during the process. The transducer will be the responsible for comprising a sensor to detect a physical property and will output a representation of this property in an electrical signal. Depending on the parameters set by the operator at the setpoint, this electrical signal will then take part in the process
- **Control block**: is the unit designed to create a stable closed-loop system and also achieve the requirements set by the operator to the equipment. its input is usually an error signal based on the difference between the actual value and the setpoint.

In this project, two PID controllers, specifically the BERUM REX-C100 controllers, have been implemented to regulate the melt temperature present in two specific stages of the process: the transition zone and the metering zone. The heat banders will not be covering the feeding section as this zone has to remain under the polymeric material's melting temperature, as referred to in previous chapters.

As to measure the melting temperature, a K type wall mounted thermocouple was positioned on top of the extruder. The K type thermocouples are made out of chromel-alumel, offering a sensitivity of approximately 41 $\mu V/℃$, being therefore suitable for application between $[-200\,℃\,;\,+1350\,℃]$ [34]. There are three types of arrangement for these types of thermocouples being only one of them is considered to be a non-invasive arrangement. While these thermocouples are quite straightforward to use and entail less maintenance, their measurements can be significantly affected by the barrel/die wall's set temperature. Additionally, they may not be able to capture melt temperature rapid variations due to their relatively slow response time, [53,82]. Therefore, it is important to exercise extra care when implementing these components into the extruder system.

After capturing temperature readings, the PID will emit an electrical signal to the band heaters. This signal will function to activate the electrical resistances, generating the heat supplied to the extruder. In order to know the amount of energy necessary to raise the temperature of a certain component to a specific temperature value, it is necessary to apply Eq.13.

Taking the example of the adaptor made of brass, with a specific heat capacity coefficient of $402\ Jkg^{-1}K^{-1}$, this indicates that raising the temperature of one kilogram of brass by 1 Kelvin (or

Celsius) would require 402 J of energy. Given that, the adaptor has a mass of 0.35 kg, raising its temperature from room temperature (25 ℃) to 230℃, would require a total of 28844 J of energy.

Performing the same calculations for transition and metering zones staged barrels, made from stainless steel as referred to in previous chapters, is a material with a specific heat capacity coefficient of $500\ \mathrm{Jkg^{-1}K^{-1}}$, as mentioned on its datasheet [83], it is possible to find that the transition stage with a mass of 0.318 kg would require 32595 J of energy to raise its temperature from 25℃ to 230℃. Similarly, the metering stage, with a mass of 0.295 kg, would require 30238 J of energy to fulfill the same temperature increase requirement as presented above.

To provide the energy requirements mentioned above, two types of heat banders were applied. The heat banders made of stainless steel are responsible for heating the staged barrels and can provide lower amounts of power, 150 W. On the other hand, the copper heat bander has a higher power output, offering 220 W, and it is responsible for heating the adaptor. Apart from their electrical properties, their dimensions are also different, being the copper heat band possible to incorporate on a 40 mm diameter piece, as the stainless-steel are only capable of incorporating 30 mm diameter components. The maximum operating temperature for the stainless-steel heat banders is between 300℃ and 400℃, and for the copper band heater, it is up to 500℃.

The datasheet from these components possibilities the current calculations as their respective resistance. The electrical power (P_e) is the rate at which electrical energy or current (I) is transferred through an electrical potential (U), Eq.20. By knowing the current passing through a component, it is then possible to calculate its resistance value by applying the Ohm's law, Eq.21.

$$\mathrm{P} = \mathrm{U} \times \mathrm{I}\ [\ \mathrm{W}\ ] \tag{20}$$

$$\mathrm{U} = R_i \times \mathrm{I}\ [\ \mathrm{V}\ ] \tag{21}$$

The stainless-steel band heaters will require an electrical current of approximately 0.68 A, meaning that its resistance value is approximately 323.7 Ω. In contrast, the brass band heater, which has a higher power rating, will require 1.14 A and presents a resistance value of 193.6 Ω.

Both of these band heaters require a 220 V AC power supply through their terminals. However, the PID controller is only capable of outputting DC (low voltage) signals. In this scenario, the most suitable component for the control of the AC power supply is the solid-state relay.

The solid-state relay is activated by a DC signal within the range of 3 and 32 V, and it is capable of switching currents up to 100 A using semiconductor devices such as thyristors and transistors. These components typically consist of three key elements: a sensor that responds to an appropriate input (control signal), an electronic switching device that switches power to the circuit and a coupling mechanism capable of enabling the control signal to switch without any mechanical parts whatsoever.

Although the solid-state relay and electro-mechanical relay share the fundamental feature of electrically isolating the low voltage input from the output responsible for switching and controlling a

circuit, electro-mechanical relays have a limited contact life cycle as well as slower switch speeds. Solid state relays have no such limitations. In fact, solid-state relays are best known for their greater lifespan, very low power consumption, silence and resistance to shocks as well as vibrations allowing high switch frequencies for very accurate adjustments. This project employs two solid-state relays, namely the FOFER solid-state relay. This really can hold up to 40 A while having 220 V through its terminals.

A summary of the melt temperature control system components as well as its corresponding electrical diagram can be seen in Table 5.1 and Figure 5.3, respectively.

Table 5.1 Melt temperature control system components list

Nº	Designation	Characteristics	Equipment
2	PID controller	• Power Supply: CA 110-240v • Deviation ± 2 °C • Temperature range: 0-400°C	
3	Stainless stell heat banders (150W)	• Maximum temperature: 300-400 °C • Input voltage: 220 V	
1	Copper band heater (220W)	• Input voltage: 220 V • Maximum temperature: 400°C	
2	K type wall-mounted thermocouple	• Sensor diameter: 4,5 mm • Temperature range: 0-400°C	
2	FOFER SSR	• Input voltage: DC 3-32v • Output voltage: 24-380 v AC • Output current: 40A	

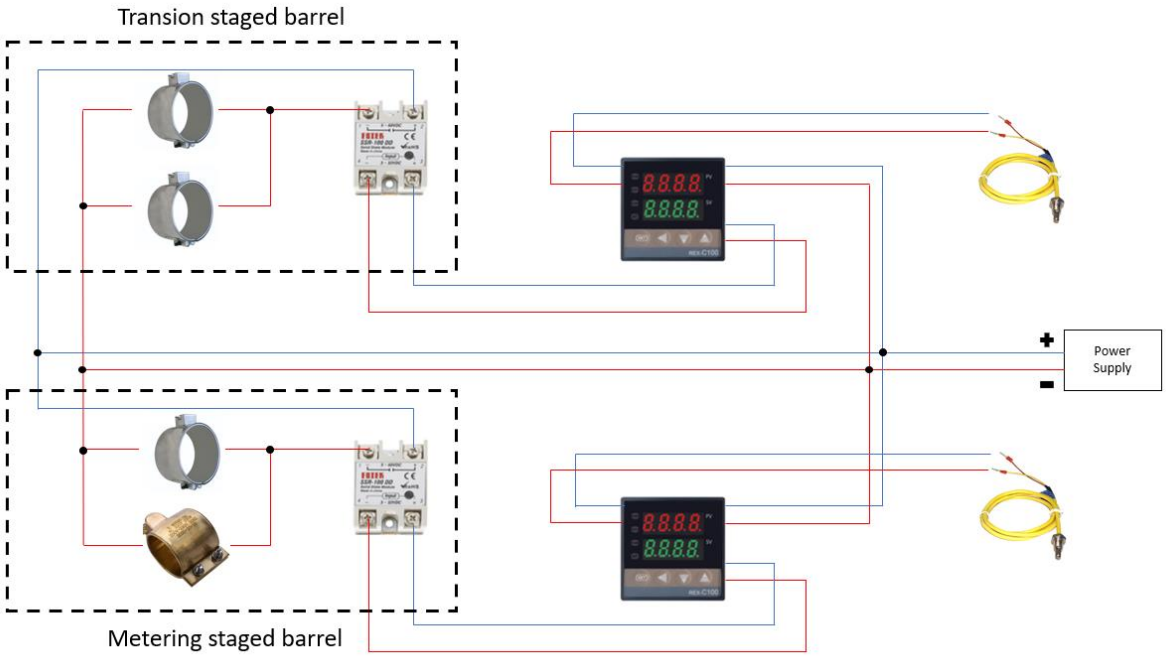

Figure 5.3 Measure control electrical diagram

It can be seen in the electrical diagram that each PID controller is responsible for controlling an extrusion stage. Both of these components will be connected to a SSR before being connected to the band heaters.

For the compression stage, the SSR will be coupled with two stainless steel band heaters, each requiring an electrical current of 0.68 A. Since they are connected in parallel, the SSR must provide a total current of around 1.36 A. Similarly, for the metering stage, as the copper band heater requires 1.14 A, the SSR must provide a total of current of around 1.82 A.

5.2 Screw rotational speed control

The screw's rotational speed is a crucial factor when determining process variables. This parameter, as previously referred, is directly related to polymer melt residence time, having therefore a great impact on thermal homogenization and throughput rate. Consequently, by accurately measuring and controlling the screw's rotational speed it is possible to boost end product quality while improving efficiency and effectiveness of the extrusion process.

In order to control the screw's rotational speed, a combination of components is implemented, visualized in Table 5.2. The electrical diagram of these components can be visualized in Figure 5.4. This setups allows for precise control and regulation of the extruder screw's speed during the extrusion process.

Table 5.2 Screw rotational speed control list of components

Nº	Designation	Characteristics	Equipment
1	Arduino UNO R3	• Input voltage: 7-12 V • Microcontroller: ATmega 328P	
1	Motor driver TB6600	• Input current: 0-5 A • Output current: 0.5-4 A • Micro Step: 1, 2/A, 2/B, 4, 8, 16, 32	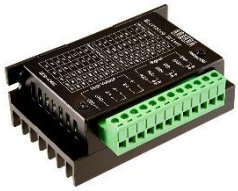
1	Astrosyn MY34HD3-8 Stepper motor	• Full step angle 1.8° • Holding Torque 8.5 Nm • Rated current: 9 A/Phase	
1	AC 24V Power Supply	• Output voltage minimum: 0 V • Output voltage maximum: 30 V • Output current minimum: 0 A • Output current maximum: 5 A	

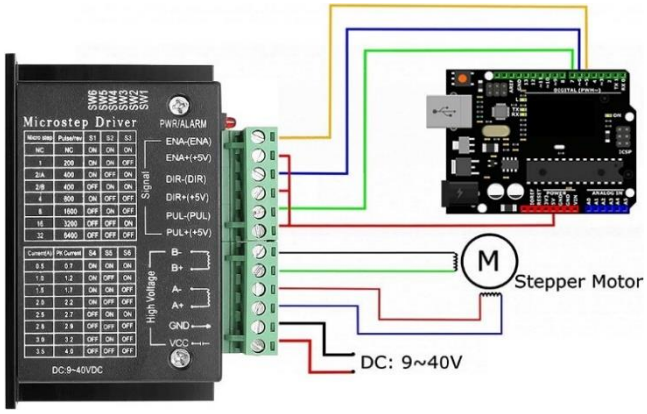

Figure 5.4 Screw's rotational speed electrical diagram

The stepper motor, as the name suggests, operates on the stepping principle. In essence, the motor completes its rotation by taking measured steps. This motor has four lead connections, meaning it has two coils within its design. Each of these coils receives pulses from the controller, which dictates the steps required to complete a rotation. To achieve a single revolution, 200 steps are needed given that the motor's step angle is 1.8°.

The stepper motor implemented in this work was the Astrosyn MY34HD3-8. These component was reused from a previous project therefore its datasheet was not obtainable, despite online research had taking place. The decision to proceed with the reuse of this component was primarily driven by budget constraints and the unavailability of suitable alternatives. In addition, this component performed a key role in the extrusion process, making it an irreplaceable component.

Choosing the Astrosyn MY34HD3-8 as a component for this project is therefore a good decision. To ensure accurate and up-to-date information about functional parameters of a more recent version of this component more recent datasheets were used, namely the datasheet from the Astrosyn MT343SP-1, Tabela 5.3. After parameters verification, a simple testing phase was conducted to ensure the capability of this component to be implemented into the extruder system, demonstrating successful outcomes.

As previously stated, this component will be in direct contact with the reduction gearbox before transmitting its energy to the conveying screw, enabling the extrusion process. However, to generate this energy, an energy supply is required. The necessary potential differential for this component to work is approximately 24 V therefore, an energy supply of 24 V was implemented.

As it is possible to visualize in Figure 5.4, to obtain the full potential of a stepper motor, a microcontroller like the Arduino Uno R3 can be implemented as a control interface. The Arduino offers a convenient platform to control stepper motors. It is capable of sending precise electrical pulses to the motor, causing it to move in well-defined steps. In this project, the implemented code, Figure 5.5, serves to define the number of steps per revolution. By only modifying rotations per minute (RPM) values

within the code, it is possible to obtain different rotational speed configurations according to the system's requirements.

Tabela 5.3 Astrosyn MT343SP-1 datasheet [84]

Specification	Value
Step angle	1.8 °
Step angle accuracy (%)	±5
Phase current (A)	9
Phase resistance (Ω)	0.2
Holding toque bipolar (Ncm)	850
Rotor Inertia (g.cm^2)	3785
Shaft configuration	Single
Number of lead connections	4

```
// Define variables and pins

const int steps_Pin = 5;    // executs a step
const int direcao_Pin = 2;  // defines a direction
const int en_Pin = 8;       // enables the motor
const int steps_volta = 200;

void setup() {

  pinMode(steps_Pin, OUTPUT);    // define output
  pinMode(direcao_Pin, OUTPUT);  // define output
  pinMode(en_Pin, OUTPUT);       // define output
  digitalWrite(en_Pin, LOW);     // enables motor in low
}

void loop() {

  int rpm = 60;  //motor rotations per minute

  // Calculate delay duration based on RPM
  int delayDuration = (60 * 1000000) / (2 * steps_volta * rpm);

  digitalWrite(direcao_Pin, HIGH);   // High rotates anti clockwise
  digitalWrite(steps_Pin, HIGH);
  delayMicroseconds(delayDuration);
  digitalWrite(steps_Pin, LOW);
  delayMicroseconds(delayDuration);
}
```

Figure 5.5 Arduino code to define number of steps per revolution

Due to the high power demands of the Astrosyn MY34HD3-8 stepper motor, a direct connection with Arduino microcontrollers is not possible. Therefore, to ensure their proper operation, a stepper motor driver should be implemented between these components.

The enable, pulse and direction pins of the respective stepper motor driver are connected to the Arduino pins. The enable pin serves to empower the driver module. The pulse pin is the step pin that controls the micro-stepping of the motor by pulse reception from the Arduino. Similarly, direction pins configures the rotation of the motor either clockwise or anticlockwise depending on its state.

6

COMPLEMENTARY COMPONENTS

In addition to the components discussed in the previous chapters, a variety of other components have been implemented to serve diverse purposes within the mechanical system.

To facilitate the reading of drawings and component identification, a coding system has been implemented. Below is an example of the second component of the first sub-group:

A01.01.02

To read this code, follow it from left to right, where the numbers correspond to:

- **A01 Project code:** This letter will be the number of the project. In case a second solution for this project was performed this would get the "A02" nomination.
- **01 Sub-group code:** The number will indicate which sub-group the component belong. Components without a specific group are considered as belonging to group "00".
- **02 Component code:** The number that corresponds to the component.

This chapter will present these additional components and provide a brief explanation of their purposes as well as its design.

6.1 Feed hopper and adaptor

The extrusion process relies significantly on two components: the adaptor and the feed hopper. These components are responsible for seamlessly introducing granulated material into the equipment.

The adaptor assumes a critical function as it must present low thermal conductivity to prevent material preheating and ensure that the material doesn't enter on the equipment on a semi-viscoelastic state. By not implementing it, it would disrupt the extrusion process by causing the conveying screw to stall. However, since the flanged coupling developed in the extrusion staged barrels functions as heat sinks, and as no heat source is added to the feeding section, it is possible to assume that the heat transmission from the staged barrel will not pose a problem in this project.

Furthermore, a different approach from what typically is done in this case was pursued. It is possible to visualize the implementation of the feeding channel and the respective adaptor, both fabricated with ABS using a 3D printer, Figure 6.1, and can be readily identified in drawings A01.00.01 and A01.00.02.

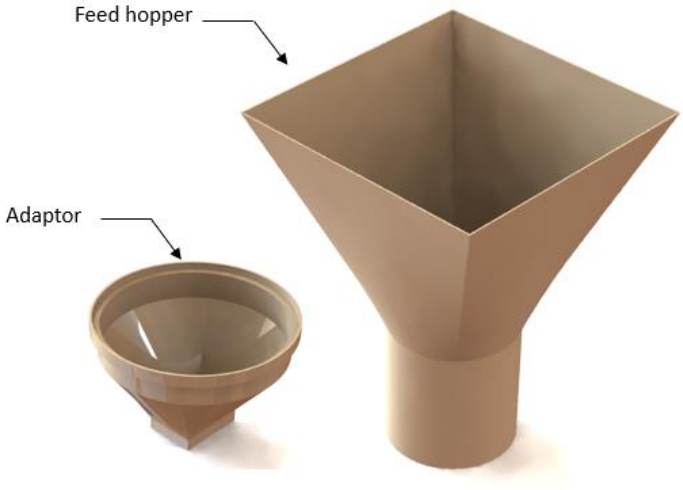

Figure 6.1 Adaptor and Feed hopper

6.2 Staged barrel support

The structural components, as their name indicates, are concerned with ensuring the structural stability of the equipment. These components are therefore the responsible for restricting the extruder's movement in all its six degrees of freedom, including three related to the axial movement and three related to their respective rotation. To obtain this type of movement restriction, two metallic components were developed resembling bearing devices, Figure 6.2.

Notice that while the lower parts are similar, the upper parts present distinct characteristics from each other. This differentiation is related to specific types of movement restrictions that each one of these components enforces during the process. Both of these components restrict the X-axis movement however only one of them restricts the respective axis of rotation.

To manufacture these components the previously mentioned CNC machine was used.

All of these support components will be duly applied so as to contact with the extrusion barrel's flange of the extrusion barrel when coupled with the group of standardized profiles implemented in this project. The position, connections and dimensions of these components can be visualized in the drawings: A01.00.05; A01.00.06 and A01.00.07.

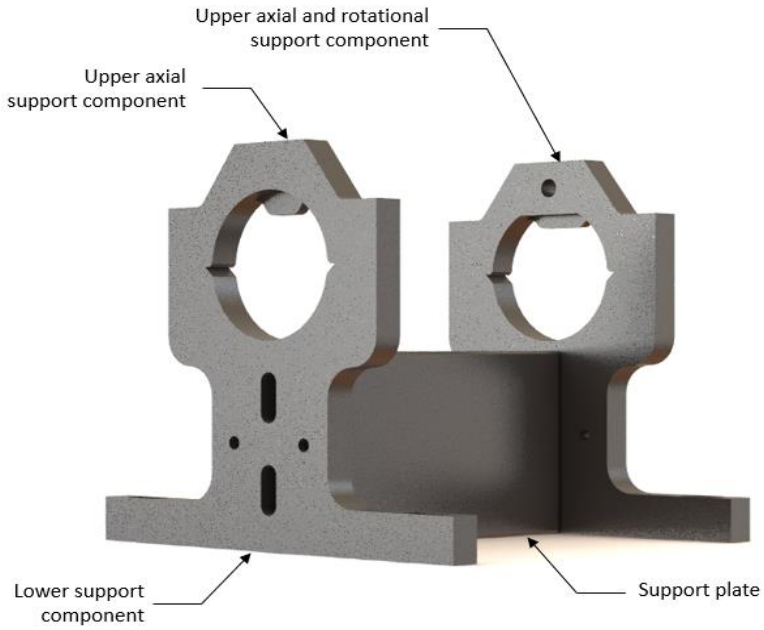

Figure 6.2 Staged barrel support

6.3 Elastic couplers

To transmit the mechanical energy supplied by the stepper motor to the conveying screw, two elastic couplers, Figure 6.3, were applied. One of these components is implemented between the motor shaft and the reduction gearbox, while the other is set between the reduction gearbox and the conveying screw.

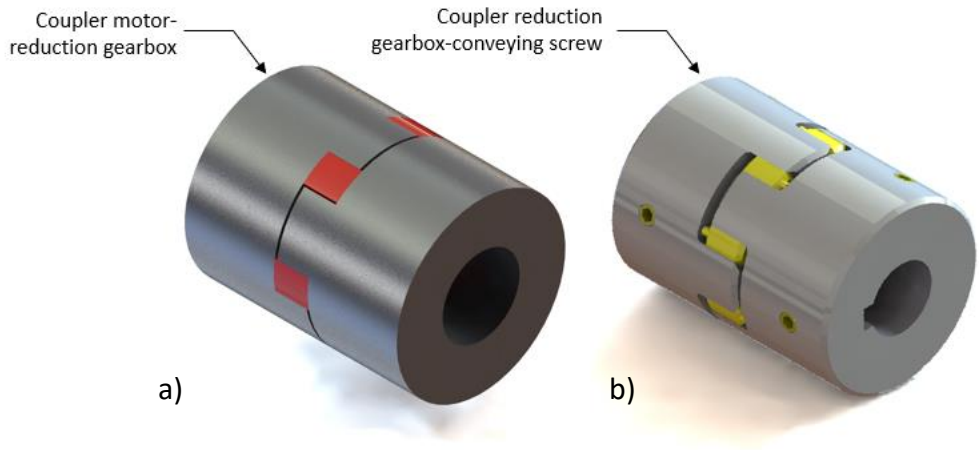

Figure 6.3 (a) Elastic coupler (motor shaft - reduction gearbox)
(b) Elastic coupler (reduction gearbox - conveying screw)

The implementation of these components is directly related to the implementation of the reduction gearbox. The reduction gearbox is set since the motor provides the necessary energy for the system on high rotational speed levels. With the implementation of the reduction gearbox, it is possible to obtain high levels of energy at lower rotational speeds, achieved by dividing energy levels by a ratio of 1:10.

The elastic coupling components used in this project must withstand the energy being transmitted through the system without failure during the extrusion process. One of these components connects the motor shaft to the reduction gearbox (12/16 mm) while the other connects the reduction gearbox to the conveying screw (25/25 mm). The later coupling must be able to withstand a rated coupling torque (T_k) of 95 Nm.

7

ASSEMBLY AND TESTING

The assembly of the extruder follows different requirements to ensure the safety of all components and optimize its functionality during use. To provide a clearer understanding of the extruder equipment assembly, Figure 7.1 is presented accompanied by a dedicated equipment identification list, Table 7.1.

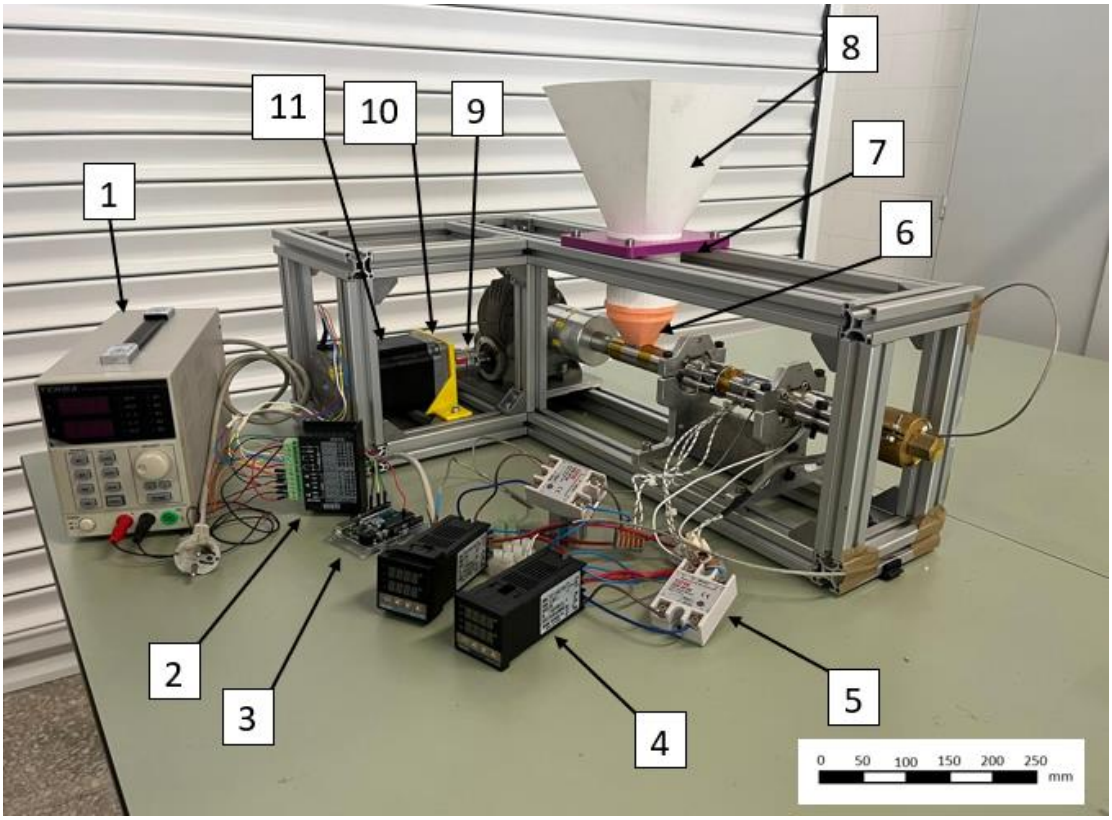

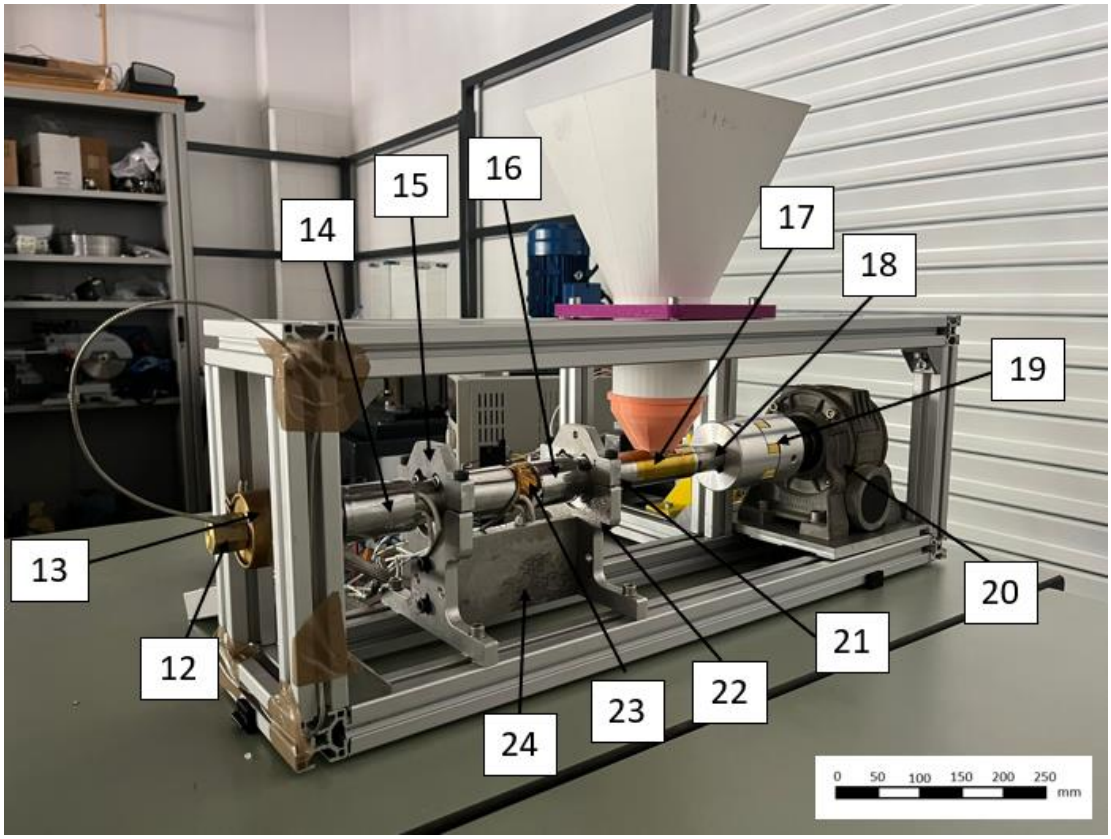

Figure 7.1 Extruder listed components

Table 7.1 Listed components

Nº	Designation	Nº	Designation
1	AC Power supply 24 V	13	Copper band heater (220 W)
2	Motor driver TB6600	14	Metering staged barrel
3	Arduino Uno R3	15	Upper axial and rotational support
4	PID Controller	16	Stainless steel band heater (150 W)
5	SSR	17	Feeding staged barrel
6	Adaptor	18	Conveying screw
7	Feed hopper support	19	Elastic coupler
8	Feed hopper	20	Reduction gearbox 1:10
9	Elastic coupler	21	Upper axial support
10	Motor Support	22	Lower support
11	Astrosyn MY34HD3-8 stepper motor	23	Transition staged barrel
12	Extrusion die	24	Support plate

The external framework of the equipment is entirely constructed of standardized Bosch profiles, measuring 30x30 mm in dimensions, having an overall dimension as presented in Figure 7.2. For a more detailed depiction of the arrangement of these structural elements, refer to drawing A01.02.

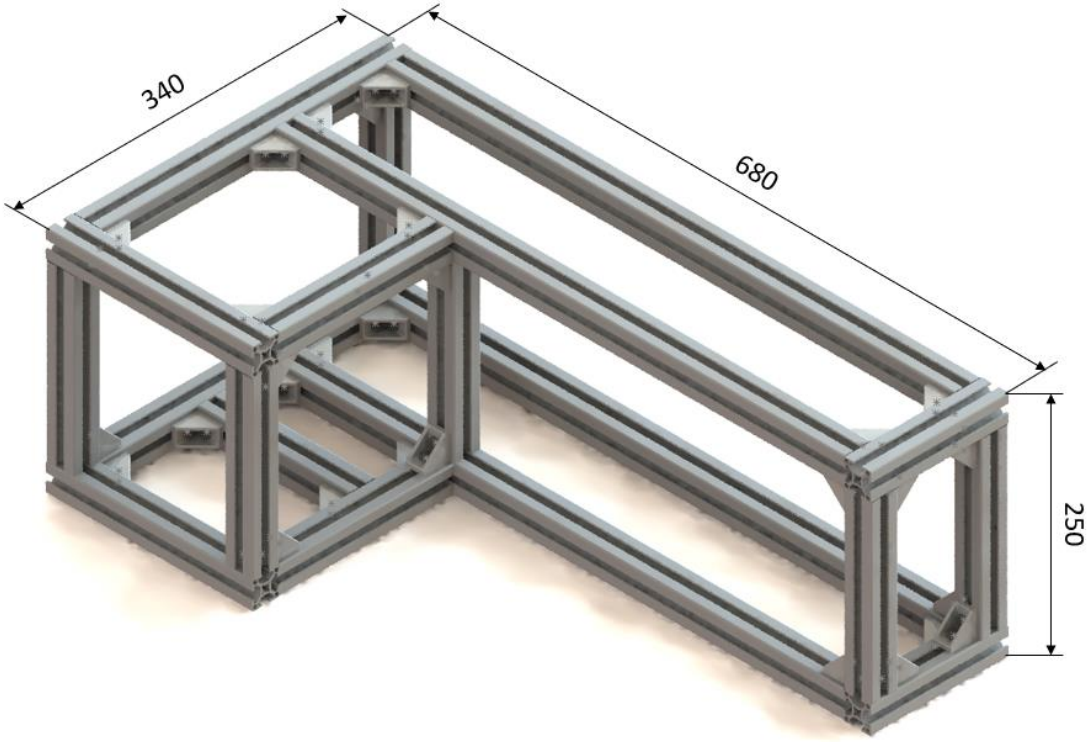

Figure 7.2 Overall structural dimensions in mm

Prior to commencing equipment operation, a preheating of the equipment for approximately 5 minutes is followed. This preheating procedure serves the purpose of achieving temperature uniformity across the barrels, thereby providing a more stable plasticizing process.

A standard rotational velocity (ω) of $5\ \mathrm{rpm}$ was selected for equipment testing. This parameter consequently results in an estimated polymer residence time of 3 minutes. Additionally, the down channel velocity, according to Eq.8 is determined as $v_{b,z} = 375\ \mathrm{mm/s}$ and the volumetric flow rate of the equipment, according to Eq.7 is established at $Q = 24750\ \mathrm{mm^3/s}$. The filament obtained from such parameters can be seen in Figure 7.3.a, where the diameter measured can also be seen in Figure 7.3.b.

An evident disparity within the extrusion die hole diameter implemented for this project becomes clear upon examination. The measured filament displays a median value of $1.42\ \mathrm{mm}$ accompanied by a deviation of $0.88\ \mathrm{mm}$. Additionally, the die swell ratio, denoted as $s = 0.88$, suggests a possible surpassing of predetermined values of screw rotational speed and melt temperature. It is important to know, however, that this deviation can be attributed to the manual pulling of the material when exiting the extruder. To solve this, a future puller machine development must be implemented following this equipment.

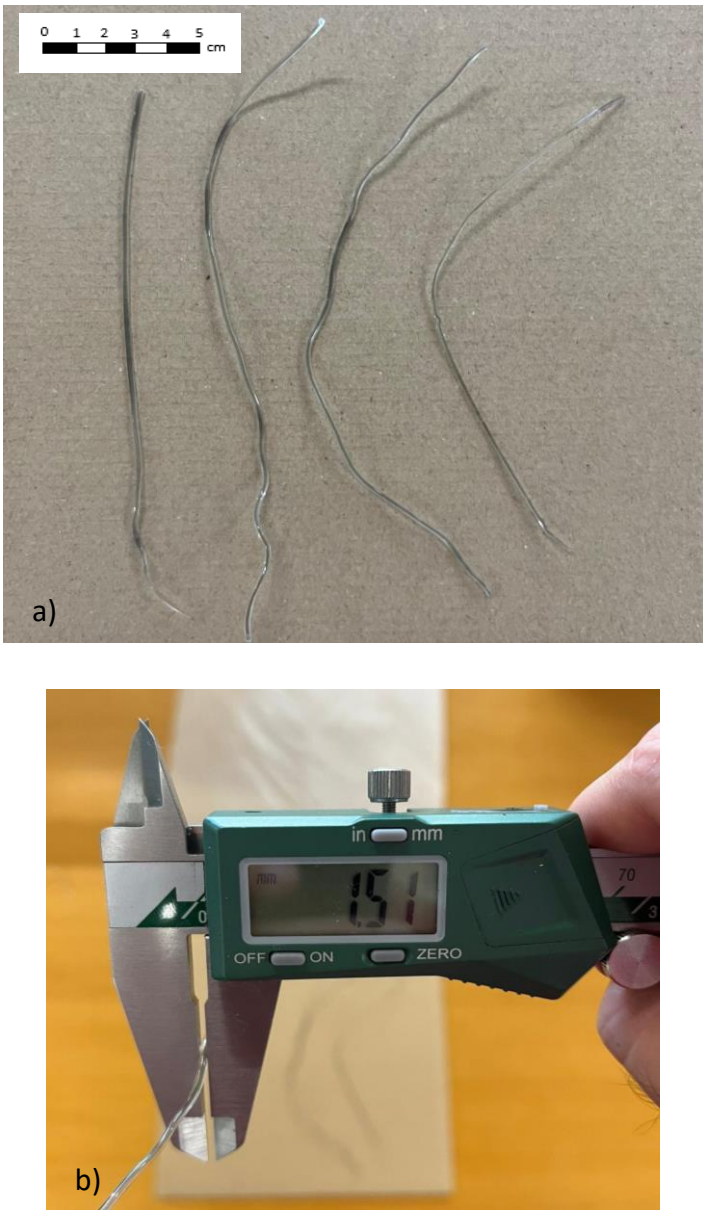

Figure 7.3 (a) Filament extruded **(b)** Filament measurements

Following these analyses, the equipment was deactivated to undertake a meticulous observation of the radial temperature profile of the extrusion die during the equipment's initiation. In order to perform this analysis, the extrusion die was uniformly coated in a heat-resistant black tint capable of withstanding temperatures up to 800°C. The temperature profile within the adaptor and the extruder die is shown in Figure 7.4. Upon initiation, the initial temperature detected from the heat bander was approximately 245°C, deviating from the set temperature imposed in the PID controller of around 200°C. However, within 30 seconds, temperature homogenization was achieved resulting in an observed average equipment temperature of 208°C.

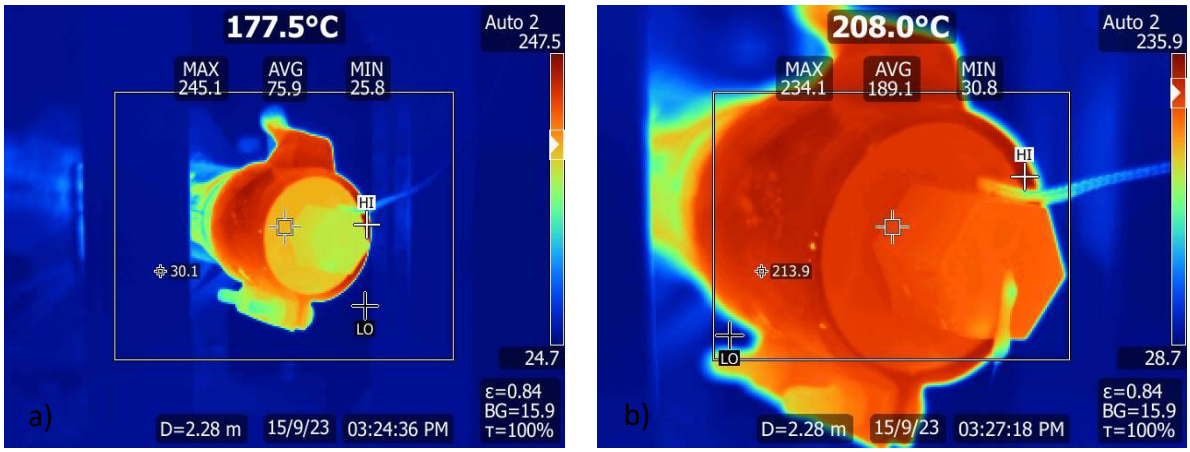

Figure 7.4 Temperature profile within the adaptor and the extrusion die in °C

It is noteworthy that the uniformized temperature observed within the equipment is 208°C. However, it should be emphasised that the temperature applied in the PID controller was 200°C signifying an observed temperature deviation of 8°C within this data acquisition equipment.

8

CONCLUSIONS

The initial prototype envisioned for this project has been successfully developed and remains fully functional for the intended purpose of extruding various types of granulate material, aligning with the project's original objectives. Notably, the equipment's reduced dimensions, when compared to its industrial-scale counterparts, emphasize the feasibility of these machines employing heat banders as the primary heat source, minimizing the reliance on frictional forces within the barrel between the screw, material and the inner surface of the barrel.

The compact dimensions of the equipment were a driving factor in the development of a fully customizable equipment, as demonstrated in this study. Each component of this equipment was designed to be easily substituted, obviating the need for a complete overhaul in the event of a part replacement, consequently increasing future project costs. This design approach means a clear reduction of manufacturing expenses as well as future material acquisition for 3D printers.

Furthermore, future components inclusion was a pivotal consideration in this project, allowing the implementation of future components such as a puller machine and enhanced data acquisition methods within the extruder. This adaptability ensures that future advancements can be incorporated without necessitating a complete redesign of the project.

In summary, the equipment is operationally sound and proficient in extruding a spectrum of low-density polymeric materials, exemplified by materials like PLA.

9

FUTURE WORKS

While this study has provided valuable insights into the design of single screw extruders, several observations and future works emerge with its conclusion:

- **Desing and implementation of a puller machine**: the development of a dedicated puller machine is recommended as it allows a consistent filament diameter measurement and immediate storage of extruded polymeric material. This advancement would enhance the efficiency and accuracy of the extrusion process.
- **Introduction of new data acquisition equipment**: the data acquisition method used in this work resulted in some temperature discrepancies and lacked pressure-related inputs within this equipment. To address this, it is suggested to integrate advanced data acquisition equipment to provide comprehensive insights into temperature and pressure dynamics during the extrusion process.
- **Optimization of process parameters:** as shown throughout this document the screw rotational speed as well as the set temperature from the band heaters is not optimized, affecting the end product and high SEC levels. Future work should focus on refining and fine-tuning these process parameters to achieve improved extrusion outcomes.

BIBLIOGRAPHY

[1] Plastics – the Facts 2010 An analysis of European plastics production , demand and recovery for 2009, Plastics Europe, Brussels, 2010.

[2] C. Abeykoon, A. Mcmillan, B. Kha, Energy efficiency in extrusion-related polymer processing: a review of state of the art and potential e ffi ciency improvements, Renew. Sustain. Energy Rev. (2021). https://doi.org/10.1016/j.rser.2021.111219.

[3] K. Ulrich, S. Eppinger, Product design and development, 5th ed., McGraw-Hill, 2022. https://doi.org/10.2166/9781789061840_0019.

[4] M. Groover, Fundamentals of modern manufacturing: materials, processes and systems, USA: Jhon Wiley & Sons, 2010.

[5] J. Vera-Sorroche, A. Kelly, E. Brown, P. Coates, N. Karnachi, E. Harkin-Jones, K. Li, J. Deng, Thermal optimisation of polymer extrusion using in-process monitoring techniques, Appl. Therm. Eng. 53 (2013) 405–413. https://doi.org/10.1016/j.applthermaleng.2012.04.013.

[6] J. Vera-sorroche, A.L. Kelly, E.C. Brown, T. Gough, C. Abeykoon, P.D. Coates, J. Deng, K. Li, E. Harkin-jones, M. Price, Chemical Engineering Research and Design The effect of melt viscosity on thermal efficiency for single screw extrusion of HDPE ☪, Chem. Eng. Res. Des. 92 (2014) 2404–2412. https://doi.org/10.1016/j.cherd.2013.12.025.

[7] C. Rauwendall, Polymer Extrusion, 5th ed., Hanser Publishers, Munich, 2021. https://doi.org/10.4325/seikeikakou.33.222.

[8] J.J. Sousa, A. Sousa, F. Podczeck, J.M. Newton, Factors influencing the physical characteristics of pellets obtained by extrusion-spheronization, Int. J. Pharm. 232 (2002) 91–106. https://doi.org/10.1016/S0378-5173(01)00908-5.

[9] J. Goff, T. Whelan, D. Delaney, Dynisco processors, 2nd Editio, DYNISCO Companies, 2015.

[10] X. Fan, Mechanics of moisture for polymers: Fundamental concepts and model study, EuroSimE 2008 - Int. Conf. Therm. Mech. Multi-Physics Simul. Exp. Microelectron. Micro-Systems. (2008) 1–14. https://doi.org/10.1109/ESIME.2008.4525043.

[11] M.J. Stevens, J.A. Covas, Extruder Principles and Operation, 2nd ed., Chapman and Hall, London, 1995.

[12] R. Kent, Energy management in plastics processing - Framework for measurement, assessment

and prediction, Plast. Rubber Compos. 37 (2008) 96–104. https://doi.org/10.1179/174328908X283285.

[13] B. Drury, The control techniques drives and controls, The Institution of Electrical Engineers, London, 2001.

[14] J.-F. Agassant, P. Avenas, P.J. Carreau, B. Vergnes, M. Vincent, Polymer Processing: Principles and Modeling, 2nd Editio, Hanser Publications, Munich, 2017.

[15] K.M. Cantor, Analyzing extruder energy consumption, SPE ANTEC Tech. (2010) 603–609.

[16] C.I. Chung, E.M. Mount, D.E. McClelland, ENERGY EFFICIENCY IN PLASTICATING SCREW EXTRUSION., ACS Symp. Ser. (1979) 21–36. https://doi.org/10.1021/BK-1979-0107.CH003.

[17] Strauch, Gliese, Menges, Energy usage and conservation in extrusion plants, Proc. Polym. Extrus. III. (1985) 2–1– 2–10.

[18] Anderson, Rauwendaal, Noriega, Troubleshooting extrusion problems, SPE ANTEC Tech. Pap. 1. (1997) 127–34.

[19] J. Deng, K. Li, E. Harkin-Jones, M. Price, N. Karnachi, M. Fei, Energy Consumption Analysis for a Single Screw Extruder, in: K. Li, S. Li, D. Li, Q. Niu (Eds.), Intell. Comput. Sustain. Energy Environ., Springer Berlin Heidelberg, Berlin, Heidelberg, 2013: pp. 533–540.

[20] R. Rasid, A.K. Wood, Effect of process variables on melt temperature profiles in extrusion process using single screw plastics extruder, Plast. Rubber Compos. 32 (2003) 187–192. https://doi.org/10.1179/146580103225002731.

[21] C. Abeykoon, A.L. Kelly, E.C. Brown, J. Vera-Sorroche, P.D. Coates, E. Harkin-Jones, K.B. Howell, J. Deng, K. Li, M. Price, Investigation of the process energy demand in polymer extrusion: A brief review and an experimental study, Appl. Energy. 136 (2014) 726–737. https://doi.org/10.1016/J.APENERGY.2014.09.024.

[22] Z. Tadmor, Fundamentals of plasticating extrusion. I. A theoretical model for melting, Polym. Eng. & Sci. 6 (1966) 185–190. https://doi.org/10.1002/pen.760060303.

[23] C. Abeykoon, A. Mcmillan, B. Kha, Energy efficiency in extrusion-related polymer processing: a review of state of the art and potential efficiency improvements, Renew. Sustain. Energy Rev. (2021). https://doi.org/10.1016/j.rser.2021.111219.

[24] R.B. Bird, W.E. Stewart, E.N. Lighfoot, Transportation Phenomena, 2nd Editio, John Wiley & Sons Inc., New York, 2002.

[25] R.M. Griffith, Fully developed flow in screw extruders, I&EC Fundam. 1 (1962) 180–187.

[26] H.J. Zamodits, J.R.A. Pearson, Flow of Polymer Melts in Extruders . Part I . The Effect of Transverse Flow and of a Flow of Polymer Melts in Extruders , Part I . The Effect of Transverse Flow and of a Superposed Steady Temperature Profile, 357 (2013). https://doi.org/10.1122/1.549136.

[27] M. V. Karwe, Y. Jaluria, Numerical Simulation of Fluid Flow and Heat Transfer in a single-

screw Extruder for non-Newtonian fluids, Numer. Heat Transf. 17 (1990) 167–190. https://doi.org/10407789008944738.

[28] C. Marschik, W. Roland, B. Löw-Baselli, J. Miethlinger, A heuristic method for modeling three-dimensional non-Newtonian flows of polymer melts in single-screw extruders, J. Nonnewton. Fluid Mech. 248 (2017) 27–39. https://doi.org/10.1016/j.jnnfm.2017.08.007.

[29] Z. Tadmor, C.G. Gogos, Principles of Polymer Processing, 2nd ed., A John Wiley & Sons, Inc., Publication, 2006.

[30] A.Y. Malkin, V. V Goncharenko, V. V Malinovskii, where h and h w are the distances from the axis of the flat channel to the layer in question, (1976) 487–492.

[31] T. Nishimura, T. Kataoka, Rheologica Acta, 407 (1984) 401–407.

[32] K. Wilczynski, A. Nastaj, A. Lewandowski, K.J. Wilczynski, Buziak, Kamila, Fundamentals of Global Modeling for Polymer Extrusion, Polymers (Basel). 11 (2019) 1–31. https://doi.org/10.3390/polym11122106.

[33] C. Abeykoon, K. Li, M. McAfee, P.J. Martin, J. Deng, A.L. Kelly, Modelling the effects of operating conditions on die melt temperature homogeneity in single screw extrusion, IET Semin. Dig. 2010 (2010) 42–47. https://doi.org/10.1049/ic.2010.0254.

[34] C. Abeykoon, Measurement : Sensors Sensing technologies for process monitoring in polymer extrusion : A comprehensive review on past , present and future aspects, Meas. Sensors. 22 (2022) 100381. https://doi.org/10.1016/j.measen.2022.100381.

[35] A.L. Kelly, E.C. Brown, P.D. Coates, The Effect of Screw Geometry on Melt Temperature Profile in Single Screw Extrusion *, (2006). https://doi.org/10.1002/pen.

[36] H.T. KIM, E.A. COLLINS, Temperature Profiles for Polymer Melts in Tube Flow. Part II. Conduction and Shear Heating Corrections, Polym. Eng. Sci. 11 (1971) 83–92.

[37] A.L. Kelly, E.C. Brown, K. Howell, P.D. Coates, Melt temperature field measurements in extrusion using thermocouple meshes, Plast. Rubber Compos. 37 (2008) 151–157. https://doi.org/10.1179/174328908X283393.

[38] E.C. Brown, A.L. Kelly, P.D. Coates, Melt temperature field measurement in single screw extrusion using thermocouple meshes, Rev. Sci. Instrum. 75 (2004) 4742–4748. https://doi.org/10.1063/1.1808895.

[39] C. Abeykoon, K. Li, M. McAfee, P.J. Martin, Q. Niu, A.L. Kelly, J. Deng, A new model based approach for the prediction and optimisation of thermal homogeneity in single screw extrusion, Control Eng. Pract. 19 (2011) 862–874. https://doi.org/10.1016/j.conengprac.2011.04.015.

[40] G.A. Campbell, M.A. Spalding, Analyzing and troubleshooting single-screw extruders, 2nd ed., Hanser Publications, Munich, 2021.

[41] C.I. Chung, Extrusion of polymers, theory and practice, 2nd ed., Hanser Publications, Munich, 2011.

[42] T.W. Womer, M.A. Spalding, The benefits of screw cooling for improved solids conveying for

smooth-bore, single-screw extruders, J. Plast. Film Sheeting. (2023). https://doi.org/10.1177/87560879231181543.

[43] H.F. Giles, J.R. Wagner, E.M. Mount, Extrusion: the definitive processing guide and handbook, William Andrew Publishing, Norwich, 2005.

[44] I.O. Mikulionok, L.. Radchenko, Screw extrusion of thermoplastics: II. Simulation of feeding zone of the single screw extruder, Russ. J. Appl. Chem. 85 (2012) 505–514.

[45] I.O. Mikulionok, Classification of Screw Cooling Devices of Single-Screw Extruders for Polymer Materials Processing (Survey of Designs), Chem. Pet. Eng. 58 (2022) 68–73. https://doi.org/10.1007/s10556-022-01057-5.

[46] T.W. Womer, W.S. Smith, R.P. Wheeler, COMPARISON OF TWO DIFFERENT COOLING METHODS FOR EXTRUSION PROCESSES, ANTEC. (2006) 796–801.

[47] B.H. Maddock, A Visual Analysis of Flow and Mixing in Extruder Screws, SPE ANTEC Tech. 15 (1959) 383.

[48] L.F. Street, Plastifying Extrusion, Intern. Plast. Eng.1. 1 (1961) 289–296.

[49] J. Frankland, Mission (Nearly) Impossible: Estimating Extrusion Melt Temperature, 2012.

[50] D.I. Marshall, I. Klein, Fundamentals of Plasticating Extrusion II, Polym.Eng.Sci. 6 (1966) 191–197.

[51] Z. Tadmor, I. Klein, Computer Programs for Plastic Engineers, Reinhold Book Corporation: New York, New York, 1968.

[52] B.H. Maddock, Measurment and Analysis of Extruder Stability, SPE Jounral. 20 (1964) 1277–1283.

[53] S. V., E. E., A. K., G. E., Dynamic temperature measurments in polymer processing, SPE ANTEC Tech. Pap. 1. (2008) 228–232.

[54] W. Obendrauf, G.R. Lagecker, W. Friesenbichler, Temperature measuring in plastics processing with infrared radiation thermometers, Int. Polym. Proc. 13 (1998) 71–77.

[55] C. Maier, Infrared temperature measurement of polymers, Polym.Eng.Sci. 36 (1996) 1502–1512.

[56] A. Bendana, M. Lamontagne, A new infrared pyrometer for polymer temperature measurement during extrusion molding, Infrared Phys. Technol. 46 (2004) 11–15.

[57] A.L. Kelly, E.C. Brown, P.D. Coates, Infrared Melt Temperature Measurement of Single Screw Extrusion, (2015). https://doi.org/10.1002/pen.

[58] C.Rauwendaal, Polymer Extrusion, 5th ed., Hanser, Munich, 2021. https://doi.org/10.4325/seikeikakou.33.222.

[59] P. Hauptamnn, N. Hoppe, A. Puttmer, Application of ultrasonic sensors in the process industry, Meas. Sci. Tech. 13 (2002) R73–R83.

[60] D.R. Franca, C.K. Jen, K.T. Nguyen, R. Gendron, Ultrasonic in-line monitoring of polymer extrusion, Polym.Eng.Sci. 40 (2000) 82–94.

[61] N.T.-F.C. Ky T, S.-S.L. Wen, C.-K. Jen, Temperature measurment of polymer extrusion by

ultrasonic techniques, Meas. Sci. Tech. 10 (1999) 139–145.

[62] A.J. Bur, M.G. Vangel, S.C. Roth, Fluorescence based temperature measurments and applications to real-time polymer processing, Polym.Eng.Sci. 41 (2001) 1380–1389.

[63] A.J. Bur, M.G. Vangel, S.C. Roth, temperature dependence of fluorescence probes for applications to polymer materials processing, Appl. Spectrosc. 56 (2002) 174–181.

[64] A.J. Bur, S.C. Roth, Fluorescence temperature measurments: methodology for applications to process monitoring, Polym.Eng.Sci. 44 (2004) 898–908.

[65] A.J. Bur, S.C. Roth, M.A. Spalding, D.W. Baugh, K.A. Koppi, W.C. Buzanowski, Temperature gradients in the channels of a single screw extruder, Polym.Eng.Sci. 44 (2004) 2148–2157.

[66] A.L. Kelly, E.C. Brown, M. Woodhead, P.D. Coates, Temperature measurement methods for polymer processing, (2002) 122.

[67] E.C. Brown, A.L. Kelly, P.D. Coates, Melt temperature field measurments in single screw extrusion using thermocouple meshes, Rev. Sci. Instrum. 75 (2004) 4742–4748.

[68] C. Abeykoon, P.J. Martin, A.L. Kelly, E.C. Brown, A review and evaluation of melt temperature sensors for polymer extrusion, Sensors Actuators, A Phys. 182 (2012) 16–27. https://doi.org/10.1016/J.SNA.2012.04.026.

[69] C.. Lee, N.. Wheeler, A study on the performance of barrier-screw extruders, Polym.Eng.Sci. 31 (1991) 831–841.

[70] E.. Steward, Barrier screws, their history and their function, SPE ANTEC Tech. (2002) 69–73.

[71] H.F. Giles, Extrusion : The Definitive Processing Guide, William Andrew Publishing, Norwich, 2005.

[72] A. Lawal, D.M. Kalyon, Mechanisms of mixing in single and co-rotating twin screw extruders, Polym. Eng. Sci. 35 (1995) 1325–1338. https://doi.org/10.1002/pen.760351702.

[73] R.S. Spencer, R.M. Wiley, The mixing of very viscous liquids, J. Colloid Sci. 6 (1951) 133–145. https://doi.org/10.1016/0095-8522(51)90033-5.

[74] J.M. Ottino, The kinematics of mixing: stretching, chaos, and transport, Cambridge university Press, 1989.

[75] J. Sun, C. Rauwendall, Analysis of flow in single screw extruders, SPE ANTEC Tech. (2002) 184–188.

[76] K.C. Mills, S.U. Yuchu, L.I. Zushu, R.F. Brooks, Equations for the calculation of the thermo-physical properties of stainless steel, ISIJ Int. 44 (2004) 1661–1668. https://doi.org/10.2355/isijinternational.44.1661.

[77] M.M. Kostic, L.G. Reifschneider, Design of Extrusion Dies, (2006) 633–649. https://doi.org/10.1081/E-ECHP-120039324.

[78] Z. Tadmor, Fundamentals of Plasticating Extrusion I, Polym.Eng.Sci. 6 (1966) 185–190.

[79] D. V. Rosato, Die design and performance, Extrud. Plast. (1998) 228–282. https://doi.org/10.1007/978-1-4615-5793-7_5.

[80] L.V. da Cunha, Desenho Técnico, 17th ed., Goulbekian, Fundação Calouste, Lisboa, 2017.

[81] M.A. Johnson, M.H. Moradi, J. Crowe, K.K. Tan, T.H. Lee, R. Ferdous, M.R. Katebi, H.P. Huang, J.C. Jeng, K.S. Tang, G.R. Chen, K.F. Man, S. Kwong, A. Sánchez, Q.G. Wang, Y. Zhang, Y. Zhang, P. Martin, M.J. Grimble, D.R. Greenwood, PID control: New identification and design methods, 2005. https://doi.org/10.1007/1-84628-148-2.

[82] X. Shen, R. Malloy, J. Pacini, An Experimental Evaluation of Melt Temperature Sensors for Thermoplastic Extrusion, Polym.Eng.Sci. 11 (1971) 83–92.

[83] I. Machinability, Technical Data Sheet UGIMA ® -X 4404, (n.d.) 1–5.

[84] Stepping Motor Technical Information, (2020).

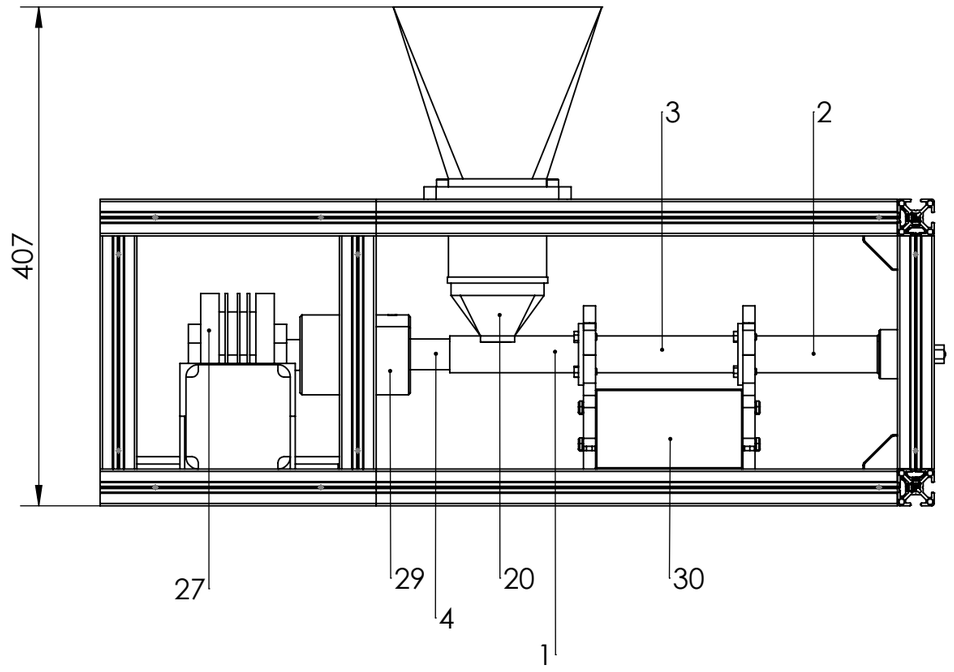

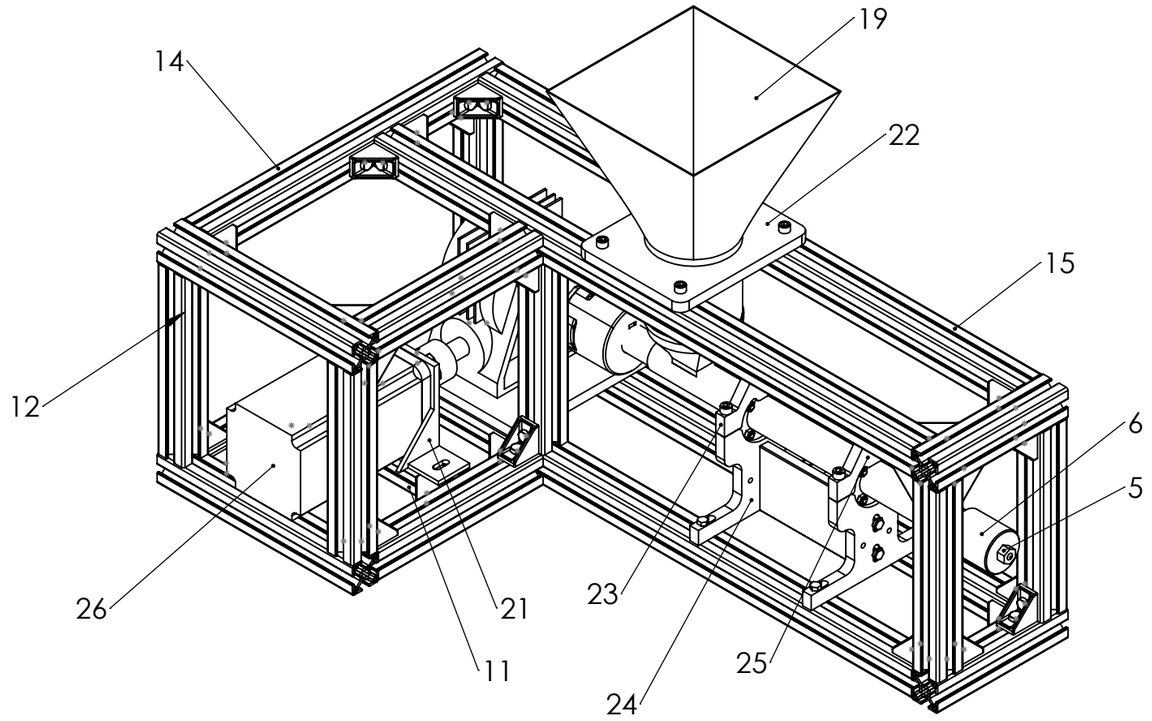

Observações:	Projetado			NOVA - S.S.T	Ricardo Manica
	Desen.	18/09/23			
	Copiado				
	Visualiz.				
	Escala 1:5			Single screw extruder	A01
	Toleran. NP-265 Médio				

Projetado		
Desen.	18/09/23	
Copiado		
Visualiz.		

NOVA - S.S.T.

Tese de mestrado

Ricardo Manica

Nº	DESIGNAÇÃO	Nº DA NORMA / Nº DO DESENHO	MATERIAL	Nº REF	PRODUTO SEMI ACABADO Nº DO MOLDE Nº DA MATRIZ	PESO	OBSERVAÇÕES
1	Feeding staged barrel	A01.01.02	AISI 316 Stainless Steel	1		226,15 g	
1	Metering staged barrel	A01.01.04	AISI 316 Stainless Steel	2		295,10 g	
1	Transition staged barrel	A01.01.03	AISI 316 Stainless Steel	3		317,55 g	
1	Conveying screw	A01.01.01	AISI 316 Stainless Steel	4		2845,53 g	
1	Extrusion die	A01.01.06	Brass	5		15 g	
1	Adaptor	A01.01.05	Brass	6		324,98 g	
8	Hexagonal M5 x 15 x 0,8			7			
8	Nut M5 x 08			8			
1	Key			9			
2	Bosch 150 mm		Aluminum 2011	10		126,36 g	Ver desenho A01.02
1	Bosch 165 mm		Aluminum 2011	11		139 g	Ver desenho A01.02
8	Bosch 190 mm		Aluminum 2011	12		160 g	Ver desenho A01.02
2	Bosch 225 mm		Aluminum 2011	13		189,54 g	Ver desenho A01.02
2	Bosch 340 mm		Aluminum 2011	14		286,42 g	Ver desenho A01.02
4	Bosch 620 mm		Aluminum 2011	15		522,30 g	Ver desenho A01.02
34	Bosch corners		Aluminum 2011	16		23 g	Ver desenho A01.02
76	M6 Nut			17			
84	M6 screw			18			
1	Feed hopper	A01.00.01	PLA	19		90,66 g	
1	Feeding adaptor	A01.00.02	PLA	20		14,26 g	
1	Motor support	A01.00.03	PLA	21		53,46 g	
1	Feed hopper support	A01.00.04	PLA	22		117,05 g	
1	Upper suport axial	A01.00.05	Stainless Steel	23		133,87 g	
1	Lower support	A01.00.06	Stainless Steel	24		132,53 g	
1	Upper support	A01.00.07	Stainless steel	25		468,14 g	
1	Astrosyn stepper motor			26			
1	Reduction gearbox			27			
1	Elastic coupler 01			28			
1	Elastic coupler 02			29			
1	Support plate			30			

Observações:

Lista de peças

A01

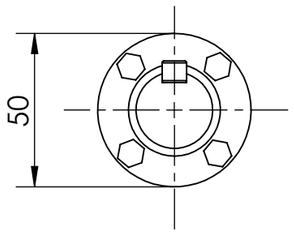

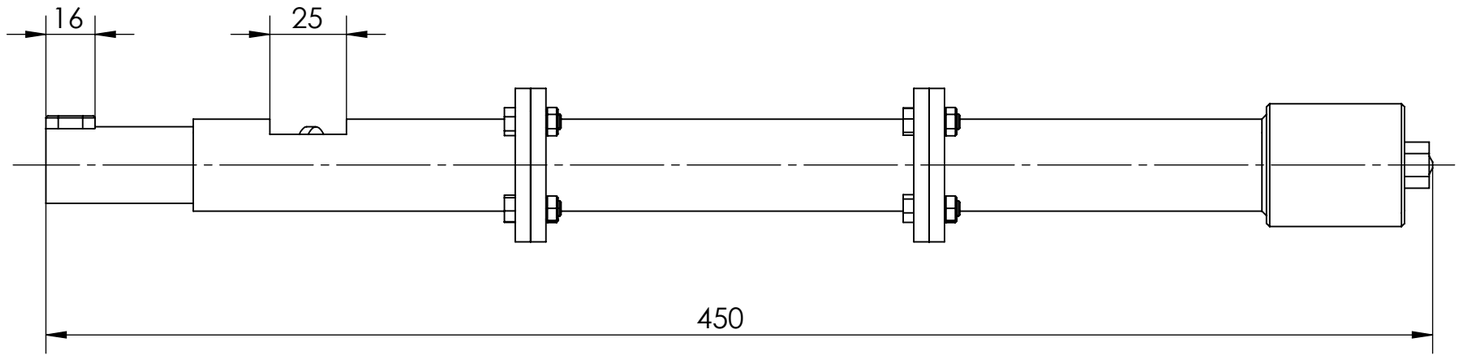

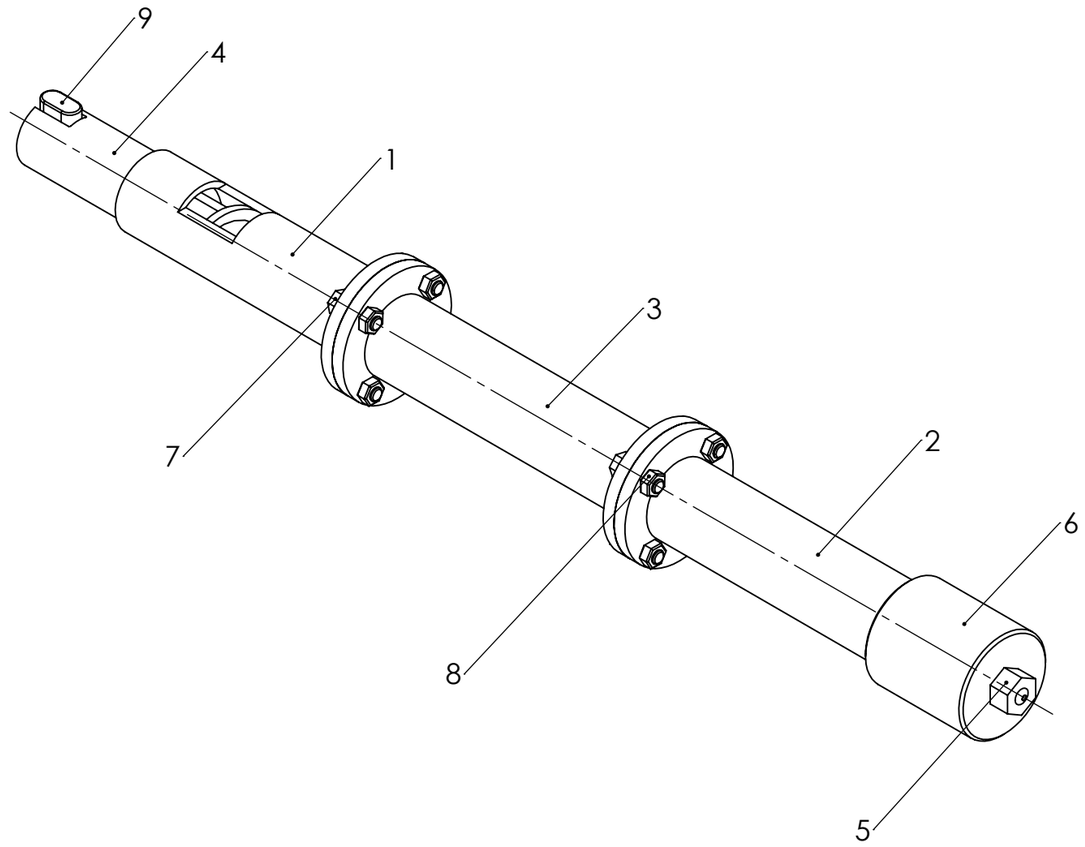

Nº	DESIGNAÇÃO	Nº DA NORMA / Nº DO DESENHO	MATERIAL	Nº REF	PRODUTO SEMI ACABADO / Nº DO MOLDE / Nº DA MATRIZ	PESO	OBSERVAÇÕES
1	Key			9			
8	M5 x 0,8 Nut			8			
8	Hexagonal screw M5 x 15 x 0,8			7			
1	Adaptor	A01.01.05	Brass	6		324,98 g	
1	Extrusion die	A01.01.06	Brass	5		15 g	
1	Conveying Screw	A01.01.01	AISI 316	4		2845,53 g	
1	Transition staged barrel	A01.01.03	AISI 316	3		317,55 g	
1	Metering staged barrel	A01.01.04	AISI 316	2		295,10 g	
1	Feeding staged barrel	A01.01.02	AISI 316	1		226,15 g	

Observações:

Projetado			NOVA - S.S.T Master Thesis
Desenhado	04/09/23		
Copiado			
Visualizado			
Escalas 1:2			Extrusion components
Toleran. NP-265 Médio			

Ricardo Manica

A01.01

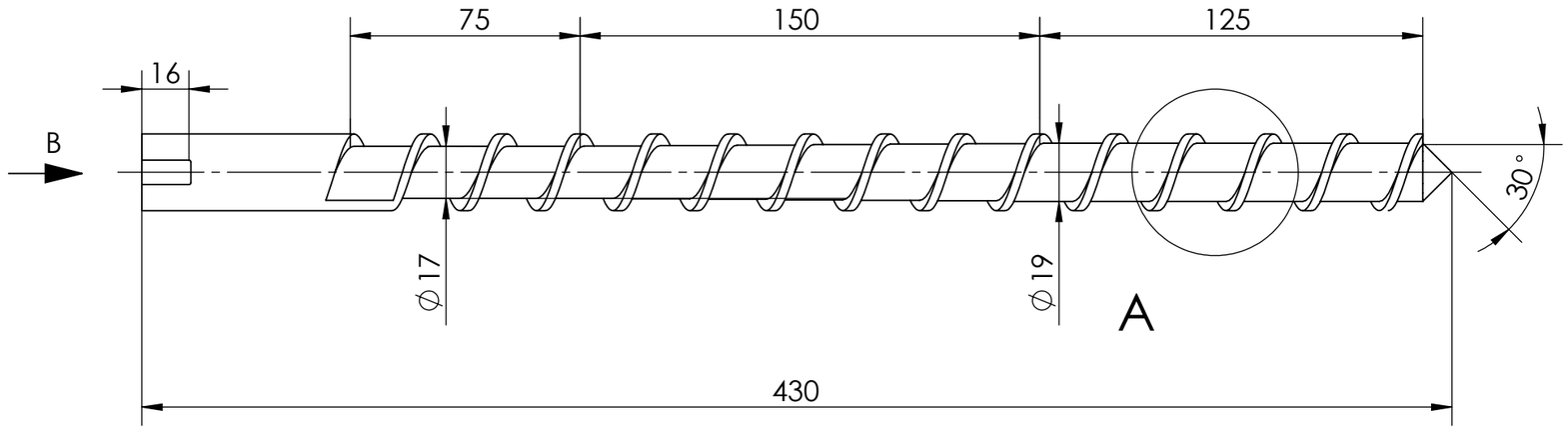

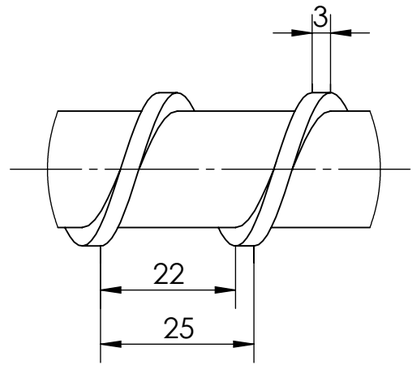

Pormenor A
Escala 2:1

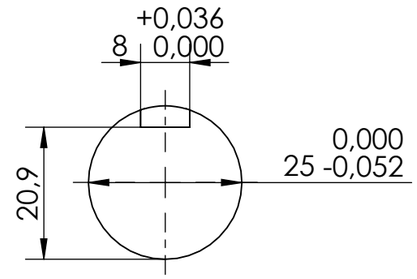

Vista B
Escala 1:1

Observações:

A zona de transição do fuso (150 mm) é a responsável pela compressão do material sendo que esta zona vai diminuir a sua profunndidade de canal inicial (4 mm) até chegar ao valor desejado na zona de metering (3 mm)

Projetado			*NOVA - S.S.T*	Ricardo Manica
Desenhado	*20/08/23*		*Master Thesis*	
Copiado				
Visualizado				
Escalas *1:2*			*Conveying Screw*	*A01.01.01*
Toleran. *NP-265* *Médio*				

Projetado			NOVA - S.S.T.	Ricardo Manica
Desen.	20/08/23		Tese de mestrado	
Copiado				
Visualiz.				

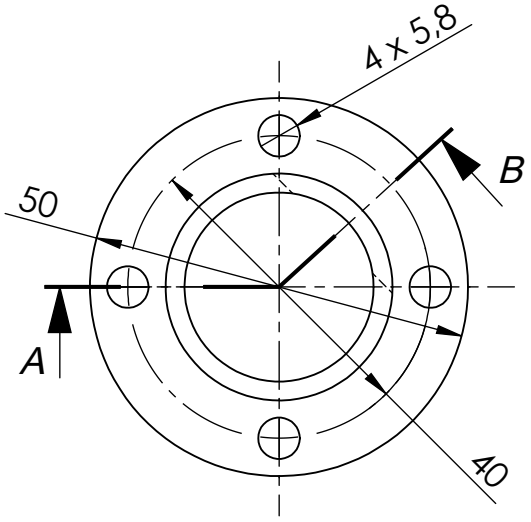

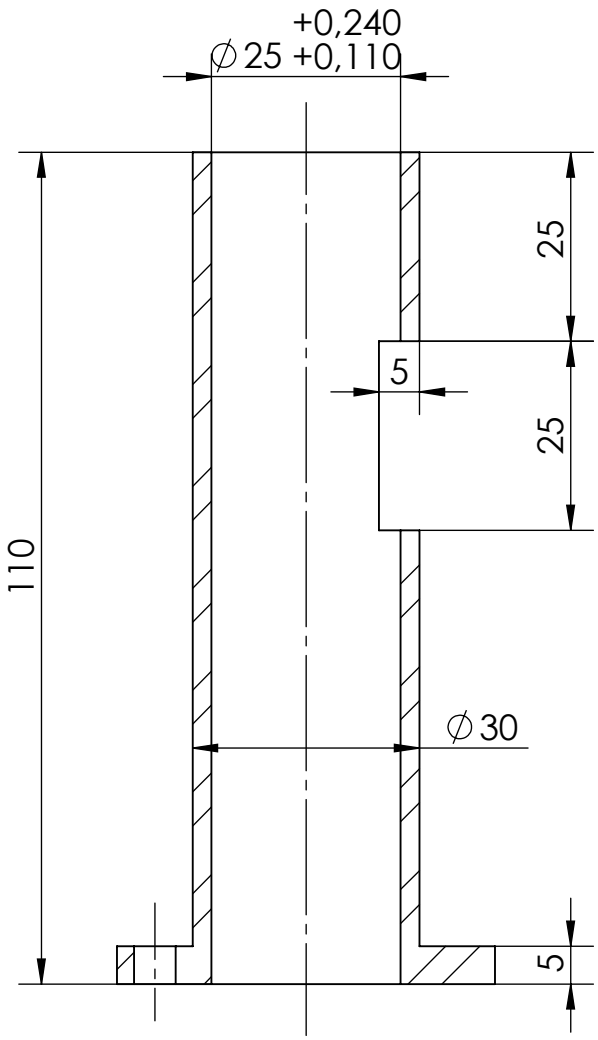

Corte A-B

Observações:	1:1 Toleran. NP-265 Médio	Feeding staged barrel	A01.01.02

Projetado			NOVA - S.S.T.	Ricardo Manica
Desen.	20/08/23		Tese de mestrado	
Copiado				
Visualiz.				

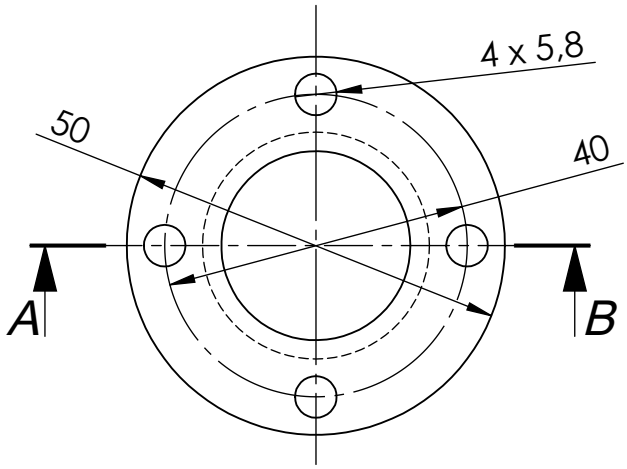

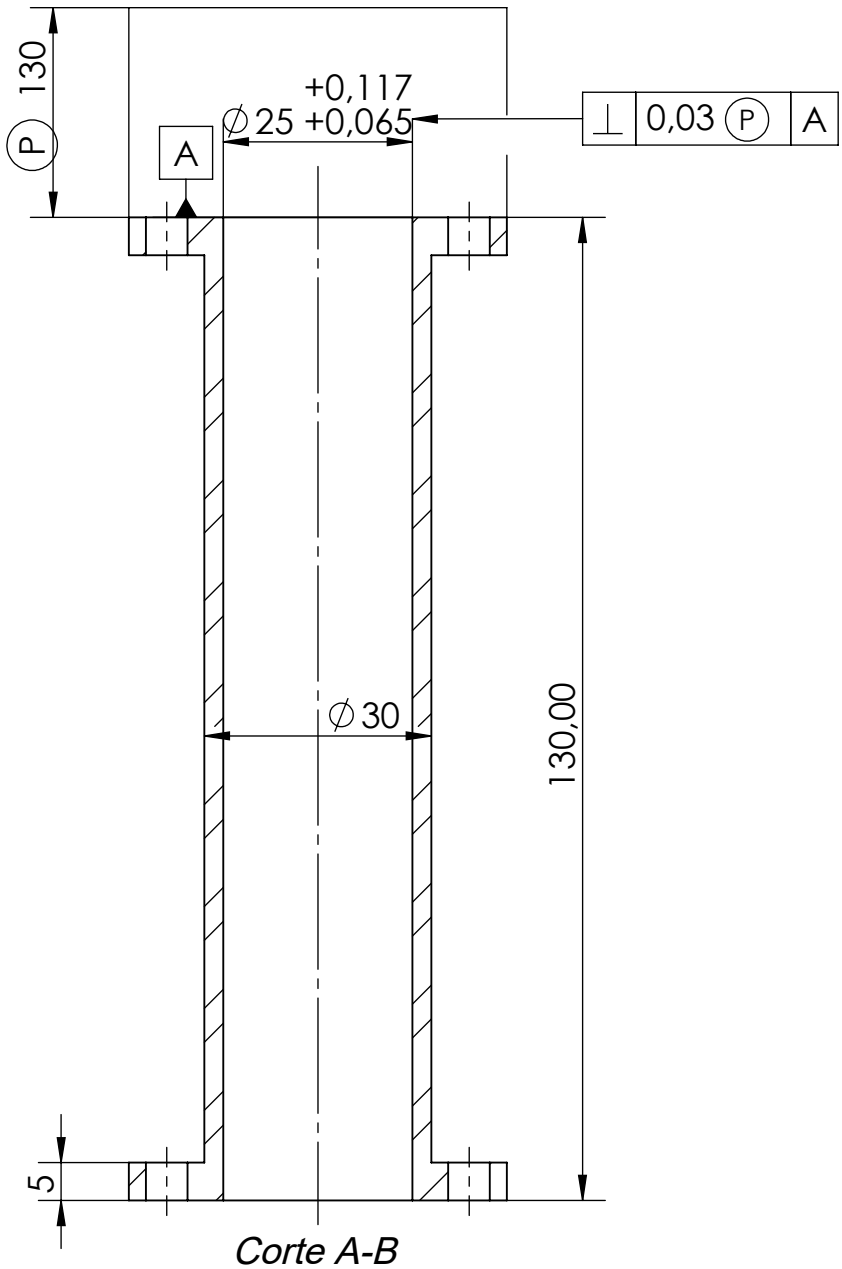

Corte A-B

Observaações:	1:1	Compression staged barrel	A01.01.03
	Toleran.		
	NP-265 Médio		

Projetado			NOVA - S.S.T.	Ricardo Manica
Desen.	20/08/23		Tese de mestrado	
Copiado				
Visualiz.				

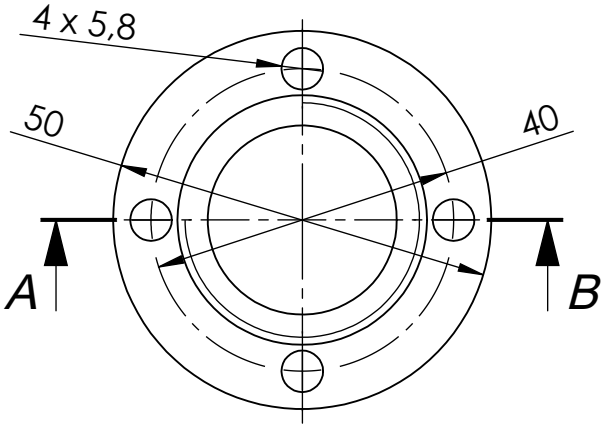

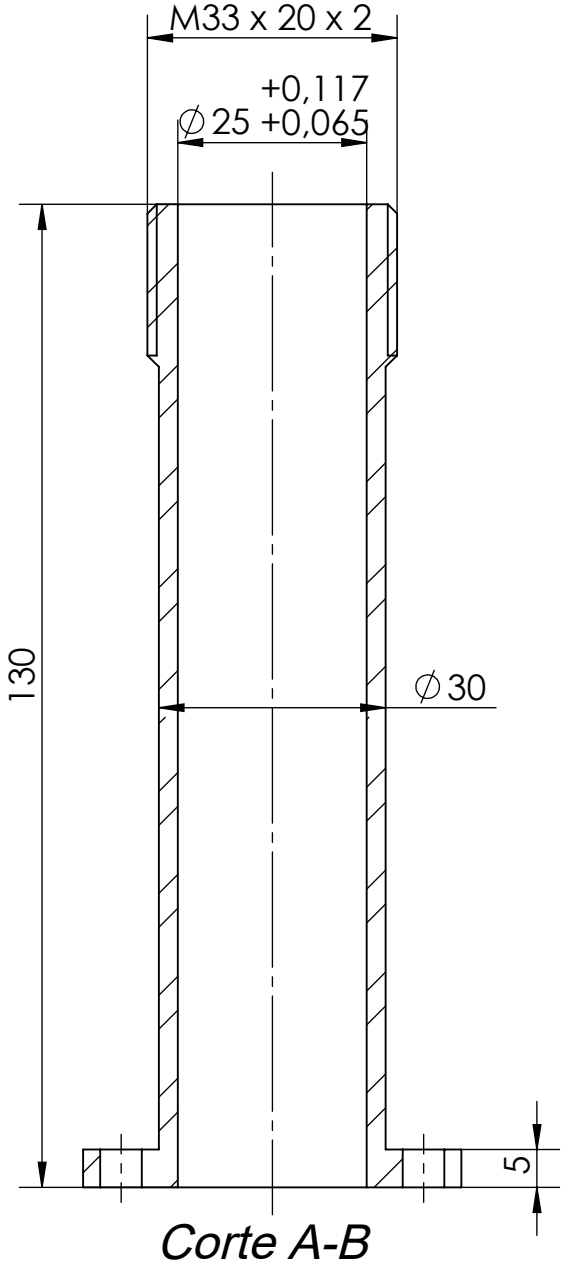

Corte A-B

Observações: Os chanfros apresentam 45 graus e têm 1 mm de distância	1:1 Toleran. NP-265 Médio	Metering staged barrel	A01.01.04

Projetado			NOVA - S.S.T.	Ricardo Manica
Desen.	20/08/23		Tese de mestrado	
Copiado				
Visualiz.				

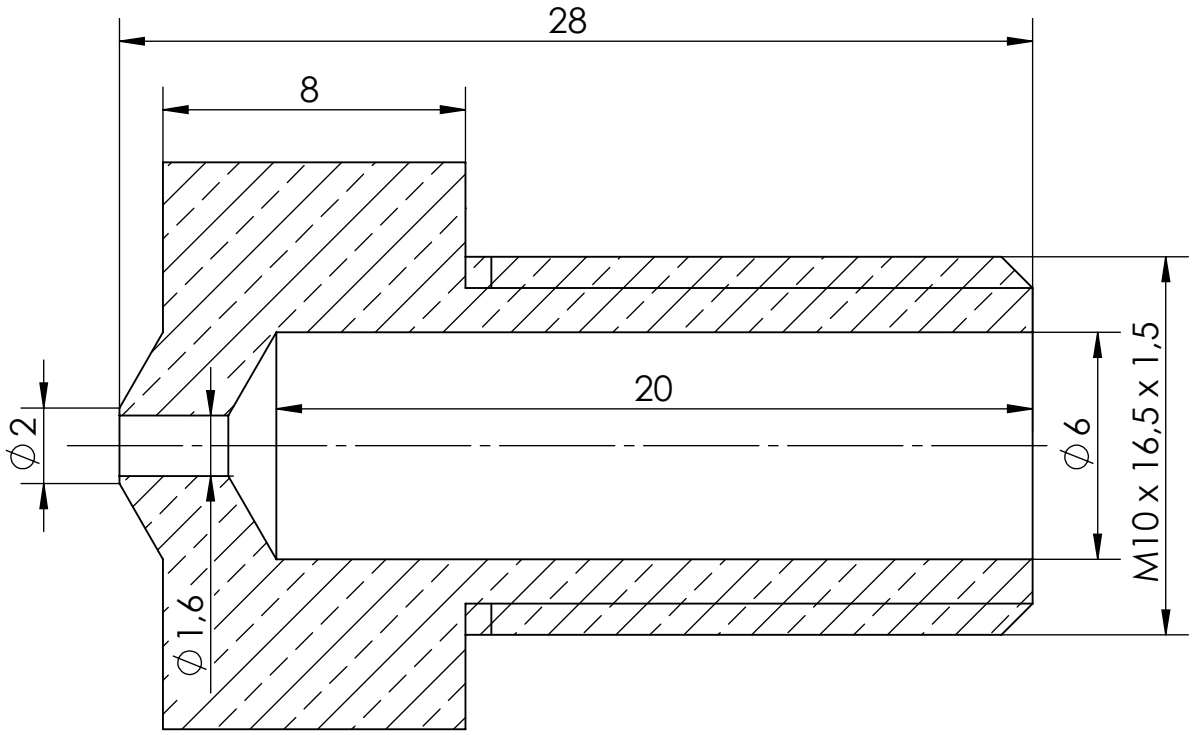

Corte A-B

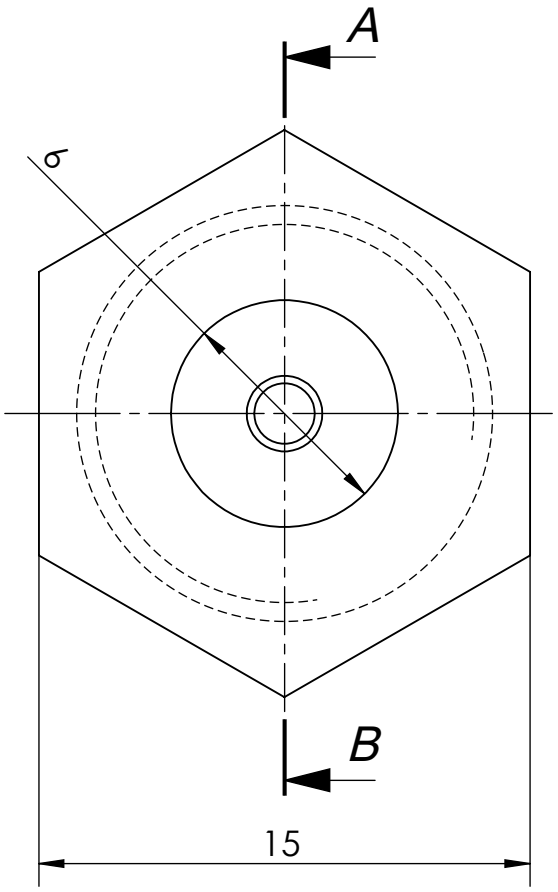

Observações: A região cónica interior apresenta as mesmas dimensões que a ponta de uma broca de 60 graus Os chanfros apresentam 45 graus e tem 1 mm de distância	5:1 Toleran. NP-265 Médio	Extrusion die	A01.01.05

Projetado			NOVA - S.S.T.	Ricardo Manica
Desen.	20/08/23		Tese de mestrado	
Copiado				
Visualiz.				

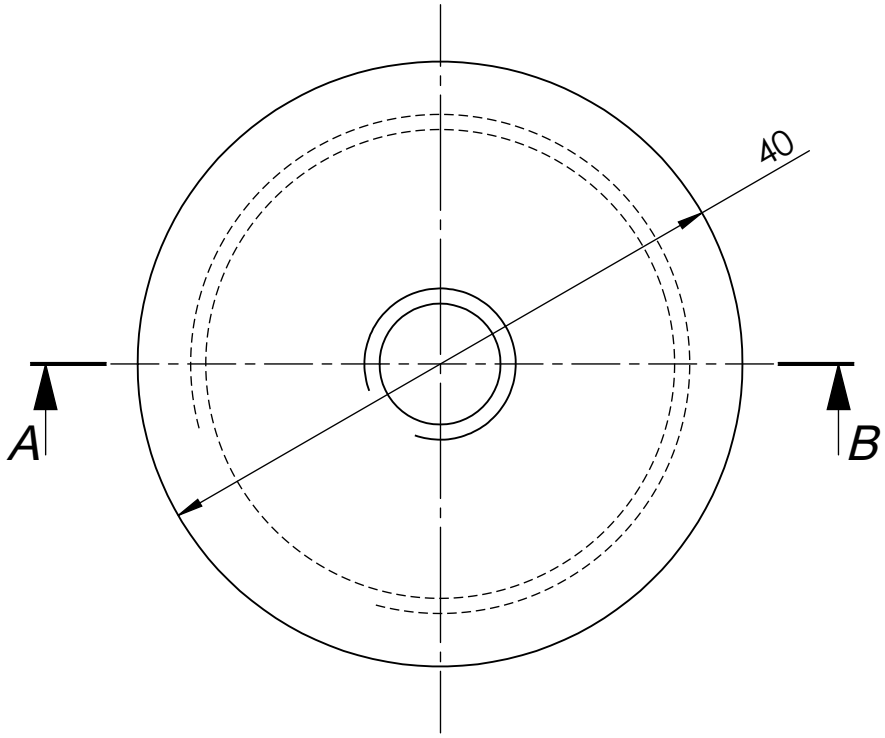

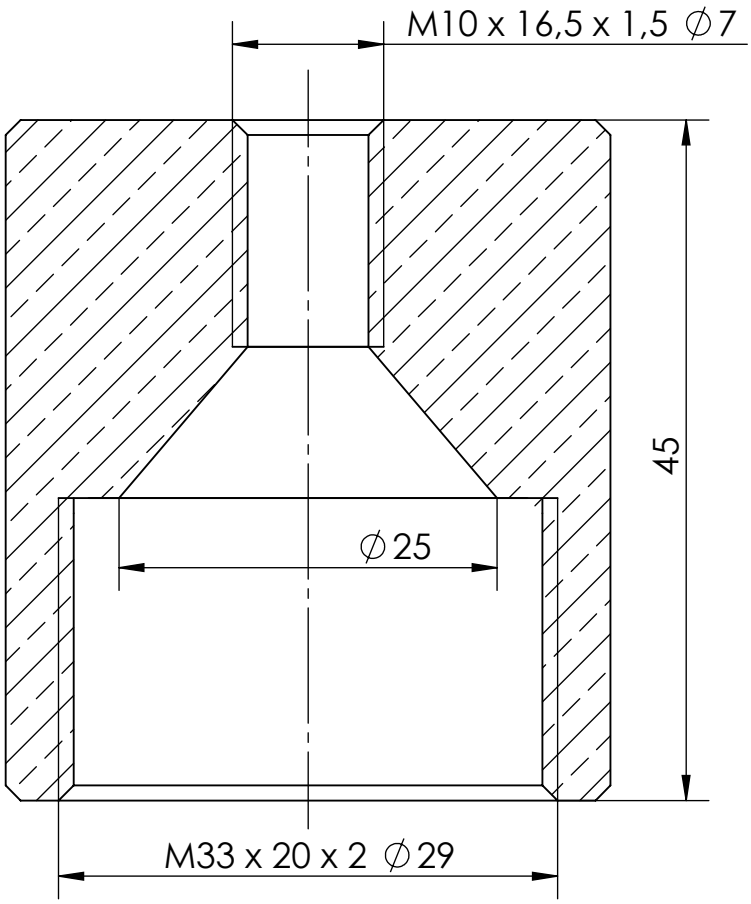

Corte A-B

Observações: Os chanfros apresentam 45 graus e medem 1 mm de distância	2:1 Toleran. NP-265 Médio	Adaptor	A01.01.06

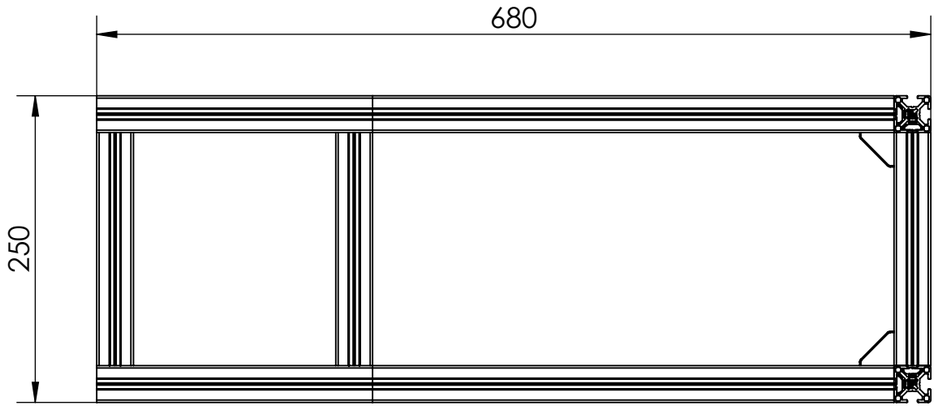

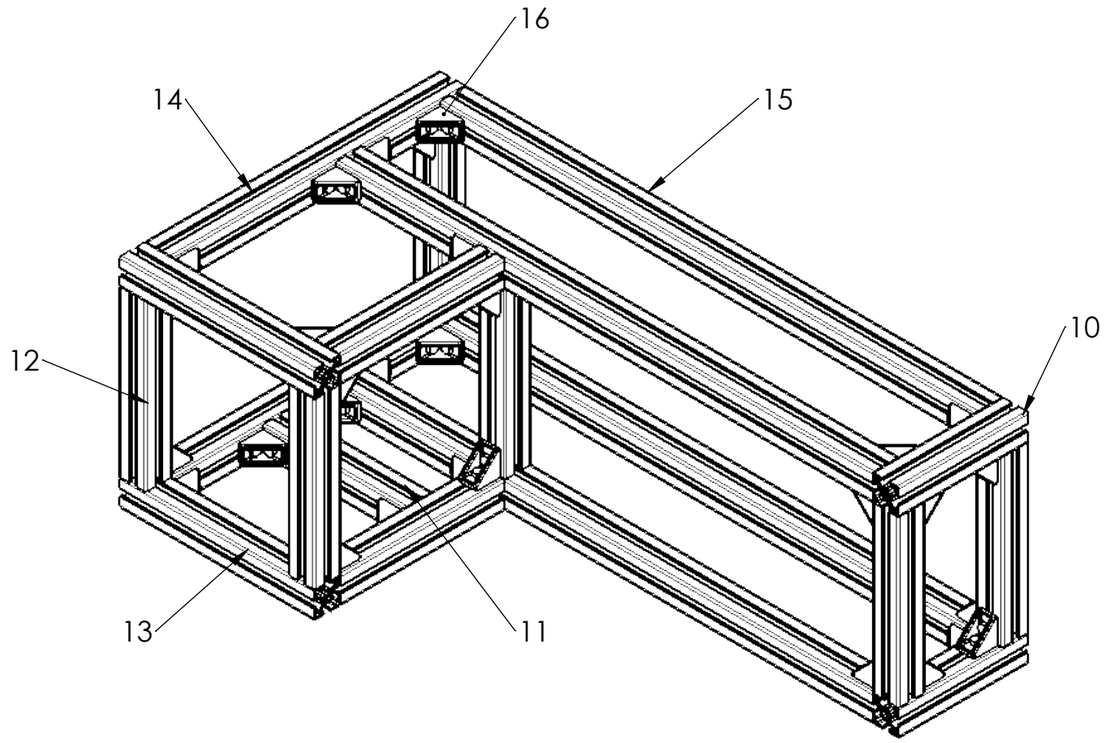

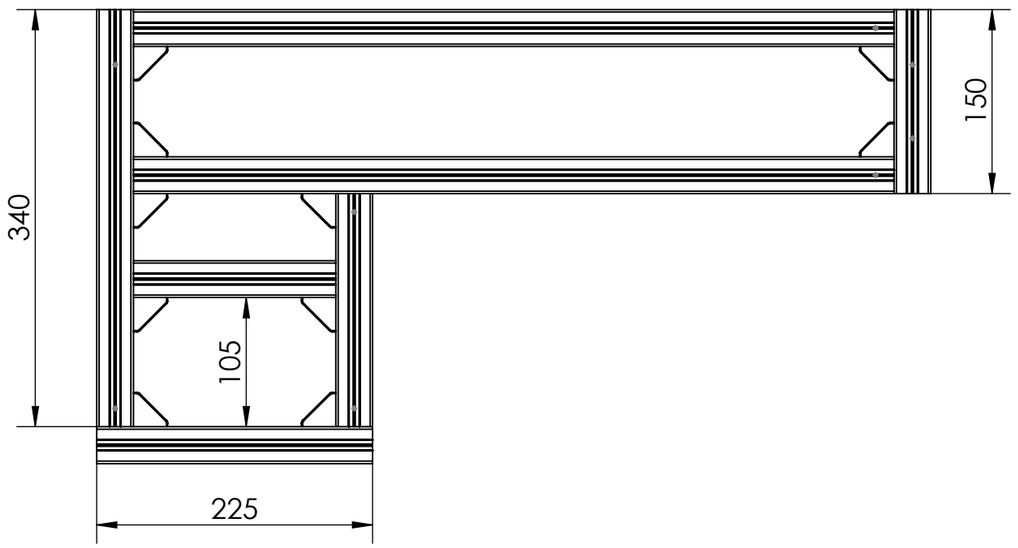

68	M6 nut			18			
68	M6 screw			17			
34	Bosch corner		Aluminum	16		23 g	
4	Bosch 620mm		Aluminum	15		522,30 g	
2	Bosch 340mm		Aluminum	14		286,42 g	
2	Bosch 225mm		Aluminum	13		189,54 g	
8	Bosch 190mm		Aluminum	12		160 g	
1	Bosch 165mm		Aluminum	11		139 g	
2	Bosch 150mm		Aluminum	10		126,36 g	
Nº	DESIGNAÇÃO	Nº DA NORMA Nº DO DESENHO	MATERIAL	Nº REF	PRODUTO SEMI ACABADO Nº DO MOLDE Nº DA MATRIZ	PESO	OBSERVAÇÕES

Observações:

Projetado			NOVA - S.S.T Master Thesis	Ricardo Manica
Desenhado	20/08/23			
Copiado				
Visualizado				
Escala 1:5			Structural support	A01.02
Toleran. NP-265 Medium				

Projetado			NOVA - S.S.T.	Ricardo Manica
Desen.	05/09/23		Tese de mestrado	
Copiado				
Visualiz.				

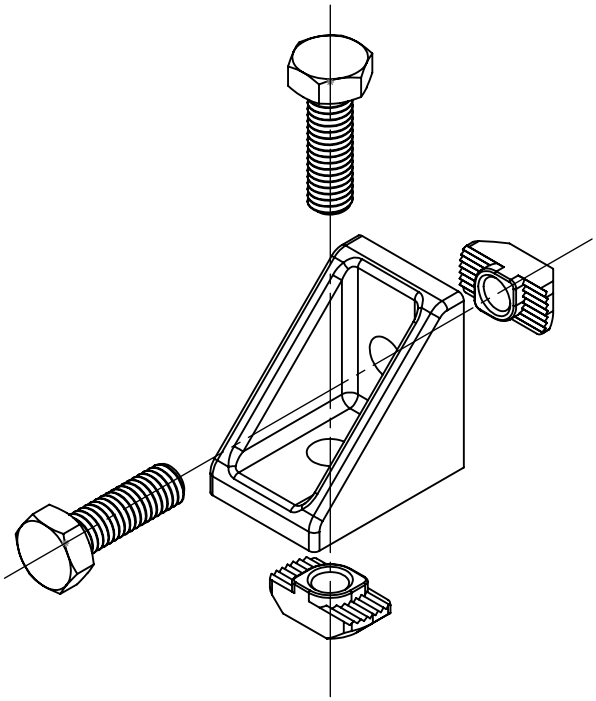

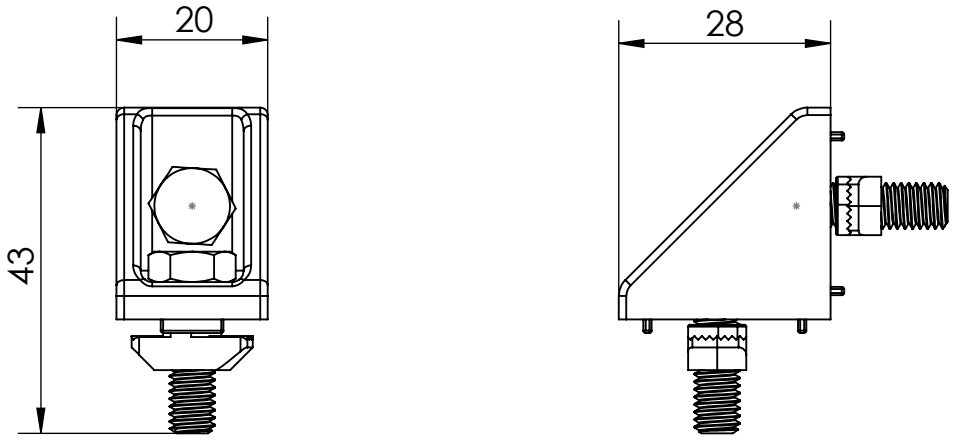

Observações:	1:1	Corner Assembly	A01.02.01
	Toleran.		
	NP-265 Médio		

Projetado			NOVA - S.S.T.	Ricardo Manica
Desen.	20/08/23		Tese de mestrado	
Copiado				
Visualiz.				

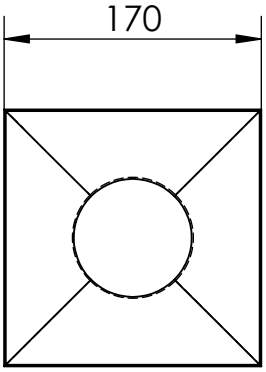

Vista A
Escala 1:5

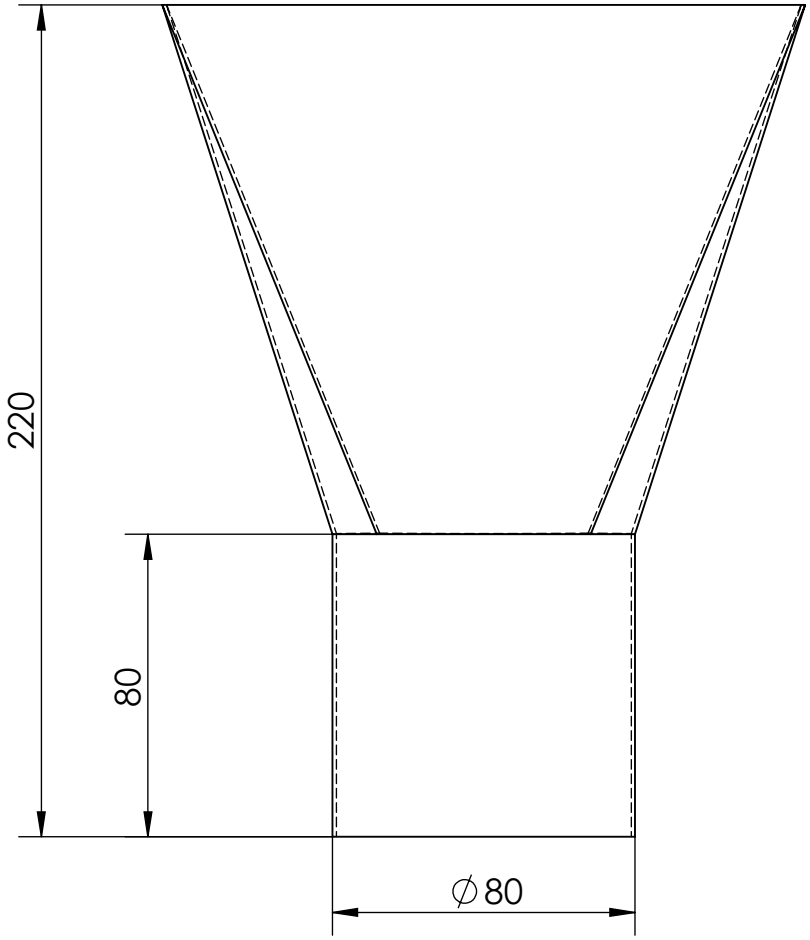

Observações: A peça tem 1 mm de espessura	1:2 Toleran. NP-265 Médio	Feed hopper	A01.00.01

Projetado			NOVA - S.S.T.	Ricardo Manica
Desen.	05/09/23		Tese de mestrado	
Copiado				
Visualiz.				

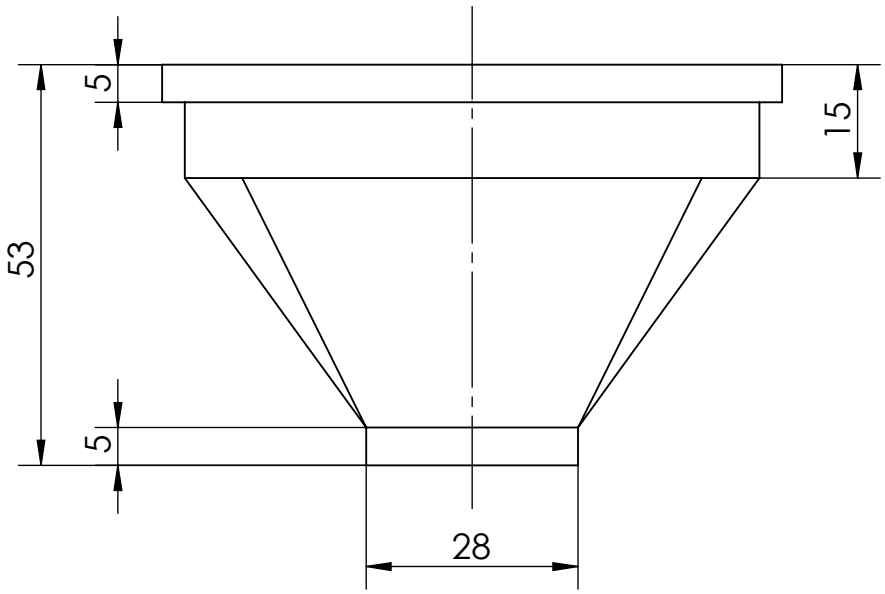

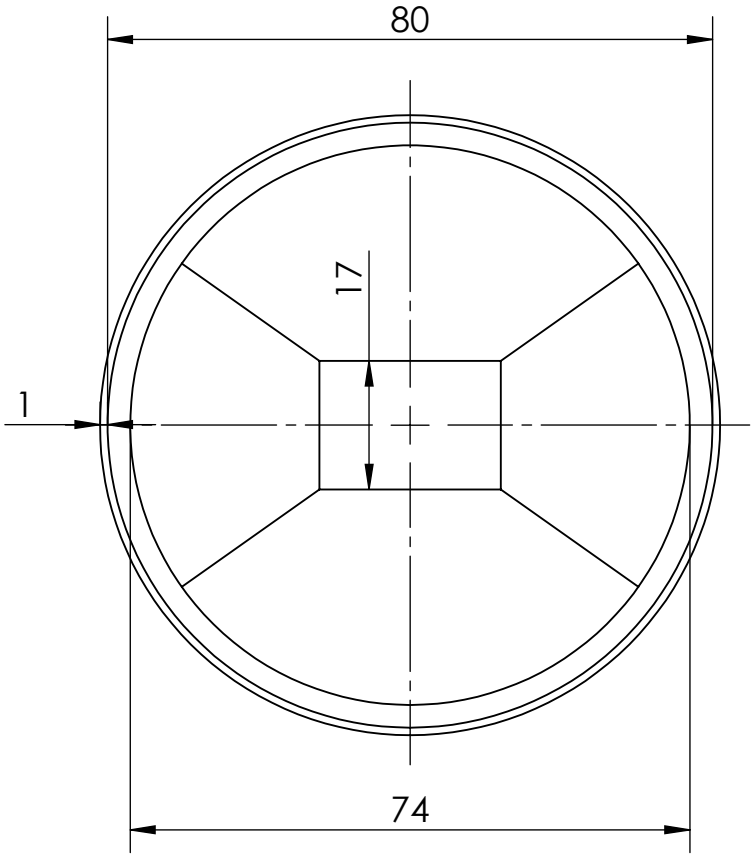

Observações:	1:1 Toleran. NP-265 Médio	Feeding adaptor	A01.00.02

Projetado			NOVA - S.S.T.	Ricardo Manica
Desen.	05/09/23		Tese de mestrado	
Copiado				
Visualiz.				

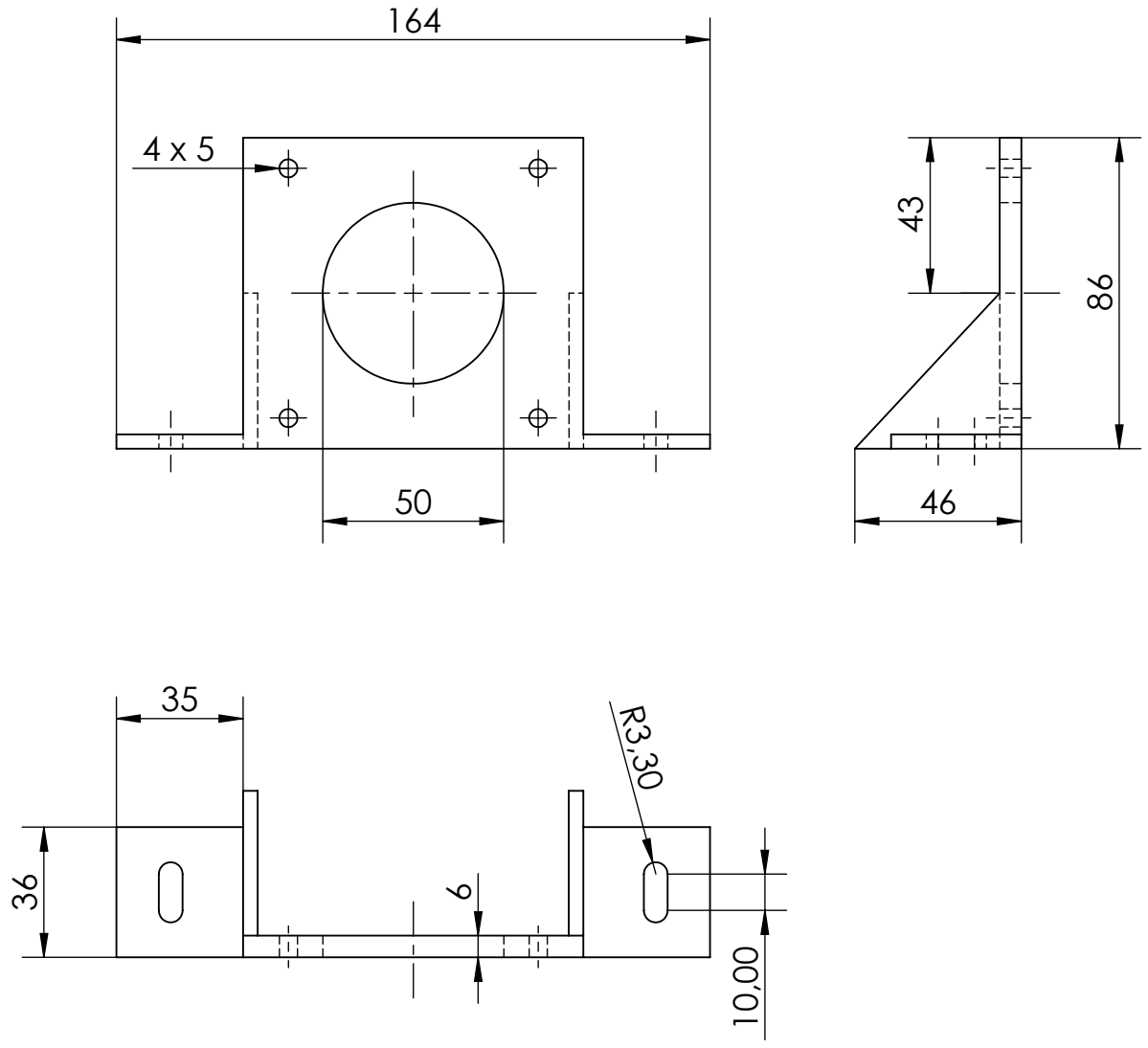

Observações: A peça tem uma espessura constante de 4 mm com exceção àquela referenciada no desenho	1:2 Toleran. NP-265 Médio	Motor support	A01.00.03

Projetado			NOVA - S.S.T. Tese de mestrado	Ricardo Manica
Desen.	05/09/23			
Copiado				
Visualiz.				

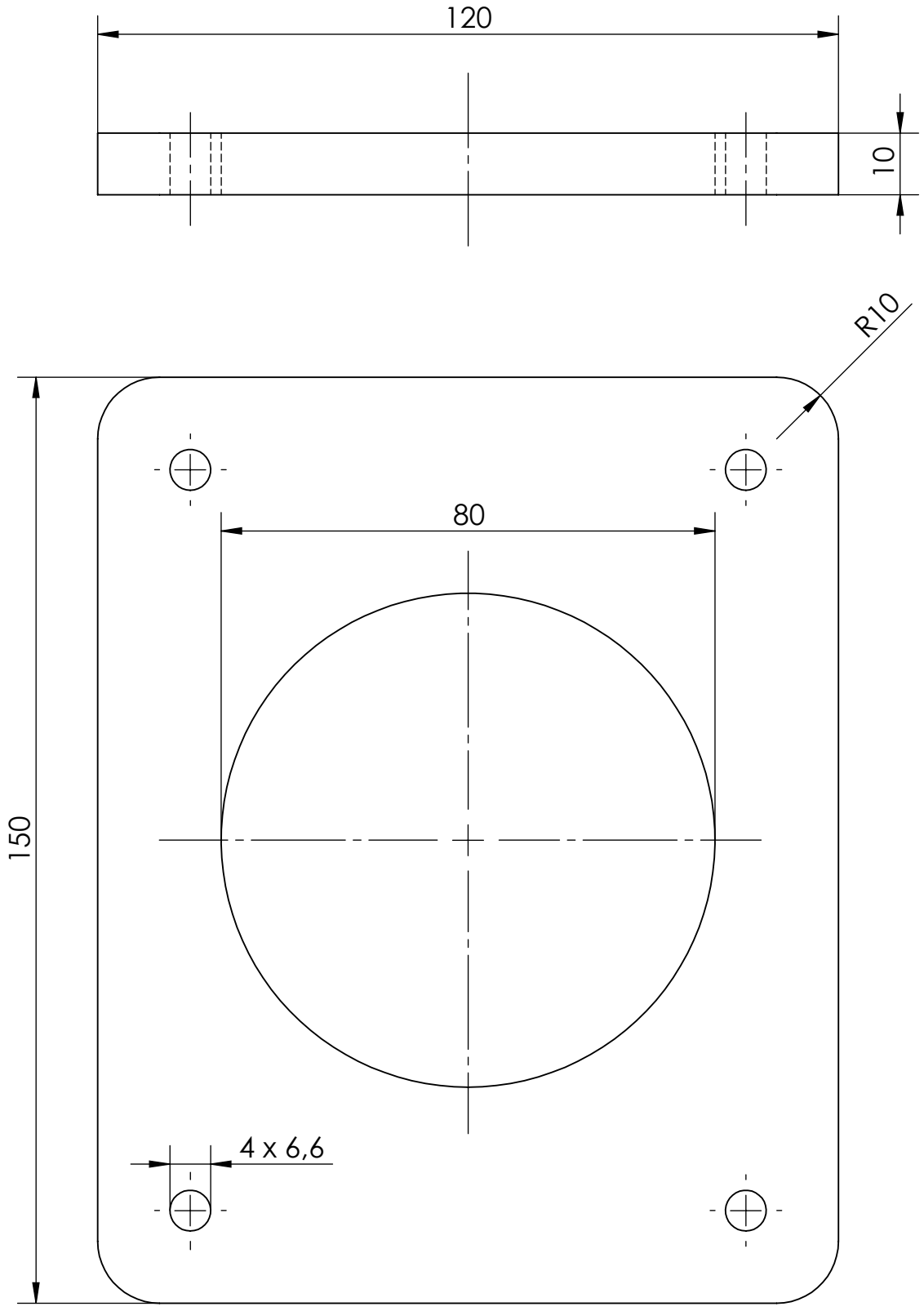

Observações:	1:1 Toleran. NP-265 Médio	Feed hopper support	A01.00.04

Projetado			NOVA - S.S.T.	Ricardo Manica
Desen.	05/09/23		Tese de mestrado	
Copiado				
Visualiz.				

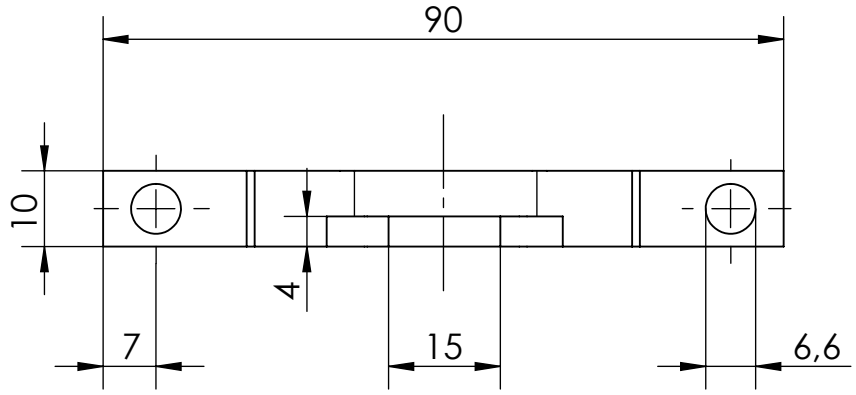

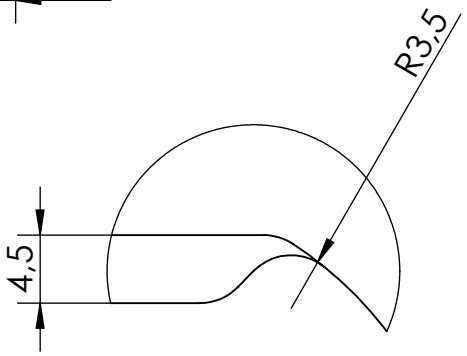

Pormenor A
Escala 2:1

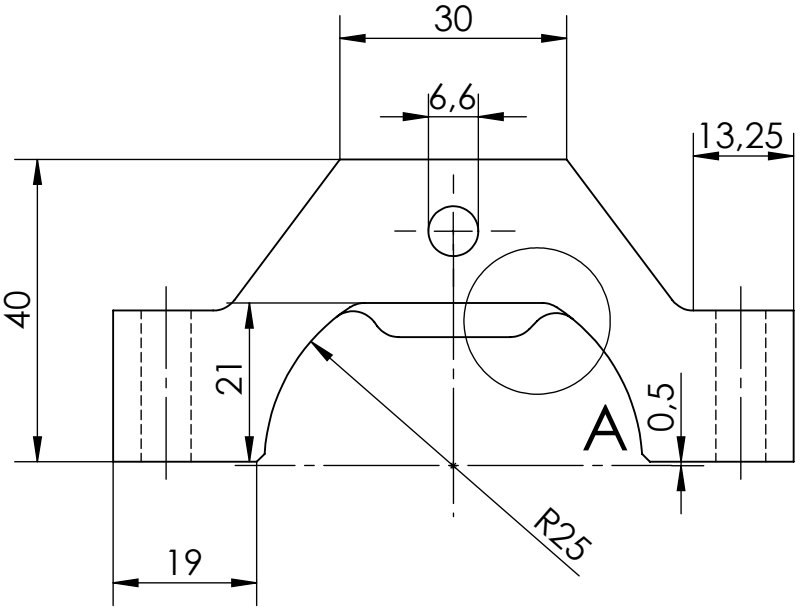

Observações:	1:1	Upper support axial	A01.00.05
	Toleran. NP-265 Médio		

Projetado		
Desen,	05/09/23	
Copiado		
Visualiz.		

NOVA - S.S.T.

Tese de mestrado

Ricardo Manica

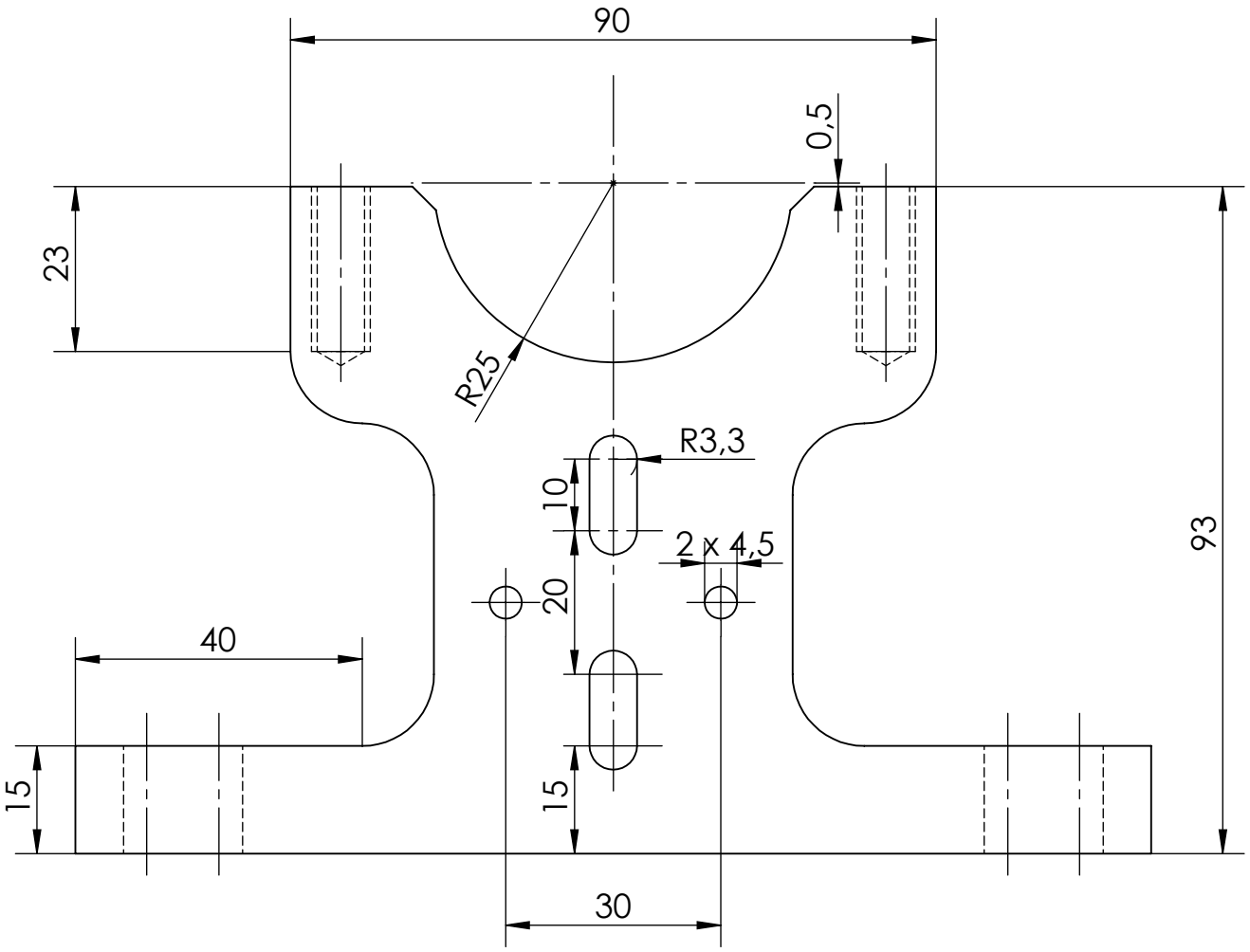

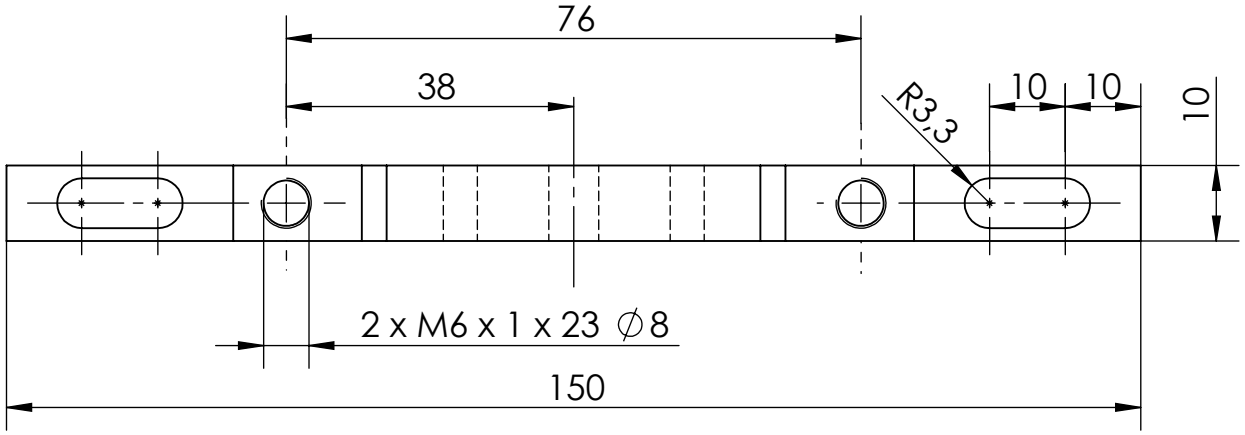

Observações: Todos os raios exteriores têm 10 mm	1:1 Toleran. NP-265 Médio	Lower Support	A01.00.06

Projetado			NOVA - S.S.T. Tese de mestrado	Ricardo Manica
Desen.	05/09/23			
Copiado				
Visualiz.				

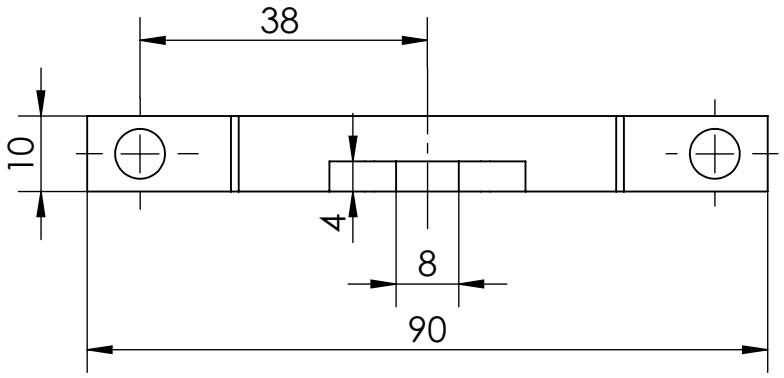

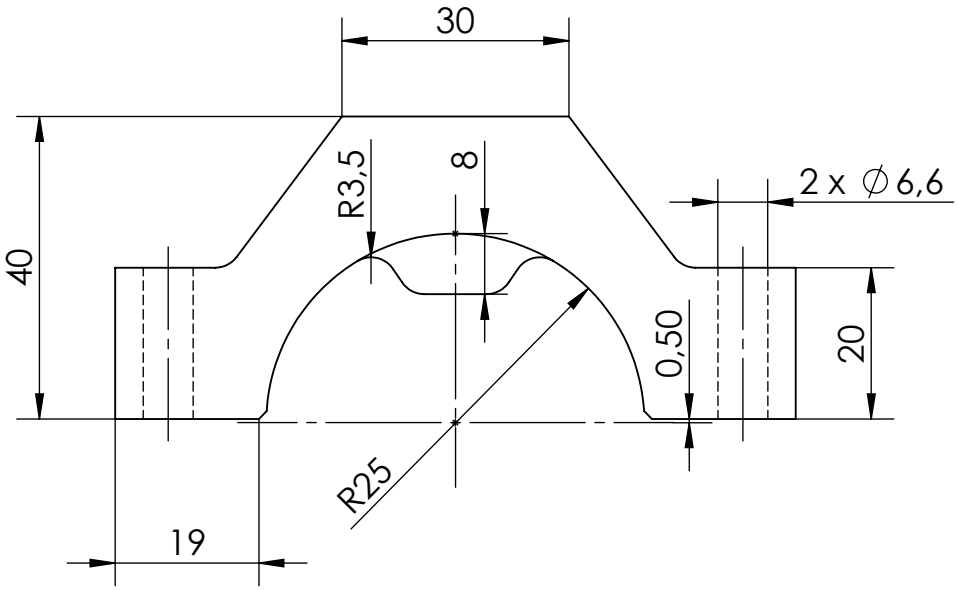

Observações:	1:1 Toleran. NP-265 Médio	Upper support	A01.00.07